Influence of the slope angle on wave overtopping at rubble mound breakwaters

Master Thesis

J. van Marrewijk

16-01-2024

TU Delft

Influence of the slope angle on wave overtopping at rubble mound breakwaters

By

Jaap van Marrewijk
4716604

in partial fulfilment of the requirements for the degree of

Master of Science
in Civil Engineering: Hydraulic Engineering

at the Delft University of Technology,
16th of January 2024

Thesis Committee

Prof. dr. ir. M.R.A. van Gent	Delft University of Technology & Deltares
Ir. D. Jumelet	De Vries & van de Wiel – DEME Group
Dr. ir. P. Mares Nasarre	Delft University of Technology

Preface

This thesis completes the master Hydraulic Engineering, which is carried out at the Delft University of Technology. This thesis is a research to the influence of the slope angle and wave steepness on the average wave overtopping discharge for rubble mound breakwaters. With this thesis, I complete my years as a student, of which I am very proud. Anyone interested is invited to read this thesis.

There are a few people that I would like to thank in particular. First of all, I would like to thank my assessment committee for their support and guidance during this project. Marcel van Gent, Daan Jumelet and Patricia Mares Nasarre: thanks for all your time and effort that you put into this project and for your valuable feedback and sharing your expert knowledge within the field of Hydraulic Engineering. Furthermore, I would like to thank Deltares for the opportunity to perform physical model tests in the Eastern Scheldt Flume and DEME-Environmental for their support. Also, I would like to thank Wesley Stet, Danny van Doeveren and Peter Alberts for all their help in the design and construction of the physical model tests. Without the help of these model technicians the experiments could not have been conducted.

Besides the experts in the field of Hydraulic Engineering, I would also like to thank my friends and family for their support. Although not everyone had the knowledge regarding some Hydraulic Engineering concepts, they have always supported and motivated me throughout this research, and in more general my entire student years, which I look back at with a smile. This thesis marks the end of my years as a student. For now all I have to say is: I hope you enjoy reading this thesis!

Jaap van Marrewijk

Den Hoorn, January 2024

Abstract

A breakwater is a type of coastal structure which has as function to protect a harbor and harbor activities against the forces of waves and currents, including effects on sedimentation and coastal erosion. One of the most common types of breakwaters is a rubble mound breakwater, of which the core consists mainly out of granular material and is protected by armour units. One of the failure modes of a rubble mound breakwater is wave overtopping. This determines the load on the inner slope of the structure as well as the amount of inconvenience by overtopping water for structures and facilities in its lee. The needed elevation of the crest of the breakwater is in general determined by the criterion for the average wave overtopping discharge or wave transmission. In the future, waves are expected to become higher due to the changing climate and the associated sea level rise and the presence of more intense storms. With this changing climate, wave overtopping can become one of the most important hazards to consider to meet the functional requirements of coastal structures.

To calculate wave overtopping at breakwaters, often available guidelines are used like the Overtopping Manual (EurOtop, 2018) and the Technical Report Wave Run-up and Wave overtopping at Dikes (TAW, 2002). One of the parameters that plays a role at wave overtopping is the slope angle of the outer slope of the rubble mound breakwater. In the current guidelines, no influence of the slope angle is accounted for in the formulas for wave overtopping for non-breaking waves at rubble mound breakwaters. However, numerical model results show that wave overtopping at rubble mound breakwaters strongly depends on the slope angle (Irías Mata & Van Gent, 2023). In the formulas for wave overtopping for breaking waves, which is mainly the case for structures with a gentle slope, the slope angle of the structure is taken into account in the guidelines, like the TAW (2002) report and the EurOtop (2018) manual. However, these formulas are mostly based on physical model tests at breakwaters or dikes with an impermeable core and therefore, the applicability of these formulas for rubble mound breakwaters with a permeable core is uncertain.

The objective of this research is to gather more information about a possible relation between the slope angle of a rubble mound breakwater and the wave overtopping at this breakwater. The following research question is covered in this thesis: What is the influence of the slope angle of rubble mound breakwaters on wave overtopping? To answer this research question, a literature study was done and physical model tests were performed at Deltares in Delft, the Netherlands. In total, tests to five different breakwater configurations were performed, with a slope of 1:1.5, 1:2, 1:4, 1:6 and 1:8. These breakwaters were exposed to varying significant wave heights (0.095 m ≤ H_{m0} ≤ 0.228 m) and wave steepnesses (0.012 ≤ $s_{m-1,0}$ ≤ 0.042). During these tests, the amount of water from waves overtopping the structure was collected in order to determine the average wave overtopping discharge for every performed test.

Results of this study show that the slope angle has a large influence on wave overtopping at rubble mound breakwaters. It follows that the steeper the slope, the larger the wave overtopping discharge for the same dimensionless crest freeboard. This trend was captured regardless the wave steepness. This relation can be seen

both for breaking and for non-breaking wave loading. However, the dependency between the slope angle and the wave overtopping discharge appears to be larger for breaking waves than for non-breaking waves.

Furthermore, it was found that the wave steepness has a large influence on wave overtopping at rubble mound breakwaters, both for non-breaking waves and for breaking waves. In general, it can be said that the lower the wave steepness, the larger the wave overtopping discharge for the same dimensionless crest freeboard. This relation was found regardless of the slope angle of the breakwater. However, it followed that the wave steepness has a larger influence on the wave overtopping discharge at gentle slopes, like 1:6 and 1:8. It should be noted that for non-breaking waves, the influence of the slope angle and wave steepness is not present in the existing manuals, while the effects are important.

Regarding non-breaking waves, four different formulas to calculate the wave overtopping discharge were compared to each other and the data. Regarding breaking waves, two different formulas were compared to each other and the data. Both for breaking and for non-breaking waves the formula, with a re-calibrated value of the roughness factor, which predicted the wave overtopping discharges best, based on the lowest RMSLE, was further modified based on the gathered data during the physical model tests to obtain even more accurate predictions for overtopping discharges.

The proposed equation to calculate the average wave overtopping discharge at permeable rubble mound breakwaters for wave loading that can be characterized as non-breaking waves reads as follows:

$$\frac{q}{\sqrt{g\,H_{mo}^3}} = 13.4\,s_{m-1,0}\;\;cot\alpha^{1.1}\;exp\left[-\frac{4.1\,R_c}{\gamma_f\gamma_\beta\gamma_b\gamma_v\gamma_p H_{mo}\xi_{m-1,0}^{0.5}}\right] \qquad \text{Equation 37}$$

The RMSLE for overtopping discharges of tests described by this equation is 0.1722.

The proposed equation to calculate the average wave overtopping discharge at permeable rubble mound breakwaters for wave loading that can be characterized as breaking waves reads as follows:

$$\frac{q}{\sqrt{g\,H_{mo}^3}} = 0.65\;\;cot\alpha\;^{-1.8}\,s_{m-1,0}^{-1}\;\gamma_b\;\;exp\left[-6.4\,\frac{R_c}{\xi_{m-1,0}H_{m0}\gamma_b\gamma_f\gamma_\beta\gamma_v}\right] \qquad \text{Equation 42}$$

The RMSLE for overtopping discharges of tests described by this equation is 0.3562.

Table of contents

List of symbols

Symbol	Description	Unit
A_c	Level of armour in front of the crest wall	[m]
B	Width of the berm	[m]
B_L	Vertical distance between the level of the berm and the level of the armour layer at the crest	[m]
$cot\alpha$	Seaward slope of the structure	[-]
C_w	Chute width	[m]
d	Water depth	[m]
D_{n50}	Median nominal grain diameter	[m]
g	Gravitational acceleration	[m/s^2]
G_c	Armour width in front of chute / crest element	[m]
h	Crest height	[m]
H_{m0}	Significant wave height at the toe based on the wave energy spectrum	[m]
$L_{m-1,0}$	Wave length	[m]
N	Number of waves	[-]
q	Mean wave overtopping discharge	[m^3/s/m]
$q_{calculated}$	Mean calculated overtopping discharge	[m^3/s/m]
q^*	Non-dimensional mean wave overtopping discharges; $q^* = q / (gH_{m0}^3)^{0.5}$	[-]
$Q_{calculated}$	Non-dimensional value of the calculated overtopping discharges; $Q_{calculated} = q_{calculated} / (g\ H_{m0}^3)^{0.5}$	[-]
$Q_{measured}$	Non-dimensional value of the measured overtopping discharge; $Q_{measured} = q_{measured} / (g\ H_{m0}^3)^{0.5}$	[-]
R_c	Crest freeboard: distance between the still water level and crest height	[m]
R_c / H_{m0}	Non-dimensional crest freeboard	[-]
$s_{m-1,0}$	Wave steepness; $s_{m-1,0}=2\pi\ H_{m0} / (g\ T_{m-1,0}^2)$	[-]
T_m	Mean wave period	[s]
$T_{m-1,0}$	Spectral wave period based on the ratio of the spectral moments m_{-1} and m_0	[s]
T_p	Spectral peak wave period	[s]
u	Flow velocity	[m/s]
β	Angle of wave attack	°
γ_b	Influence factor for a berm	[-]
γ_f	Influence factor for the roughness	[-]
γ_p	Influence factor for a recurved parapet on a crest wall	[-]
γ_v	Influence factor for a vertical crest wall	[-]
γ_β	Influence factor for oblique waves	[-]
γ_*	Combined influence factor for crest elements	[-]
$\xi_{m-1,0}$	Iribarren number or breaker parameter; $\xi_{m-1,0}=\tan(\alpha) /(s_{m-1,0})^{0.5}$	[-]

List of figures

List of tables

1. Problem Analysis

In this chapter, first, a short introduction to wave overtopping at breakwaters is given, followed by a problem statement. Next, the objective and research questions of this thesis are introduced. Finally, the methodology to answer the research questions is shown and the outline of this thesis is presented.

1.1 Introduction

A breakwater is a structure which is typically built in the water near the shore. The main function of a breakwater is to protect a harbor and harbor activities against the forces of waves and currents, including effects on sedimentation and coastal erosion. Breakwaters work by reducing the energy of waves as they reach the shoreline by either absorbing or redirecting the energy of waves (Schiereck & Verhagen, 2019). They can be important for protecting coastal communities and infrastructure from the damaging effects of storms and erosion. They can be built in all kinds of shapes and sizes which is depending on the different needs and characteristics of the area they are built in and need to protect.

The most common types of breakwaters are a vertical wall breakwater and a rubble mound breakwater. The vertical type breakwaters mainly consist of masonry concrete or sheet steel plates which are filled with gravel and laid on rip rap rocks as toe protection. The rubble mound breakwaters consist mainly of granular material inside their core and are protected by armour units (Arkash & Chaudhary, 2022). A typical cross section of a rubble mound breakwater with its various components and a vertical type breakwater can be seen in Figure 1. A composite breakwater, where a combination is made between a vertical type and a rubble mound type breakwater, is also possible.

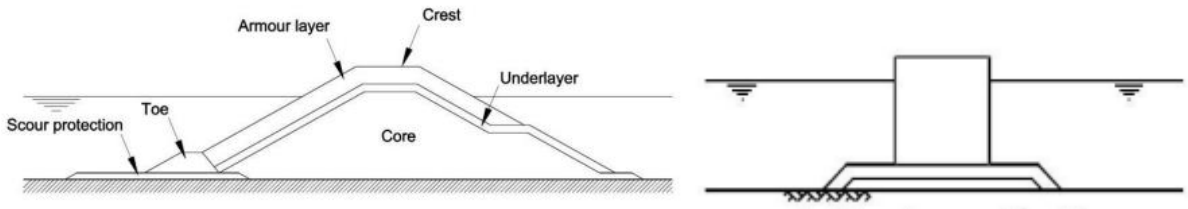

Figure 1 Typical Cross section of a rubble mound breakwater (left) and a vertical type breakwater (right) (CIRIA, et al., 2007).

Rubble mound breakwaters are often preferred over other types of breakwaters due to several reasons. First of all, the seaward slope of a rubble mound breakwater forces storm waves to break and hereby dissipate their wave energy (CIRIA, et al., 2007). This causes only partial wave reflection. Secondly, the material from which the rubble mound breakwater is built is, in general, readily available. The main building material is rock and armour stone, which can often be supplied by local quarries. Also, the structures can be built without the need for complicated equipment, resources and

professional skills. This makes it often an economically attractive solution. Another advantage is the flexibility of the structure. They have the potential to accommodate small changes in the seabed or beach and therefore are not very sensitive to these differential settlements (CIRIA, et al., 2007). Lastly, damage to rubble mound breakwaters often occurs gradually rather than rapidly. Therefore, design and construction errors can often be seen and repaired before complete failure of the structure occurs (CIRIA, et al., 2007).

In order to make a proper safe design for a rubble mound breakwater, all possible failure modes have to be considered. Failure of rubble mound breakwaters can either occur due to wave action or geotechnical factors, such as slope failure, foundation failure and internal erosion. An overview of the individual failure mechanisms of rubble mound breakwaters with a crest element is shown in Figure 2.

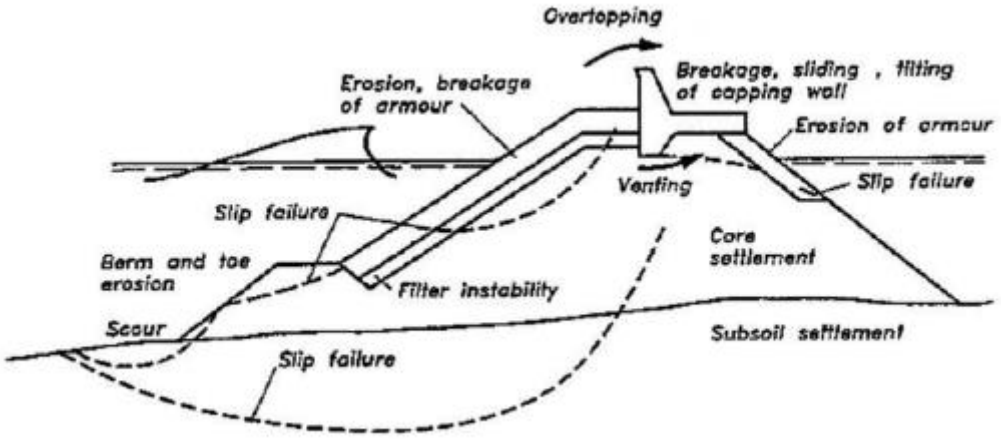

Figure 2 Individual failure mechanisms of a rubble mound breakwater with a crest element (Burcharth & Liu, 1995).

The needed elevation of the crest of the breakwater is generally determined by the criterion for the wave overtopping discharge or wave transmission. The overtopping discharge is the quantity which determines the load on the inner slope of the structure and it determines the amount of inconvenience by overtopping water for the structures and facilities in its lee (Schiereck & Verhagen, 2019). It may damage and erode the inner slope of the breakwater which can possibly lead to failure of the whole breakwater, which in its turn can have severe consequences for the hinterland or harbour. Also, it can cause major inconvenience for people and vehicles behind the defence structure, as well as damage to property, operation or infrastructure in the defended area (EurOtop, 2018).

Wave overtopping occurs when the wave run-up level exceeds the crest level of the breakwater. This principle can be seen in Figure 3. Here R_c is the free crest height (freeboard), which is defined as the difference in height between the crest height of the structure and the still water line SWL.

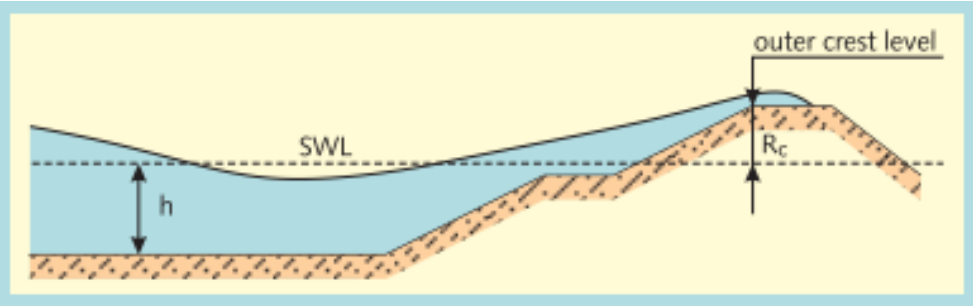

Figure 3 Wave overtopping at a dike (TAW, 2002).

In order to determine the needed free crest height of a breakwater for a safe design, the overtopping discharge needs to be analyzed. There are several parameters that have an influence on the wave overtopping discharge like the wave height, wave period, presence of a berm, roughness of the structure, obliquely incident waves and the presence of a crest element on the breakwater.

In the future, waves are expected to become higher due to the changing climate and the associated sea level rise and the presence of more intense storms. With this changing climate, wave overtopping can become one of the most important hazards to consider to meet the functional requirements of coastal structures.

1.2 Problem Statement

To calculate wave overtopping at breakwaters, often available guidelines are used like the Overtopping Manual (EurOtop, 2018) and the Technical Report Wave Run-up and Wave overtopping at Dikes (TAW, 2002). Influencing parameters on wave overtopping like the roughness of the structure and obliquely incident waves have already been investigated extensively and are therefore included in these guidelines. One of the parameters that is less widely investigated is the slope angle of the outer slope of the rubble mound breakwater. Most physical model tests that have been performed at rubble mound breakwaters are only performed with one slope angle, or a limited amount of different slope angles of the outer slope.

Therefore, in the current guidelines no influence of the slope angle is accounted for in the formulas for wave overtopping for non-breaking waves at rubble mound breakwaters. However, numerical model results show that wave overtopping at rubble mound breakwaters strongly depends on the slope angle (Irías Mata & Van Gent, 2023). It is stated that this effect is so large that it cannot be neglected. In order to reduce this knowledge gap, more research needs to be done.

In the formulas for wave overtopping for breaking waves, which is mainly the case for structures with a gentle slope, the slope angle of the structure is taken into account in the guidelines, like the TAW (2002) and EurOtop (2018) manual. However, these formulas are mostly based on physical model tests at breakwaters or dikes with an impermeable core and it is therefore uncertain to what extent these formulas are applicable for rubble mound breakwaters with a permeable core. Hence, more

research needs to be done to the influence of the slope angle for wave overtopping for breaking waves at rubble mound breakwaters.

1.3 Objective

This thesis has the aim to get a better understanding of the influence of the slope angle on wave overtopping at rubble mound breakwaters. The objective of this research is to gather more information about a possible relation between the slope angle of a rubble mound breakwater and the wave overtopping at this breakwater. In order to achieve this objective, the following research question is studied during this master thesis:

What is the influence of the slope angle of rubble mound breakwaters on wave overtopping?

To answer this research question multiple sub-questions will be answered first. Four sub-questions have been formulated to support the main research question.

1. *Which parameters have an influence on wave overtopping at rubble mound breakwaters?*

2. *What is the influence of the slope angle on wave overtopping when the wave characteristics stay the same and what is the difference between non-breaking and breaking waves?*

3. *What is the influence of the wave steepness on wave overtopping at different slope angles?*

4. *What is the difference between the results of the physical model tests and the existing guidelines for wave overtopping and how can the guidelines be improved in order to obtain more accurate predictions of wave overtopping at rubble mound breakwaters?*

1.4 Methodology

In order to fulfill the research objective and answer the research questions, first a literature study was performed to get an overview of the current state of knowledge regarding wave overtopping and to find out what the existing knowledge gaps are. An overview of previous research on wave overtopping at rubble mound breakwaters was given and the existing guidelines that are mainly used to calculate wave overtopping were discussed. Also, a summary was given of the scale and model effects that can result from physical modelling.

Then, to answer the main research question, physical model tests were performed. These tests have taken place at the laboratory at Deltares in Delft, the Netherlands. During these tests several different permeable rubble mound breakwaters, each with a different slope angle at the seaside of the breakwater, were exposed to waves with varying hydraulic parameters. During these tests the amount of water from waves overtopping the structure was collected in order to determine the average wave overtopping discharge for every performed test. Besides the average wave overtopping discharge, during the physical model tests also the number of overtopping events and the individual overtopping volumes per wave were measured with a wave gauge in the overtopping box. However, it must be noted that the emphasis in this thesis was at the average wave overtopping discharge. To get an impression of the physical model tests, a sketch of the situation can be seen in Figure 4.

Collection and processing of the data was required to determine the average overtopping discharges for all different tests that were performed in the previous step. After this, the processed data was analyzed and the influence of the parameters that play a role at wave overtopping was discussed. Then, a comparison was made between the performed physical model tests and the existing guidelines for wave overtopping. New expressions for wave overtopping at rubble mound breakwaters for breaking and non-breaking waves were proposed, to obtain more accurate predictions of wave overtopping discharges at rubble mound breakwaters.

Finally, a discussion about the research was given and a conclusion was drawn. Furthermore, some recommendations for further research were given.

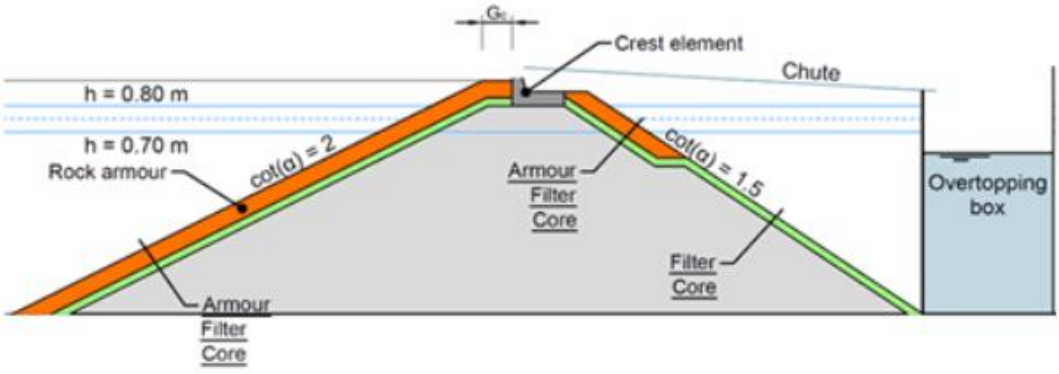

Figure 4 Sketch of the tested breakwater configuration with a seaward slope of 1:2.

1.5 Reading Guide

This thesis can be divided into several different parts. In chapter 1, the main subject is introduced and the research questions are formulated. In chapter 2, a literature study to the state of the art knowledge regarding wave overtopping at breakwaters can be found, as well as some information on physical modelling. The literature study also provides some information regarding the current knowledge gaps that were discussed earlier in section 1.2. Then, in chapter 3, the set-up of the physical model tests is described and the test program that was used for the physical model tests is discussed.

Next, in chapter 4, an analysis of the gathered data is given and a comparison with the existing guidelines regarding wave overtopping is made. Also, a modification to these guidelines is done and two new formulas to predict wave overtopping discharges at rubble mound breakwaters are proposed. After this, a discussion can be found in chapter 5 and a conclusion is drawn in chapter 6. Also, some recommendations for future research are given.

2. Literature Study

In this chapter a literature study is performed to the state of the art knowledge regarding wave overtopping at breakwaters. This is done in order to get an understanding of the physical processes and the influencing parameters that play a role in wave overtopping and to find out the most widely used formulae to calculate wave overtopping at breakwaters. Additionally information regarding physical modelling is given.

2.1 Wave overtopping at breakwaters

2.1.1 Current Guidelines

Many formulas that are used to determine the amount of wave overtopping are empirical formulas. These empirical formulas are often validated with either physical model tests, numerical modelling, or a combination of both. Widely used equations related to wave overtopping are given in the EurOtop manual (EurOtop, 2018) and the TAW report (TAW, 2002).

The magnitude of wave overtopping is often described as the overtopping discharge, averaged over time, which is given as m^3/s or l/s per running meter. According to the EurOtop (2018) guideline the general formulae for the average wave overtopping discharge on a slope (dike, levee or embankment) are given as follows:

$$\frac{q}{\sqrt{g\,H_{mo}^3}} = \frac{0.023}{\sqrt{tan\alpha}}\gamma_b\,\xi_{m-1,0}\,exp\left[-\left(2.7\frac{R_c}{\xi_{m-1,0}H_{m0}\gamma_b\gamma_f\gamma_\beta\gamma_v}\right)^{1.3}\right] \qquad \text{Equation 5}$$

With a maximum of :

$$\frac{q}{\sqrt{g\,H_{mo}^3}} = 0.09\,exp\left[-\left(1.5\frac{R_c}{H_{m0}\gamma_*\gamma_f\gamma_\beta}\right)^{1.3}\right] \qquad \text{Equation 6}$$

Where q [$m^3/s/m$] is the mean wave overtopping discharge, g [m/s^2] is the gravitational acceleration, R_c [m] is the crest freeboard, which is the height of the crest above the still water level, tanα [-] is the seaward slope of the structure, $\xi_{m-1,0}$ is the breaker parameter or Iribarren number, γ_f is the influence factor for the roughness, γ_b is the influence factor for a berm, γ_β is an influence factor for oblique waves and γ_v is an influence factor for a vertical wall. H_{m0} [m] is the significant wave height based on the wave energy spectrum which can be defined as follows: $H_{m0} = 4(m_0)^{1/2}$, where m_0 [m^2] is the zero-th moment of the incident wave spectrum, which represents the total wave energy.

The dimensionless Iribarren number or breaker parameter $\xi_{m-1,0}$ is important in all kinds of shore protection problems. It is a function of the slope angle of the structure and the wave steepness, as can be seen in equation 7. The Iribarren number determines the interaction between waves and a coastal structure like a breakwater. It determines the way in which waves break as can be seen in Figure 5. According to the EurOtop (2018) manual, the transition from breaking (plunging) waves to non-breaking

(surging) waves lies at $\xi_{m-1,0}$=1.8. Again it is noted that here by breaking waves, waves which break on the structure slope are meant. So no depth-limited wave breaking occurs.

The breaker parameter can be described as follows:

$$\xi_{m-1,0} = \frac{tan\alpha}{\sqrt{s_{m-1,0}}} \qquad \text{Equation 7}$$

With:

$$s_{m-1,0} = \frac{2\pi H_{m0}}{gT_{m-1,0}^2} \qquad \text{Equation 8}$$

Where $s_{m-1,0}$ is the wave steepness and $T_{m-1,0}$ is the spectral wave period based on the ratio of the spectral moments m_{-1} and m_0 of the incident wave spectrum. This is the most suitable wave period to account for the influence of the spectral shape of the wave energy spectra on wave run-up and wave overtopping (Van Gent, 1999).

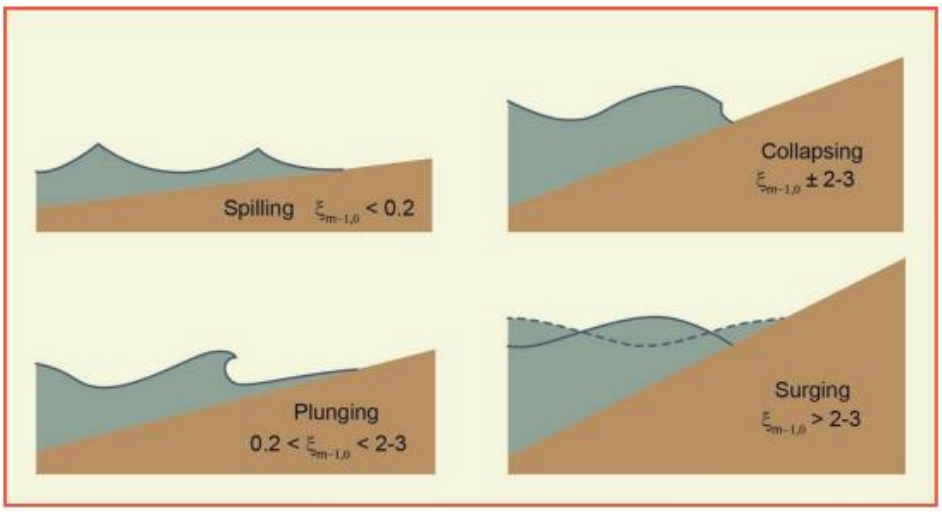

Figure 5 Types of wave breaking on a slope (EurOtop, 2018).

According to the EurOtop (2018) manual, the wave overtopping discharge increases with an increasing breaker parameter, until a maximum is reached for non-breaking (surging) waves. Thus, there seems to be a maximum amount of the wave overtopping discharge because wave overtopping for non-breaking waves is assumed to be independent of the breaker parameter for the same non-dimensional freeboard R_c/H_{m0}. Besides the breaker parameter, also the influence of the slope angle of the structure and the influencing factors for a berm and a vertical crest wall, disappear in the formula for non-breaking waves.

For wave overtopping at permeable rubble mound structures, the EurOtop (2018) manual suggests that equation 6 can be used. However it is mentioned that this equation can only be used for steep slopes ranging from 1:2 to 1:4/3. It is stated that rubble mound structures often have steep slopes of about 1:1.5, which leads to non-breaking waves at the structure and hence the wave overtopping equation that gives the maximum can be used (EurOtop, 2018). No further information is given about wave overtopping at rubble mound breakwaters with slopes more gentle than 1:2.

Also the TAW (2002) report gives two separate formulae for average wave overtopping discharges that are linked to each other: one for breaking waves and one for non-breaking waves.

$$\frac{q}{\sqrt{g\,H_{mo}^3}} = \frac{0.067}{\sqrt{tan\alpha}}\gamma_b\,\xi_{m-1,0}\,exp\left[-4.75\frac{R_c}{\xi_{m-1,0}H_{m0}\gamma_b\gamma_f\gamma_\beta\gamma_v}\right] \quad \text{Equation 9}$$

With a maximum of :

$$\frac{q}{\sqrt{g\,H_{mo}^3}} = 0.2\,exp\left[-2.6\frac{R_c}{H_{m0}\gamma_f\gamma_\beta}\right] \quad \text{Equation 10}$$

Again, just as the proposed formula in the EurOtop (2018) manual, the overtopping discharge increases with increasing breaker parameter until a maximum is reached for non-breaking waves. From that point onward no influence of the breaker parameter or slope angle is included in the formula.

From the general average wave overtopping discharge formulas, both in the EurOtop (2018) manual as in the TAW (2002) report, it can be said that the wave overtopping discharge is dependent on several different wave characteristics and influence factors. The expressions for breaking waves in these guidelines, as shown in equations 5 and 9, include an influence of the slope of the structure, the wave steepness (included via the breaker parameter), the presence of a berm, the presence of a crest wall, oblique waves and roughness of the structure. However, the expressions for breaking waves are mainly developed for wave overtopping at impermeable structures.

The general expressions for surging (non-breaking) waves, which are given in equations 6 and 10, do not include an influence of the slope angle, the presence of a crest wall and a berm and the wave steepness on the overtopping discharges. However, according to Van Gent et al. (2022), who performed physical model tests to study wave overtopping at rubble mound breakwaters, a crest wall, the berm width, berm level and wave steepness all have an influence on the wave overtopping discharge. Therefore a new set of expressions was suggested to describe wave overtopping at rubble mound breakwaters for non-breaking waves:

$$\frac{q}{\sqrt{g\,H_{mo}^3}} = 0.016\,s_{m-1,0}^{-1}\,exp\left[-\frac{2.4\,R_c}{\gamma_f\gamma_\beta\gamma_b\gamma_v\gamma_p H_{mo}}\right] \quad \text{Equation 11}$$

Where:

$$\gamma_f = 1 - 0.7\left(\frac{D_{n50}}{H_{mo}}\right)^{0.1} \quad \text{Equation 12}$$

$$\gamma_v = 1 + 0.45\left(\frac{R_c - A_c}{R_c}\right) \quad \text{Equation 13}$$

$$\gamma_b = 1 - 18\left(\frac{s_{m-1,0}B}{H_{mo}}\right)^{1.3}\left(1 - 0.34\left(\frac{B_L}{s_{m-1,0}A_c}\right)^{0.2}\right) \quad \text{Equation 14}$$

$$\gamma_\beta = 0.65cos^2\beta + 0.35 \quad \text{Equation 15}$$

Where: γ_f is the influence factor for roughness, γ_β is the influence factor for oblique waves, γ_b is the influence factor for a berm, γ_v is the influence factor for a crest wall, γ_p is the influence factor for a recurved parapet on a crest wall, D_{n50} is the median nominal grain diameter of the armour stone [m], $R_c - A_c$ is the protruding part of the crest wall, B is the width of the berm, B_L is the vertical distance between the level of the berm and the level of the armour layer at the crest, and β is the angle of incident waves (for perpendicular waves β = 0°).

The ranges of the parameters that were used in these physical model tests cover a wide range of rubble mound structures. However, there are still limitations to the ranges of validity of the formula, outside the ranges of the parameters that were used in the tests (Van Gent, et al., 2022). For example, the derived expressions are only obtained based on tests to rubble mound structures with a 1:2 seaward slope and for rock armoured structures with a permeable core.

To confirm the trends that have been observed in the physical model tests and examine the validity of the developed set of expressions, outside the range of the parameters that were used, numerical modelling was performed by Irías Mata & Van Gent (2023). This numerical modelling confirmed, among other things, the dependency of the wave overtopping discharge on the wave steepness. It also showed that wave overtopping at rubble mound breakwaters strongly depends on the slope angle of the structure.

In Figure 6 some results of the numerical model are shown. In the left part of the figure the dependency between the slope angle and the overtopping discharge can be seen. Regardless of the varying waves steepness it was found that, the gentler the slope, the lower the overtopping discharges (Irías Mata & Van Gent, 2023).

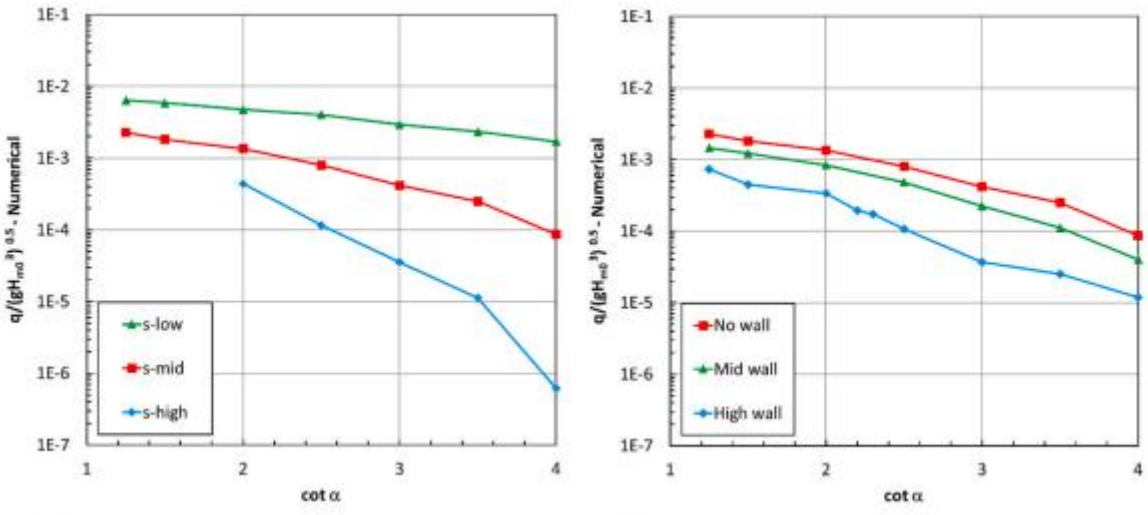

Figure 6 Non-dimensional overtopping discharges as a function of the slope angle of the structure according to numerical modelling (Irías Mata & Van Gent, 2023).

As a result the influence of the slope angle on wave overtopping discharges at rubble mound structures has been included in a new expression as proposed by Irías Mata & Van Gent (2023). This resulted in the following formula:

$$\frac{q}{\sqrt{g\,H_{mo}^3}} = 0.032\; s_{m-1,0}^{-1}\; cot^{-1}\alpha\; exp\left[-\frac{2.4\;R_c}{\gamma_f\gamma_\beta\gamma_b\gamma_v\gamma_p H_{mo}}\right] \qquad \text{Equation 16}$$

Also a new guideline based on physical reasoning was proposed:

$$\frac{q}{\sqrt{g\,H_{mo}^3}} = 0.03\; s_{m-1,0}^{-0,5}\; cot\alpha\; exp\left[-\frac{4\;R_c}{\gamma_f\gamma_\beta\gamma_b\gamma_v\gamma_p H_{mo}\xi_{m-1,0}^{0,5}}\right] \qquad \text{Equation 17}$$

With a re-calibrated expression to account for a berm:

$$\gamma_b = 1 - 8\left(\frac{s_{m-1,0}B}{H_{m0}}\right)\left(1 - 0.36\left(\frac{B_L}{s_{m-1,0}A_c}\right)^{0.15}\right) \qquad \text{Equation 18}$$

According to the proposed set of expressions, the slope angle of the structure has a relevant influence on the expected amount of wave overtopping discharge, since it is incorporated both directly in the formula, by the factor cotα, as well as in the breaker parameter $\xi_{m-1,0}$. However, the influence of the slope angle on wave overtopping discharges at rubble mound structures still needs to be verified with physical model tests (Irías Mata & Van Gent, 2023). Also, it must be noted that these expressions are still only valid for non-breaking waves on the structure.

Hence, there are multiple formulas available in order to calculate the expected wave overtopping discharge at coastal structures. However, they all have their own limitations. Equations 5 and 9, for breaking waves, do include a factor for the slope angle of the structure and also the wave steepness is included via the breaker parameter. However, these equations are mainly developed for impermeable structures and therefore it is not known to what extent these formulas are also applicable for permeable rubble mound structures.

For non-breaking waves, equations 6, 10, 11 and 17 are proposed in various guidelines. Equations 11 and 17 both include factors for the wave steepness, berm and vertical crest wall and equation 17 includes a factor for the slope angle. Both equations are valid for permeable rubble mound structures. However, since they are only applicable for non-breaking waves, which either means a steep slope of the structure or long wave conditions, these expressions can probably not be used for rubble mound structures with gentle slopes. At these gentle slopes, from 1:4 and gentler, most waves will break on the sloping structure. This will have a relevant impact on the wave overtopping discharge.

Furthermore, the formulas as given in the above sections all describe the average wave overtopping discharge over a certain structure. Thus this is not the instantaneous amount of water flowing over a dike or breakwater at a certain moment, but the total overtopping quantities averaged over a period of time. Conventionally, the average wave overtopping discharge is used as a design criterion for coastal structures (Koosheh, et al., 2021). However nowadays, research indicates that large overtopping quantities are much more important than small quantities and therefore, the average overtopping discharge may not be sufficient and additional criteria may be required to describe extreme overtopping events. For instance, a criterion related to volumes within individual waves may be a suitable addition (Franco, et al., 1994). Large

overtopping quantities can be the result of extreme overtopping events. This can cause high flow velocities and a thick water layer at the structure, which can cause damage at the dike or breakwater.

It must be noted that, although these extreme overtopping events might be important as well, in this master thesis the focus will be on the average wave overtopping discharge.

2.1.2 Influencing factors for wave overtopping at rubble mound breakwaters

As explained in the section above, there are different parameters that play a role in determining the wave overtopping discharge at rubble mound breakwaters. These parameters can be divided into two different categories: wave characteristics and other influence factors which mainly depend on the structure's geometry. In the following sections these parameters will be described in more detail.

2.1.2.1 Wave characteristics (wave height and steepness)

The main wave characteristics that play a role in determining the wave overtopping discharge at rubble mound breakwaters are the significant wave height and the wave period. When all other influencing parameters stay the same, an increase in significant wave height will result in an increase in overtopping discharge. Together the significant wave height and wave period form the wave steepness.

Both in the EurOtop (2018) manual as in the TAW (2002) report, the wave steepness is not included in the formulas for wave overtopping at rubble mound breakwaters for non-breaking waves. However, for example Van Gent et al. (2022) concluded that wave overtopping discharges at rubble mound breakwaters depend on the wave steepness. They proposed a new set of expressions, see equations 11-15, where the wave steepness is taken into account both directly in the formula, as well as in the influence factor for the presence of a berm. It was concluded that a lower wave steepness leads to more wave overtopping than a higher wave steepness for the same non-dimensional crest freeboard. This dependency was supported by Irías Mata and Van Gent (2023), however it was only shown for non-breaking waves.

Thus a rise in wave steepness results in a lower overtopping discharge. A higher wave steepness corresponds to a lower breaker parameter. Plunging waves with a lower breaker parameter lose more energy while breaking compared to surging waves with a higher breaker parameter (Schiereck & Verhagen, 2019). This results in less wave overtopping for waves with a lower breaker parameter. Also, a lower breaker parameter corresponds to a lower wave run-up. This decreases the likelihood of waves overtopping the breakwater which results in a lower overtopping discharge.

2.1.2.2 Roughness and permeability

The surface roughness of the slope of a dike or breakwater can have a relevant influence on the amount of wave overtopping. A rubble mound slope, which has a rough surface, increases the frictional resistance on the approaching waves. Therefore a

rubble mound slope dissipates more wave energy than a smooth and impermeable slope (EurOtop, 2018). This effect is caused by both the roughness and the porosity of the armour layer, but also the permeability of the whole structure has a contribution to it. More dissipation of wave energy on the slope results in less wave overtopping.

A structure with a permeable core has less wave run-up than a structure with an impermeable core. This has to do with the fact that for structures with an impermeable core and a steep slope, the surging waves which run up and down the slope cause the water to stay in the permeable armour layer. This leads to a high wave run-up (EurOtop, 2018). The surging waves do not feel the roughness as much as before because of the layer of water in the armour layer and therefore there is less dissipation of energy and so likely more wave overtopping.

For structures with a permeable core the water does not stay in the armour layer, but can penetrate into the core which decreases the wave run-up. There is more energy dissipation and therefore the likelihood of wave overtopping at structures with a permeable core is smaller (EurOtop, 2018). So for breakwaters with the same dimensions and wave characteristics, a breakwater with a permeable core results in less wave overtopping than a breakwater with an impermeable core.

In the EurOtop (2018) and TAW (2002) manual, constant values of roughness factors for a large variety of roughness elements are given. However Chen et al. (2019) found that the roughness factors do not have constant values and therefore do not only depend on the type of material, but also depend on the wave conditions and dike configurations. It was found that the crest freeboard, significant wave height and Iribarren number also play a role in determining a value for the roughness factor. For non-breaking waves at a breakwater with a permeable core, Van Gent et al. (2022) proposed an expression for the roughness factor that depends on the non-dimensional stone diameter (D_{n50}/H_{m0}), which can be seen in equation 12.

2.1.2.3 Oblique waves

Obliquely incident waves are waves that do not approach the structure perpendicularly. The angle of wave attack is defined as the angle between the direction of propagation of waves and the axis perpendicular to the structure (EurOtop, 2018). This can be seen in Figure 7.

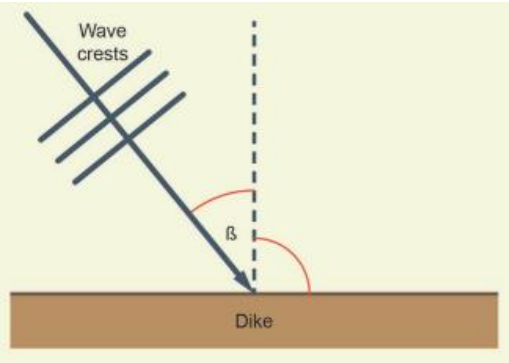

Figure 7 Definition of angle of wave attack (EurOtop, 2018).

Compared to normally incident waves with the same height and period, obliquely incident waves have a reducing effect on wave overtopping. This is valid for structures with a permeable and impermeable core. When waves approach the structure under an angle, the energy of the waves is distributed over a larger area. This reduces the concentration of wave energy at the structure and therefore decreases the likelihood of waves overtopping the structure. The larger the angle of wave attack, the less wave overtopping at the structure (Van Gent, 2020).

2.1.2.4 Berm

An influence factor for a berm on wave overtopping for non-breaking waves at rubble mound structures is missing in the EurOtop (2018) manual and TAW (2002) report. However according to Van Gent et al. (2022), the presence of a berm has an influence on wave overtopping. A new empirical expression is proposed which is shown before in equation 11 which, among other influence factors, includes a factor for the presence of a berm. It must be noted that this expression is only valid for non-breaking waves.

As can be seen in equation 14, the berm influence factor depends on the width of the berm, the level of the berm, and the wave steepness. Wave overtopping is reduced by a stable berm at the seaward slope of a rubble mound breakwater. The larger the berm width, the larger the reduction in overtopping discharge (Van Gent, et al., 2022). This effect is stronger for conditions with a high wave steepness. Furthermore the higher the level of the berm, the lower the wave overtopping discharge. Here the wave steepness is affecting the importance of the berm (Van Gent, et al., 2022). A permeable berm causes more penetration of water into the berm. This causes more dissipation of wave energy and therefore a reduction in wave overtopping.

For breaking waves, an influence factor for a berm on wave overtopping is taken into account in the EurOtop (2018) manual and TAW (2002) report. According to the EurOtop (2018) manual, a berm reduces wave overtopping since the equivalent slope angle of the structure becomes smaller. This influence factor also depends on the width of the berm and the level of the berm. However, it must be noted that these equations for breaking waves are mainly developed for structures with an impermeable core.

2.1.2.5 Crest Wall

Adding a crest wall clearly leads to a reduction in wave overtopping for impermeable structures compared to an impermeable structure without a crest wall but with the same elevation of the armour layer. However, for rubble mound breakwaters the roughness and permeability of the armour layer can be more effective in reducing the wave overtopping discharge than a crest wall (Van Gent, et al., 2022).

The influence factor for a crest wall depends on the ratio of the protruding part of the crest wall and the crest elevation. A definition of this influence factor can be seen in equation 13. Since it followed that the structures with a crest wall lead to more overtopping than the corresponding structures with the same crest level, but without a crest wall, the influence factor becomes larger than one (Van Gent, et al., 2022).

2.1.3 Qualitative review of the potential influence of the slope angle

As explained earlier, the slope angle of a rubble mound structure might have an influence on the expected amount of wave overtopping discharge, both for breaking and for non-breaking waves. In this section, the possible influence of the slope angle on wave overtopping will be described qualitatively.

A steeper slope, which means a higher Iribarren number if the wave steepness stays the same, tends to reflect more of the incoming wave energy. A vertical impermeable wall fully reflects incoming waves. This wave reflection can help to minimize the wave overtopping.

The slope angle also affects the run-up of waves on the breakwater. Run-up is defined as the maximum water level on a slope during a wave period. Waves at a steeper slope have a higher upward velocity in the run-up (Van Doorslaer, et al., 2015). This increases the momentum and energy of the waves at the breakwater which causes more water to spill over the crest. So a higher wave run-up increases the likelihood of wave overtopping, and therefore a higher wave overtopping discharge can be expected.

Furthermore, the slope angle influences the wave tongue that would reach a certain level above the crest level. This is longer for a more gentle slope compared to a steep slope (Irías Mata & Van Gent, 2023). This makes likely that the volume of a wave overtopping a structure with a gentle slope is larger compared to a structure with a steep slope. An impression of this can be seen in Figure 8. So in this case, a more gentle slope leads to a higher wave overtopping discharge due to a higher volume of the waves overtopping the structure.

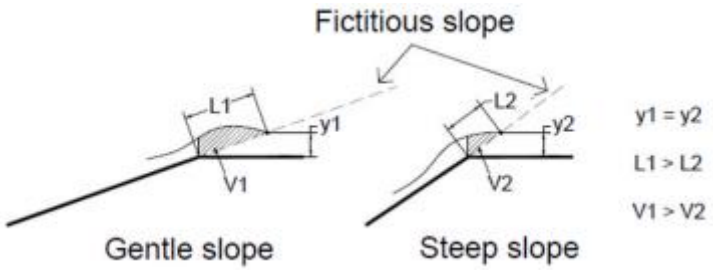

Figure 8 Larger volumes in longer wave tongues at more gentle slopes (Irías Mata & Van Gent, 2023).

It is important to note that the influence of the slope angle on wave overtopping depends on several different mechanisms. On the one hand a steeper slope causes more wave reflection and less volume of the waves overtopping the structure, and so less wave overtopping can be expected. On the other hand a steeper slope causes a higher wave run-up which increases the likelihood of wave overtopping. To get a better understanding of the relationship between the slope angle of the breakwater and wave overtopping, for this thesis physical model tests were performed.

2.2 Physical Modelling

Physical modelling in hydraulic engineering is a technique to study and understand the behaviour of water or other fluids or to study the impact of water in physical systems. Many hydraulic processes are complicated and therefore are missing an analytical formulation (Peña & Anta, 2021). Physical modelling can then be a useful method to develop empirical formulas that can be useful for the design of all kinds of coastal structures.

A lot of different parameters and processes influence wave overtopping at dikes or breakwaters. The individual and combined influences of these parameters are still largely unknown. Theoretical and many numerical approaches to wave overtopping are not well developed yet due to, among other things, the large number of influencing parameters. Also the fluid motion at coastal structures is very complex which makes it difficult to understand the hydraulic processes that play a role in wave overtopping. Therefore, regarding wave overtopping, physical model tests are widely used to develop empirical formulas which can predict wave overtopping discharges.

In physical modelling, it is important for the model to behave in the same way as the real scale structure, which is further referred to as the prototype. Similitude between the model and prototype can mainly be required in three different categories: geometric (shape), kinematic (velocities), and dynamic (force) similitude (Schiereck & Verhagen, 2019). Several laws of similitude can be derived based on the forces that are dominant in a specific test.

In this case hydraulic model tests are performed concerning waves. The viscosity and surface tension of water usually do not play a significant role in this kind of tests and therefore inertia and gravitational factors are the governing factors. Therefore, in this situation the Froude scaling law can be applied. The main principle of this law is that the Froude number in the model and the prototype should be equal (Schiereck & Verhagen, 2019).

$$Fr = \frac{u}{\sqrt{gh}} \qquad \text{Equation 23}$$

$$\frac{u_m}{\sqrt{g_m L_m}} = \frac{u_p}{\sqrt{g_p L_p}} \qquad \text{Equation 24}$$

Where u is the velocity [m/s], g the gravitational acceleration [m/s^2] and L a length [m]. In Froude scaling a geometric scale factor is defined as an indication of how much smaller the model is compared to the reality.

$$n_L = \frac{L_p}{L_m} \qquad \text{Equation 25}$$

Combining the above equations and assuming a scale factor of the gravitational acceleration of 1 (g_m=g_p), the scale factor for velocity becomes:

$$n_v = \frac{u_p}{u_m} = \sqrt{n_L} \qquad \text{Equation 26}$$

Based on the equations above this scaling law also dictates that the scale factor for time [s] equals $n_L^{0.5}$ and for discharge [m^3/s] equals $n_L^{2.5}$.

2.2.1 Scale and model effects

Empirical formulas for predicting wave overtopping discharges are not always very accurate. This might be due to the scale and model effects that are always present to some degree in physical models. Scale and model effects are caused by an incorrect reproduction in the model of the interaction between water and a structure on the real scale.

Scale effects can occur when the physical conditions from the prototype are not correctly reproduced at model scale by the scaling law (Wolters, et al., 2009). As explained earlier, in hydraulic model tests the models are mostly scaled by the Froude Law. However, reliable results from the model tests can only be expected if also the Reynold's law for viscosity forces, Cauchy's law for elasticity and Weber's law for surface tension are fulfilled . This is not possible to achieve and therefore these forces need to be negligible. If these forces are however not completely negligible, scale effects can occur. Scale effects cause inaccuracies in predicting wave overtopping discharges. To reduce the scale effects in model tests some generic rules are given in Wolters et al. (2009) and somewhat modified in the EurOtop (2018) manual:

- The minimum water depth in the physical model should be much larger than h = 2.0 cm.
- Wave periods in the model should be larger than 0.35 s.
- Wave heights in the model should be larger than 5.0 cm to avoid surface tension effects.
- For rubble mound breakwaters the minimum Reynolds number should be Re > 3E+04 ,for which the stability of the breakwater armour can be modelled correctly (Hughes, 1993).
- For coastal dikes the minimum Reynolds number should be Re > 1E+04
- The stone size in the core of rubble mound breakwaters has to be scaled according to the velocities in the core rather than the stone dimensions.

Besides scale effects, the physical model tests might also be disturbed by model and measurement effects. Model effects can be caused by an incorrect reproduction of the structure, geometry and waves and currents of the prototype by the laboratory itself. They can also be the result of the boundary conditions of a wave flume like the side walls (Wolters, et al., 2009).

Measurement effects can be caused by the use of different measuring equipment for collecting data in the physical model and the prototype. They can have a significant influence when the results between the prototype and physical model are compared.

3. Physical Model tests

Physical model tests were performed in the Eastern Scheldt Flume at Deltares in Delft, the Netherlands. In this chapter the physical model tests are described more briefly. Firstly, the set-up of the physical model will be discussed. This includes the composition of the breakwater, the configuration of the wave flume and the overtopping basin. Secondly, the parameters which are used in the several different tests that were performed will be discussed and the measurement program will be shown.

3.1 Physical model set-up

Tests were performed to five different breakwater configurations. For each configuration only the seaward slope of the structure, which is the side of the breakwater subjected to waves, was varied. The different slopes that were tested were: 1:1.5, 1:2, 1:4, 1:6 and 1:8. The different breakwater constructions can be seen in Figure 9.

For each configuration, the breakwater consisted out of three different layers: an armour layer, a filter layer and the core. The armour layer had a D_{n50} of 31.7 mm, the filter layer of 16.8 mm and the core of 6.5 mm, with D_{n50} being the nominal stone diameter for the median armour stone size for the rock grading. The thickness of the armour layer is 2 times the D_{n50}. In order to make sure that no problems occured regarding the stability of the armour layer, the stones in the armour layer were glued together with epoxy so that the stones were fixed at one position.

The armour layer that covered the full slope at the configuration with a 1:1.5 slope, was reused in the upper part of the slopes of the other configurations by using a steel framework. By using this framework, the armour layer could be removed from one structure and be put in the next structure. This resulted in an armour layer that was similar for every structure. This implies that for every test and every configuration the positioning of the stones as well as the porosity of the armour layer at the part where the waves run up the slope is equal. Because of this, the roughness of the breakwater was also equal for every breakwater configuration. Therefore, this method is particularly suitable to make comparisons between the configurations since it reduces inaccuracies in the measurements due to a difference in roughness which can have an influence on the wave overtopping discharge. Furthermore, the breakwater is fully permeable for every configuration.

For all configurations, the slope at the rear side of the breakwater consisted of three layers at the upper part of the slope, and two layers further down the slope. The rear side of the breakwater had a slope of 1:1.5 for every configuration. A sketch of the construction of the breakwater with a 1:2 seaward slope can be seen in Figure 10. The full composition of the breakwater can be seen in more detail in a technical drawing in Appendix A.

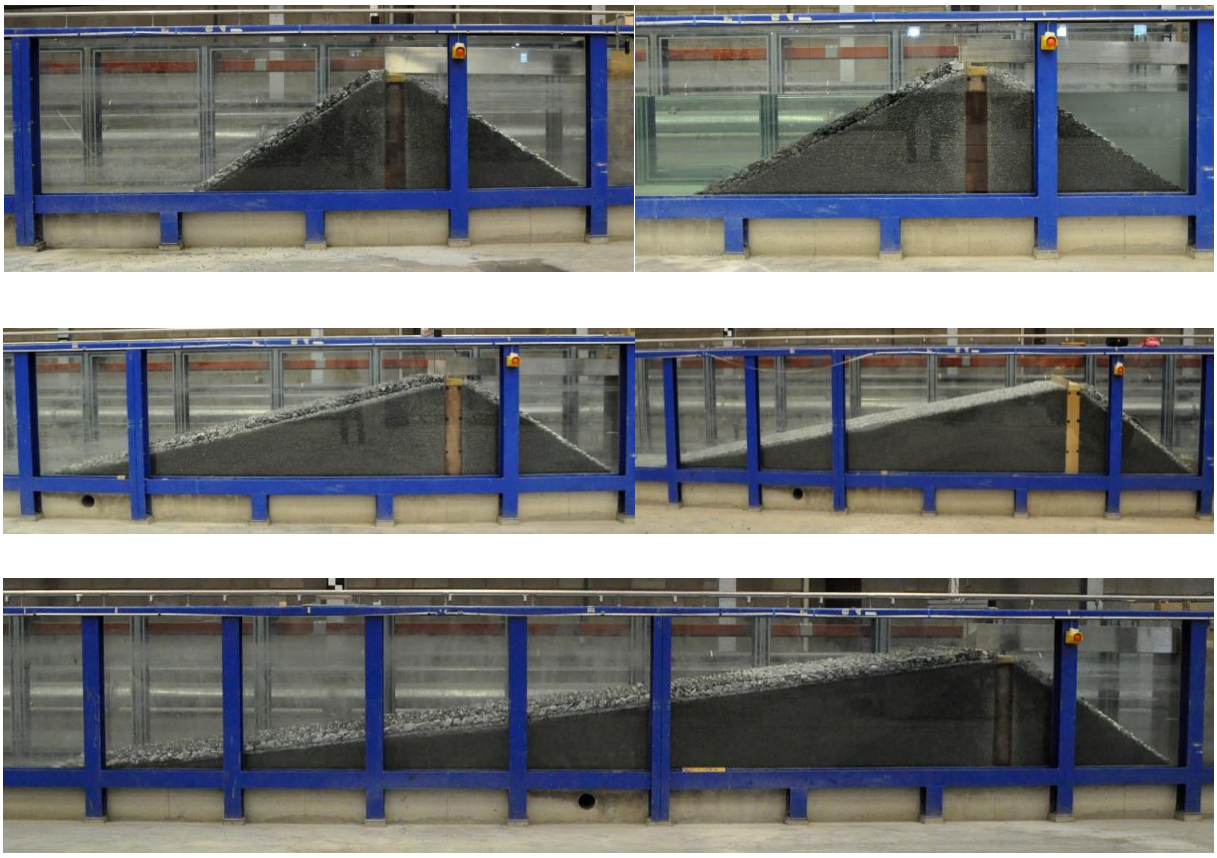

Figure 9 Construction of the different breakwater Configurations. Top left: slope 1:1.5, Top right: slope 1:2, Middle left: slope 1:4, Middle right: slope 1:6, bottom: slope 1:8.

The total height of the construction, which corresponded to the crest height of the breakwater, was 0.9 m for every configuration. A crest element was present but it did not protrude above the stones at the crest. A steel chute was connected to this crest element which conducted the water that overtopped the breakwater to the overtopping basin. This connection can be seen in Figure 11. Three different chutes were used with a width of 0.9 m, 0.5 m and 0.25 m, respectively. The choice for the chute width depended on the expected wave overtopping discharge for the specific test that was performed to keep the pumping time as low as possible but on the other hand to gather as much of the overtopping wave volume as possible. This was a consideration that needed to be made before each test.

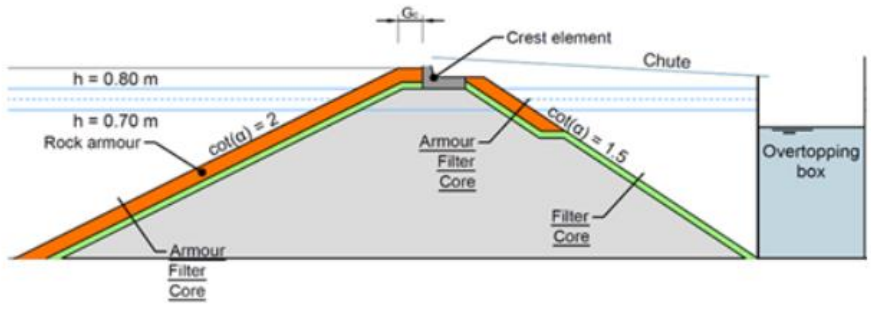

Figure 10 Sketch of the breakwater configuration with seaward slope 1:2.

The overtopping box was a wooden box with a total volume of 120 L. Inside the overtopping box a pump was placed with a hose connected to it so that water could be pumped from inside the overtopping box back into the flume when the box started to fill up. Two wave gauges were placed in the overtopping box to measure the water depth. When the water depth inside the box became too high, the pump was switched on automatically.

Figure 11 Chute connection between crest element and overtopping box (left) and pump inside overtopping box (right).

3.2 Experimental Facilities

3.2.1 Flume Configuration

The Eastern Scheldt Flume has a total length of 55 meter. The breakwater construction was placed at the 3 m long observation windows that are present in the flume, so that a large part of the seaward slope as well as the crest element was clearly visible. At one side of the wave flume a wave generator was present. This wave generator is equipped with Active Reflection Compensation. This means that waves propagating towards the wave boards are measured and that the wave boards compensate for these reflected waves (Deltares, sd).

3.2.2 Wave Gauges

In total 17 wave gauges (WHM's) were used for the experiments. Two sets of WHM's were positioned inside the wave flume to be able to measure the wave characteristics that occurred during the tests. The first set of WHM's, which consisted out of 7 wave gauges, were placed at deep water. The positioning of the second set of WHM's, also consisting of 7 wave gauges, was based on the last WHM of this set. It was placed at a distance of 0.4 times the maximum expected wave length from the toe of the breakwater configuration with a 1:8 slope. This finally corresponded to a distance of WHM14 of 26.95 m from the wave generator.

The internal spacing between the WHM's was based on the ELA method (De Ridder, et al., 2023) and MF-method, to separate the incoming and reflected waves (Mansard & Funcke, 1980). A sketch of the positioning of the wave gauges in the wave flume can be seen in Figure 12, which can be seen in more detail in Appendix B.

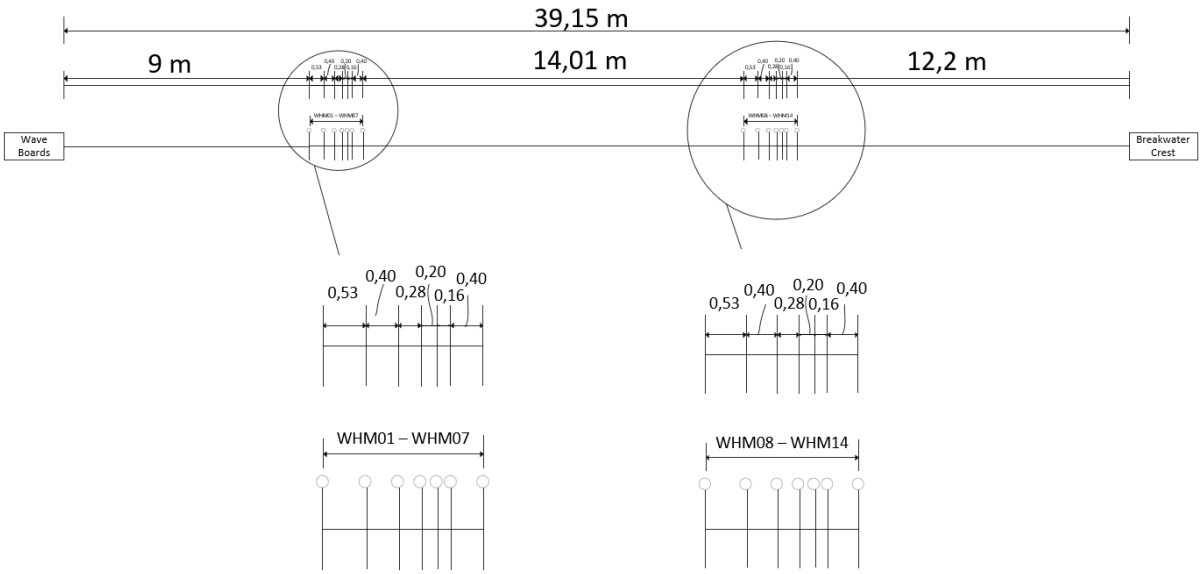

Figure 12 Positioning of wave gauges in wave flume.

Furthermore, one wave gauge was placed on top of the crest of the breakwater to measure the number of overtopping events. Another two wave gauges were placed inside the overtopping box to measure the water depth in this box. From this measured water depth the overtopping volume per test was determined. The average wave overtopping discharge could then be determined from the wave overtopping volume and the duration of the test.

3.3 Test Program

As said earlier, tests with five different breakwater configurations were performed, each with another slope of the seaward side of the breakwater. In all tests a JONSWAP spectrum was used for the incoming waves. This is a wave spectrum that describes young sea states that are not fully developed and it is used to generate random realistic waves. An enhancement factor of 3.3 has been applied. Every test consisted out of 1,000 waves since then the series is long enough to schematize a full wave height and period distribution over the frequency domain and for stabilizing statistical properties of wave overtopping.

Each breakwater configuration was tested with various wave characteristics. For three different wave steepnesses: a low steepness, a middle steepness and a high steepness, the wave height was increased gradually. In order to perform tests with an increasing wave height, but a wave steepness that needed to stay the same, the wave period needed to be adjusted accordingly for every test. The water depth was adjusted for the tests based on the expected wave overtopping discharge to stay in a certain range of discharges.

This resulted in the execution of at least 18 tests per breakwater configuration and therefore, 90 tests in total. However, sometimes it was interesting to see the difference in wave overtopping discharge for tests with the same wave height and steepness but different water depth, or a test was redone with a smaller chute width in order to reduce the pumping time. Therefore, in total 119 tests were performed. A wave running up the slope during a test can be seen in Appendix C.

Incident significant wave heights at the toe of the breakwaters were in the range between H_{m0} = 0.095 m and 0.228 m. The wave steepness at the toe of the structures varied between $s_{m-1,0}$ = 0.012 and 0.042. Four different water depths were applied (0.825 m, 0.75 m, 0.7 m and 0.6 m). Since the crest height stayed the same in every configuration, this resulted in four different values of the crest freeboard R_c (0.075 m, 0.15 m, 0.2 m and 0.3 m). Eventually, the non-dimensional freeboard was in the range between R_c/H_{m0} = 0.88 and 2.08. In Table 1 the ranges of the most important parameters of the test program can be seen. The full test program with the most important parameters can be found in Appendix D.

Table 1 Ranges of most important parameters of the test program.

Parameter	Symbol	Values / Ranges
Seaward Slope [-]	$\cot \alpha$	1.5; 2; 4; 6; 8
Median nominal grain diameter of armour stone [m]	D_{n50}	0.0317
Water depth [m]	d	0.6 – 0.825
Crest height [m]	h	0.9
Incident significant wave height at toe [m]	H_{m0}	0.095 – 0.228
Freeboard [m]	R_c	0.075 – 0.3
Wave Steepness [-]: $s_{m-1,0}=2\Pi H_{m0}/gT^2_{m-1,0}$	$s_{m-1,0}$	0.012 – 0.042
Iribarren number [-]: $\xi_{m-1,0}=\tan\alpha/s^{0.5}_{m-1,0}$	$\xi_{m-1,0}$	0.612 – 6.04
Number of waves [-]	N	1,000
Armour width in front of chute / crest element [m]	G_c	0.100
Chute width [m]	C_w	0.25; 0.5; 0.9
Non-dimensional Freeboard [-]	R_c/H_{m0}	0.33 – 2.08
Non-dimensional armour width in front of chute [-]	G_c/H_{m0}	0.44 – 1.05
Non-dimensional stone diameter [-]	D_{n50}/H_{m0}	0.14 – 0.33

3.4 Scaling of hydrodynamics

The hydraulic physical model tests that were performed in this study were not based on any prototype model. Therefore, although scaling laws are important to correctly reproduce the behaviour of the model just as on the real scale as explained in section 2.2, in these experiments the used parameters were not scaled from prototype.

4. Data Analysis

In this chapter an analysis of the gathered data during the physical mode tests is given. In the first part, the results of these tests can be found and the influence of different parameters on the wave overtopping discharge is described qualitatively. In the second part, these results are compared with existing guidelines regarding wave overtopping, which were described earlier in chapter 2. In the third part modifications to these guidelines are performed in order to improve the prediction of wave overtopping discharges.

As explained earlier in chapter 3, the overtopping volume was collected in the overtopping box during the tests. For some tests with large overtopping discharges, the water depth in this overtopping box became so high that a pump inside the overtopping box was switched on to empty the box during these tests. The waves that overtopped the breakwater during this pumping time were not taken into account in the total overtopping volume and thereby influencing the average wave overtopping discharge.

To keep these inaccuracies as low as possible while using as much data as possible, it was decided to disregard the tests with a total pumping time, as percentage of the total duration of the specific test, higher than 11%. This seemed to be the threshold where the deviation of the average wave overtopping discharge between a test were pumping was needed and the same test where pumping was not needed, due to the use of a chute with a smaller width, did not exceed 5%. This is assumed to be accurate enough to include in the data analysis.

4.1 Test Results

Data gathered during the physical model tests can be seen in Figure 13. In this figure, the dimensionless measured wave overtopping discharge is plotted against the dimensionless crest freeboard for all tests, including the mean trend of observations. Also, a distinction is made between the different breakwater configurations and the associated different slope angles. What stands out first is the influence of the slope angle on the wave overtopping discharge. In general, the steeper the slope of the breakwater, the larger the wave overtopping discharge for the same dimensionless crest freeboard.

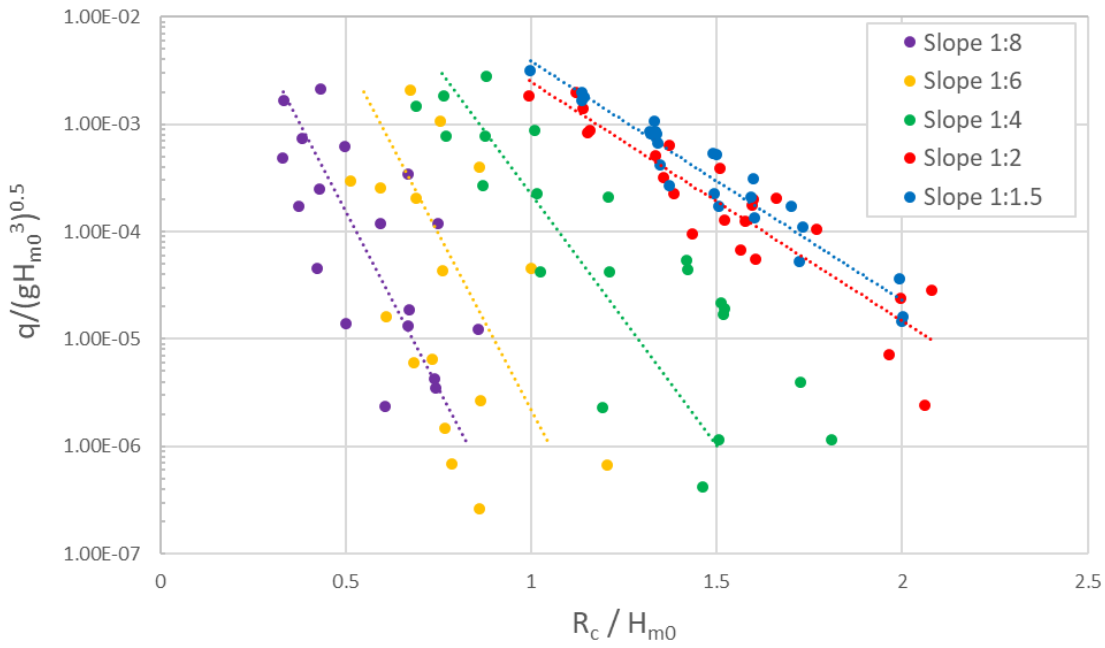

Figure 13 Measured dimensionless wave overtopping discharges plotted against dimensionless crest freeboard including mean trends of observations.

4.1.1 Influencing parameters

4.1.1.1 Dimensionless crest freeboard

As can be seen from the mean trends of observations in Figure 13, there is a more or less linear relationship for every breakwater configuration between the dimensionless crest freeboard R_c/H_{m0} and the dimensionless wave overtopping discharge on logarithmic scale. Therefore, the relationship between the dimensionless crest freeboard and the wave overtopping discharge is of exponential nature, which is in line with the TAW (2002) report, but not in line with the EurOtop (2018) manual. The latter includes an exponential function, but the dimensionless crest freeboard is to the power 1.3. This would lead to a curved rather than a straight line in Figure 13.

4.1.1.2 Wave steepness

The wave overtopping discharges, divided per breakwater configuration and wave steepness, plotted against the dimensionless crest freeboard can be seen in Figure 14. In this case, low waves steepness is defined as $s_{m-1,0} < 0.015$, middle wave steepness is defined as $0.015 \leq s_{m-1,0} \leq 0.030$ and high wave steepness as $s_{m-1,0} > 0.030$. It should be noted that this distinction will also be made in the remaining part of this data analysis.

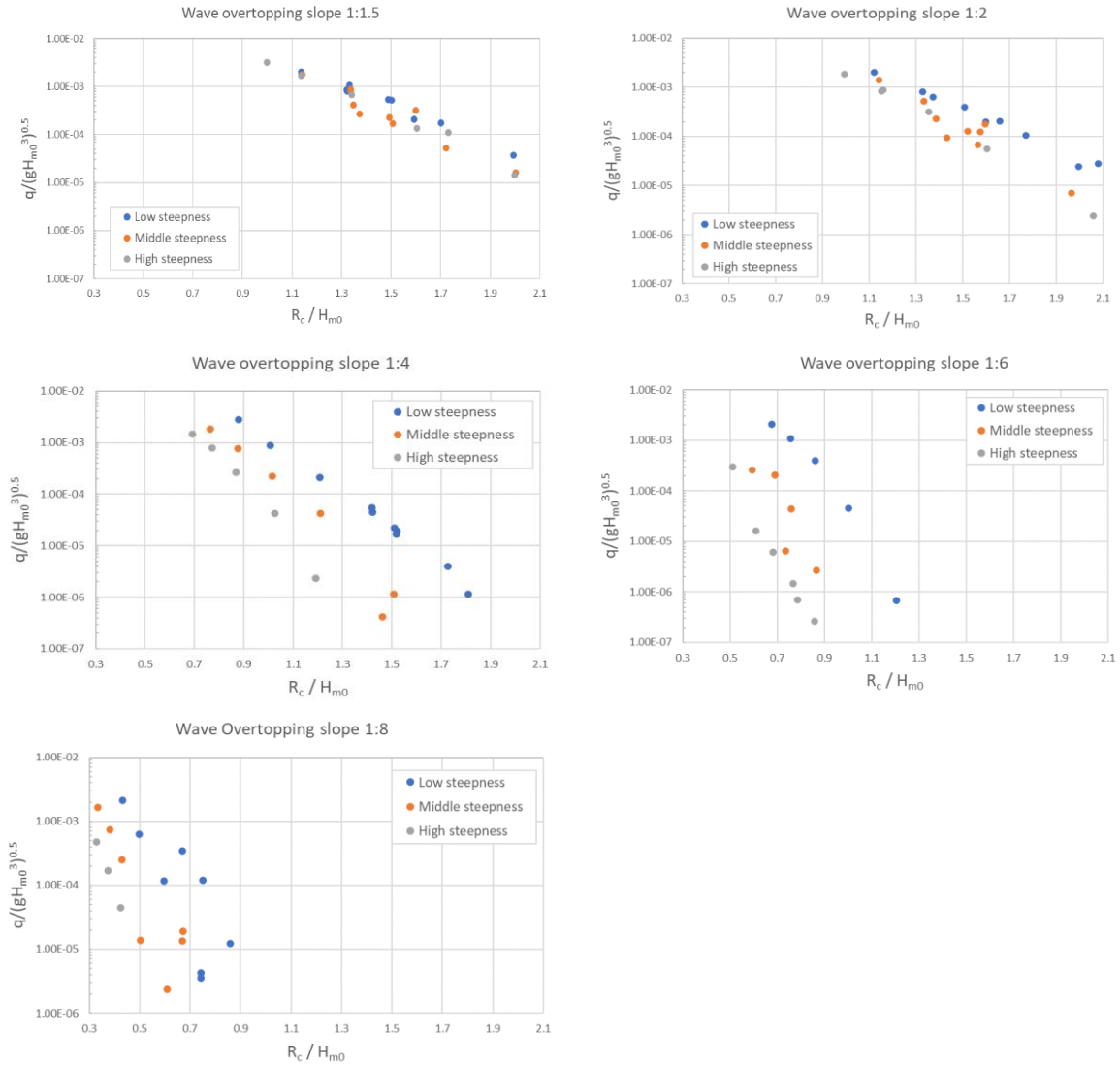

Figure 14 Measured wave overtopping discharges per breakwater configuration.

Figure 14 shows that, in general, the lower the wave steepness, the higher the wave overtopping discharge, regardless the slope angle of the breakwater. However, for the same dimensionless crest freeboard, the difference between the wave overtopping discharge for low wave steepnesses and high wave steepnesses is less for steeper slopes (1:1.5 and 1:2) and becomes bigger for more gentle slopes (1:4, 1:6 and 1:8). Therefore, it seems that for steeper slopes of the breakwater, the dependency between the wave overtopping discharge and the wave steepness becomes less compared to more gentle breakwater slopes. This can also be seen in Figure 15, where a distinction is made between breaking and non-breaking waves.

The difference in this analysis between breaking and non-breaking waves is made in line with EurOtop (2018) and is based on the breaker parameter $\xi_{m-1,0}$, which was earlier described in equation 7. Waves with a breaker parameter lower than 1.8 are considered to be breaking or plunging waves. Waves with a breaker parameter above this value are considered to be non-breaking or surging waves. In the TAW (2002) report, a value of $\xi_{m-1,0}$ of 1.86 is used for the transition between the two.

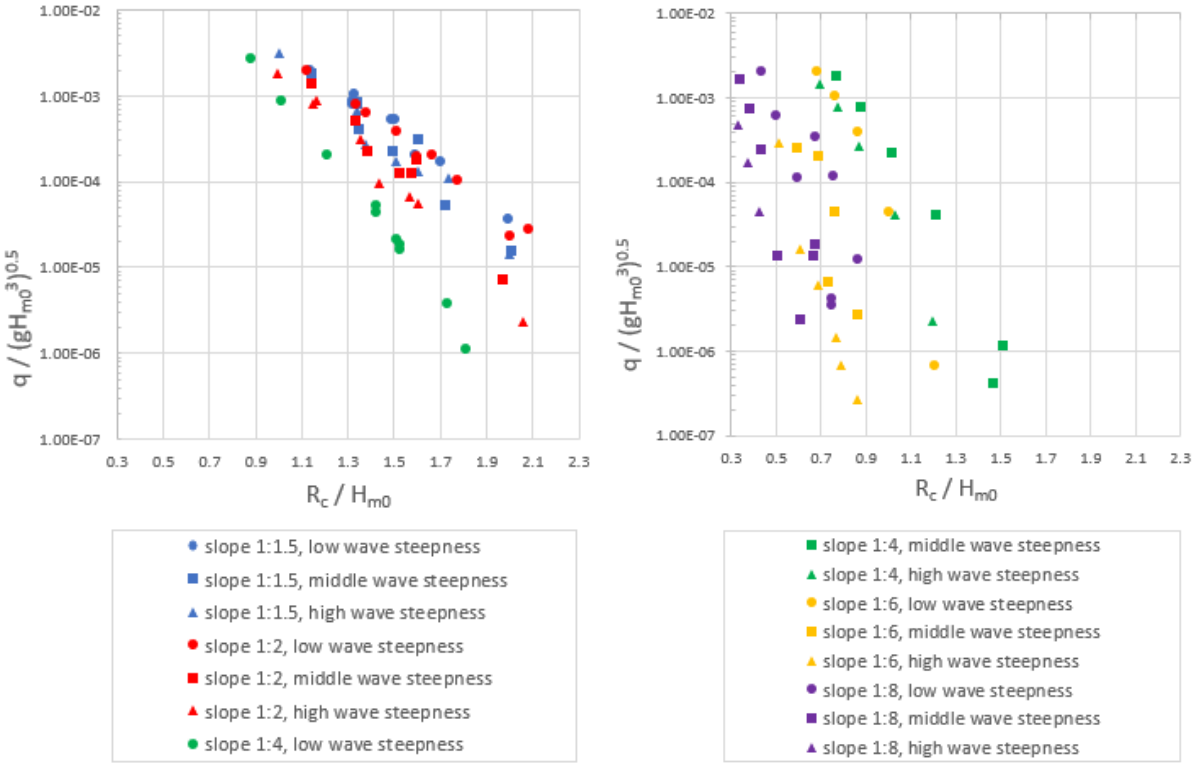

Figure 15 Measured wave overtopping discharges for non-breaking waves (left) and breaking waves (right).

Figure 15 illustrates a bigger spread in wave overtopping discharges for the same slope angle for breaking waves compared to non-breaking waves. This supports the idea that the wave steepness has a larger influence on the wave overtopping discharge at gentle slopes, since the breaker parameter strongly depends on the slope angle of the breakwater. However, also at steeper slopes (1:1.5 and 1:2) the influence of the wave steepness on the overtopping discharge is still noteworthy.

Based on the measurements, it can be concluded that the wave steepness has a large influence on wave overtopping at rubble mound breakwaters, both for non-breaking waves and for breaking waves. The qualitative influence of the wave steepness on the wave overtopping discharge at rubble mound breakwaters is in line with previous research by Van Gent et al. (2022) and Irías Mata & Van Gent (2023), who reported that wave overtopping at rubble mound breakwaters depends on the wave steepness, for wave loading that can be characterized as non-breaking waves.

Regarding breaking waves, the wave steepness is included in the formulas for the average wave overtopping discharge for impermeable dikes or breakwaters in the TAW (2002) report and EurOtop (2018) manual. Here, the influence of the wave steepness for breaking waves can also be seen for permeable rubble mound breakwaters.

4.1.1.3 Slope angle

In Figure 13 it is shown that the seaward slope angle of the breakwater has an influence on the wave overtopping discharge. Figure 16 illustrates the dependency between the wave overtopping discharge and the slope angle of the breakwater, with a distinction between non-breaking and breaking waves. For wave loading that can be characterized as breaking waves, it follows that the steeper the slope, the larger the overtopping discharge for the same dimensionless crest freeboard. This is also described in the TAW (2002) and EurOtop (2018) guidelines for impermeable dikes or breakwaters. Here, this trend can be seen for permeable breakwaters. This trend can also be observed for wave loading that can be characterized as non-breaking waves.

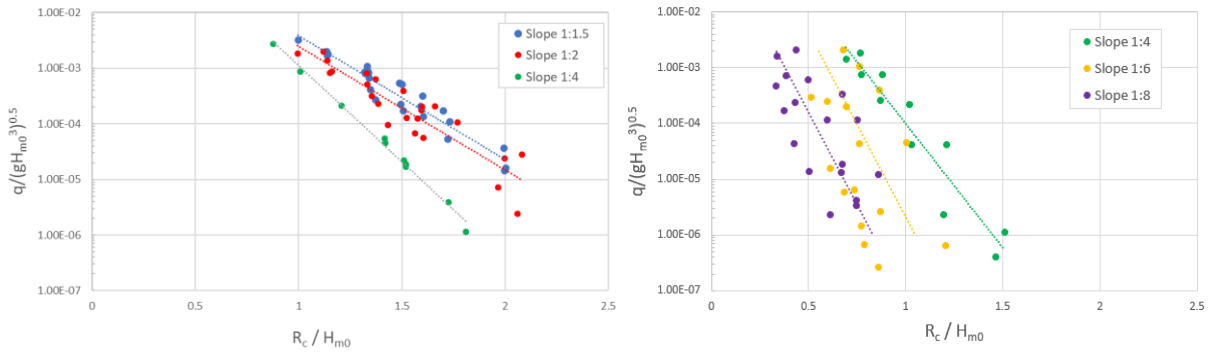

Figure 16 Measured wave overtopping discharges for non-breaking waves (left) and breaking waves (right) including mean trend of observations.

In general, it can be said that the gentler the slope of the breakwater, the lower the wave overtopping discharge for the same dimensionless crest freeboard. This can also be seen in Figure 17 where this trend is also captured regardless the wave steepness. This is in line with research performed by Irías Mata & Van Gent (2023), who already found this trend for non-breaking waves based on numerical model results.

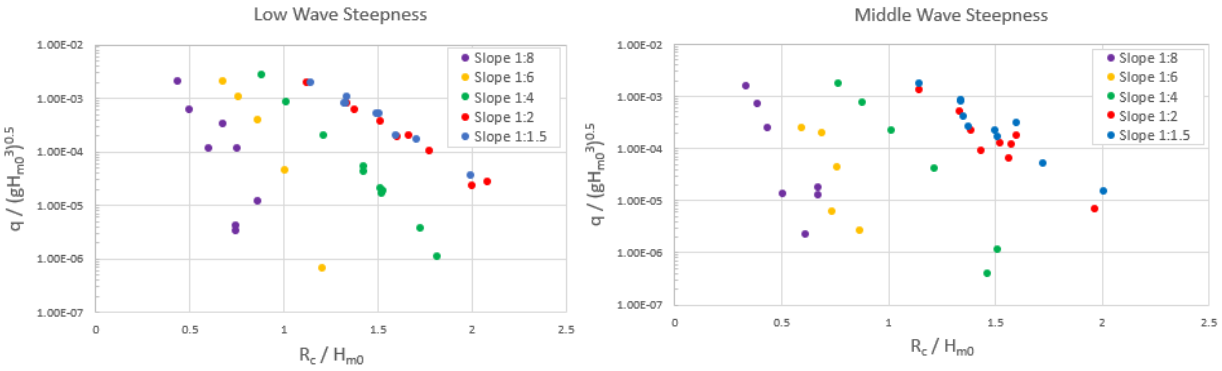

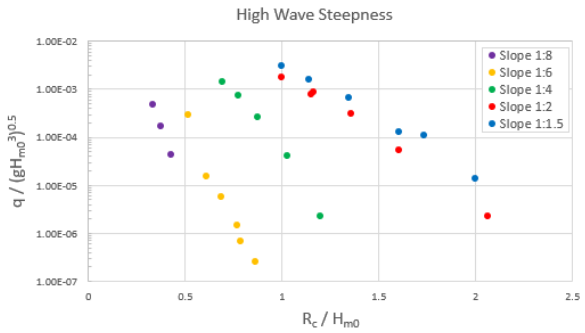

Figure 17 Measured wave overtopping discharges per wave steepness.

The influence of the slope angle on the wave overtopping discharge optically seems larger for breaking waves compared to non-breaking waves, based on the larger spread in the data of breaking waves in Figure 16. However, the influence of the slope angle on wave overtopping for non-breaking waves cannot be neglected.

The difference in wave overtopping discharges between the configurations with a slope of 1:1.5 and 1:4 seems to be one to two orders of magnitude for the same dimensionless crest freeboard based on Figure 16. This effect of the slope angle on overtopping discharges for non-breaking waves was also found by Irías Mata & Van Gent (2023). The difference in wave overtopping discharges between the configurations with a slope of 1:4 and 1:8 is even larger than two orders of magnitude for the same dimensionless crest freeboard. This confirms the idea of a larger dependency between the wave overtopping discharge and the slope angle for breaking waves compared to non-breaking waves.

4.1.1.4 Breaker parameter

As described in section 4.1.1.2 and 4.1.1.3, the wave steepness and slope angle have a relevant influence on the overtopping discharge, both for breaking wave loading and for non-breaking wave loading. The breaker parameter is a combination of these parameters and determines the type of wave breaking on the slope as can be seen in Figure 5. The type of wave breaking on the slope determines the distribution of energy dissipation along the breakwater slope, which might influence the wave run-up along this slope and thus the wave overtopping.

In Figure 18, measured wave overtopping discharges can be seen where a distinction is made between different values of the breaker parameter. It appears that for the same dimensionless crest freeboard, a higher breaker parameters corresponds to a higher overtopping discharge based on the mean trends of observation in the figure. This is of course in line with the earlier findings. A lower wave steepness, corresponding to a higher breaker parameter, leads to a higher overtopping discharge as was found in section 4.1.1.2. A steeper slope, corresponding to a higher breaker parameter, also leads to a higher overtopping discharge as was found in section 4.1.1.3.

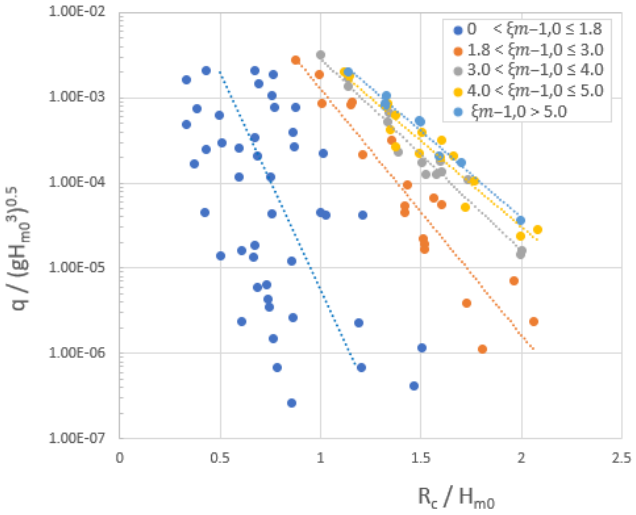

Figure 18 Measured wave overtopping discharges for breaking waves with a distinction in breaker parameter.

Regarding breaking wave loading ($\xi_{m-1,0} \leq 1.8$) the type of wave breaking can either be spilling or plunging. Jumelet et al. (2024) found that for values larger than $\xi_{m-1,0}=1.0$, all waves were plunging waves. For values of the breaker parameter smaller than 1.0 it was found that the fraction of plunging waves F_p can be described by:

$$F_p = \frac{N_{plunging}}{N_{total}} = -1.7\xi_{m-1}^2 + 3.2\xi_{m-1,0} - 0.5$$

For $0.4 \leq \xi_{m-1,0} \leq 1.0$

From this relation it follows that a higher value of the breaker parameter results in a higher percentage of plunging waves, or a smaller percentage of spilling waves. In Figure 19, a relation between the wave overtopping discharges regarding breaking wave loading and the fraction of plunging waves can be seen.

In general, it appears that a higher fraction of plunging waves corresponds to a higher wave overtopping discharge for the same dimensionless crest freeboard. Although, it must be noted that only a limited amount of tests are available which had a fraction of plunging waves F_p below 0.95.

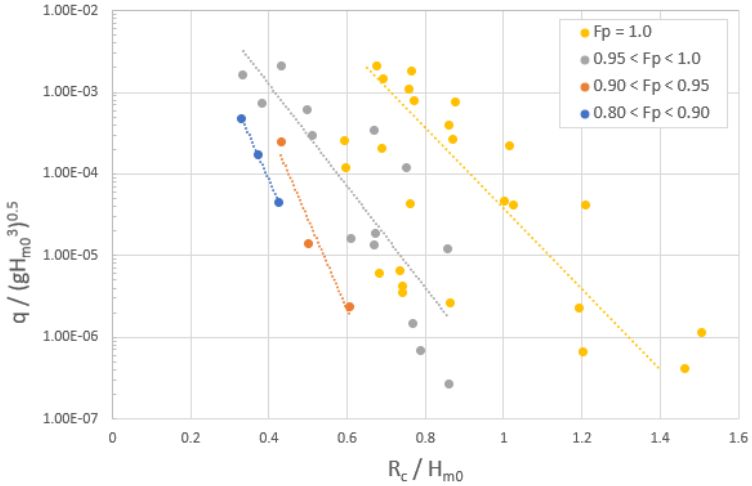

Figure 19 Measured wave overtopping discharges for breaking waves with a distinction in fraction of plunging waves.

4.2 Comparison of tests with current guidelines

The results of the physical model tests are compared with the existing wave overtopping guidelines to check whether these guidelines fit the measurements and to what extent differences between the measurements and guidelines occur. In both the TAW (2002) and the EurOtop (2018) guidelines, a distinction is made between plunging (breaking) and surging (non-breaking) waves. In Figure 20, it can be seen that also in the results of the performed physical model tests, breaking and non-breaking waves show a somewhat different behavior and therefore, also in this analysis a difference is made between wave loading that can be characterized as either breaking or non-breaking waves, based on the breaker parameter $\xi_{m-1,0}$.

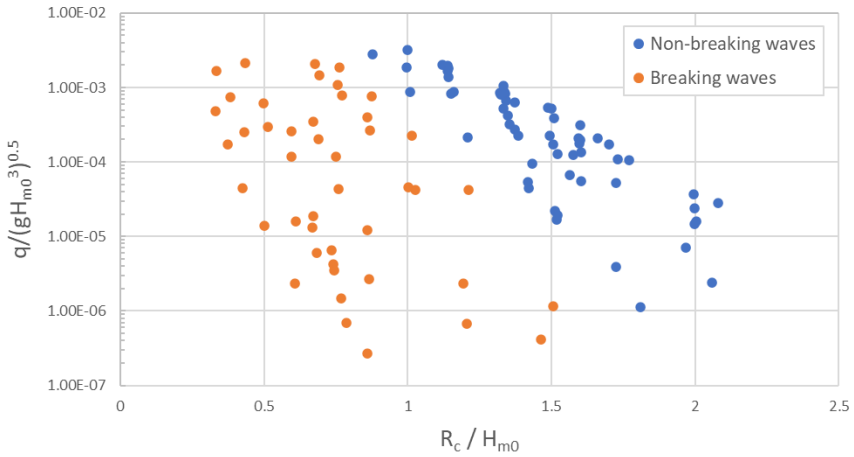

Figure 20 Measured wave overtopping discharges for breaking and non-breaking wave loading.

4.2.1 Non-breaking waves

Wave overtopping for non-breaking waves is described in different guidelines. In this analysis, the measurements will be compared with four different approaches, which were earlier introduced in chapter 2. The formulas for the wave overtopping discharge for non-breaking waves, as presented in the TAW (2002) report and EurOtop (2018) manual, are repeated here in equation 27 and 28, respectively.

$$\frac{q}{\sqrt{g\,H_{mo}^3}} = 0.2\ exp\left[-2.6\frac{R_c}{H_{mo}\gamma_f\gamma_\beta}\right] \qquad \text{Equation 27}$$

$$\frac{q}{\sqrt{g\,H_{mo}^3}} = 0.09\ exp\left[-\left(1.5\frac{R_c}{H_{mo}\gamma_*\gamma_f\gamma_\beta}\right)^{1.3}\right] \qquad \text{Equation 28}$$

These formulas are displayed together with the measurements in Figure 21. The roughness factor γ_f in the TAW (2002) formula is set to $\gamma_f = 0.55$, which coincides with the value for a double-layer rock armour (rubble mound) as given in the TAW (2002) report. The roughness factor in the EurOtop (2018) formula is set to $\gamma_f = 0.40$, which coincides with the value for a double-layer rock armors with a permeable core as given in the EurOtop (2018) manual.

Figure 21 shows that the TAW (2002) formula is a better fit than the EurOtop (2018) formula when the standard tabulated values, as given in the guidelines, for the roughness factor are used. The deviations of the overtopping discharge computed by the TAW (2002) formula appear to be quite consistent. On the other hand, the EurOtop (2018) formula underestimates the measured wave overtopping discharges by a relatively large amount.

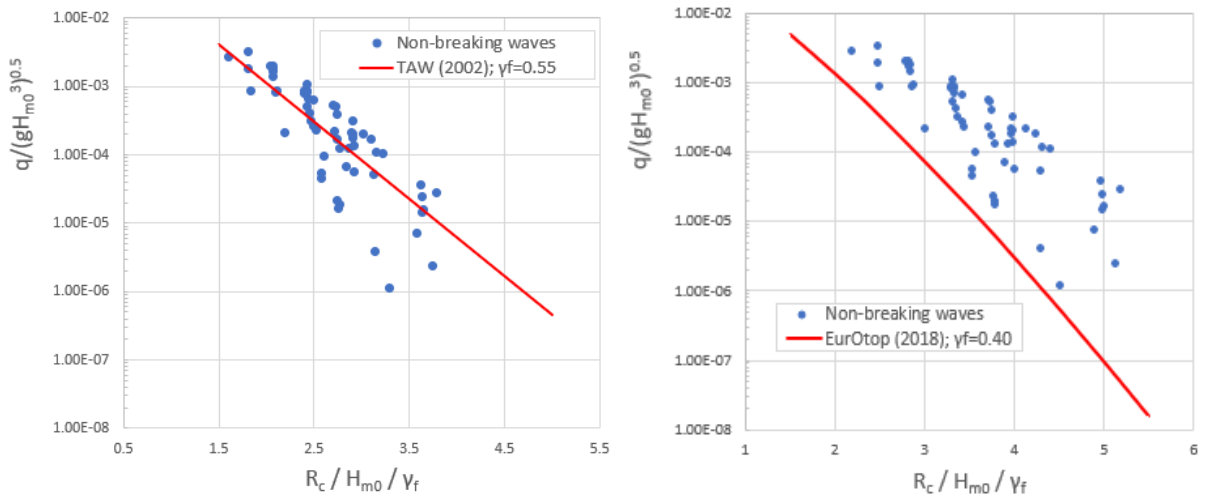

Figure 21 Measured wave overtopping discharges regarding non-breaking waves compared with TAW (2002) (left) and EurOtop (2018) (right) formulas.

To make a better comparison between the two formulas, the roughness factor γ_f should be optimized for both formulas separately, such that the data fits the expression best. This means that the bias for overtopping discharges of tests described by the specific formula should be as close to zero as possible. The bias quantifies the average difference in wave overtopping discharge to be expected between an estimator's expected value (a value following from the specific formula used) and the underlying true value of the parameter that is being estimated (in this case the measurements). If this difference is equal to zero, the formula is called unbiased. This means that the formula does not show any systematic differences and therefore does not overestimate or underestimate the true value of the parameter (Joosten, 2017).

Both roughness factors in the formulas are re-calibrated separately to find the expression which results in zero bias. This is the case for $\gamma_f = 0.582$ and $\gamma_f = 0.562$ for the TAW (2002) report and EurOtop (2018) manual, respectively. Both formulas can be seen in Figure 22 together with the measurements.

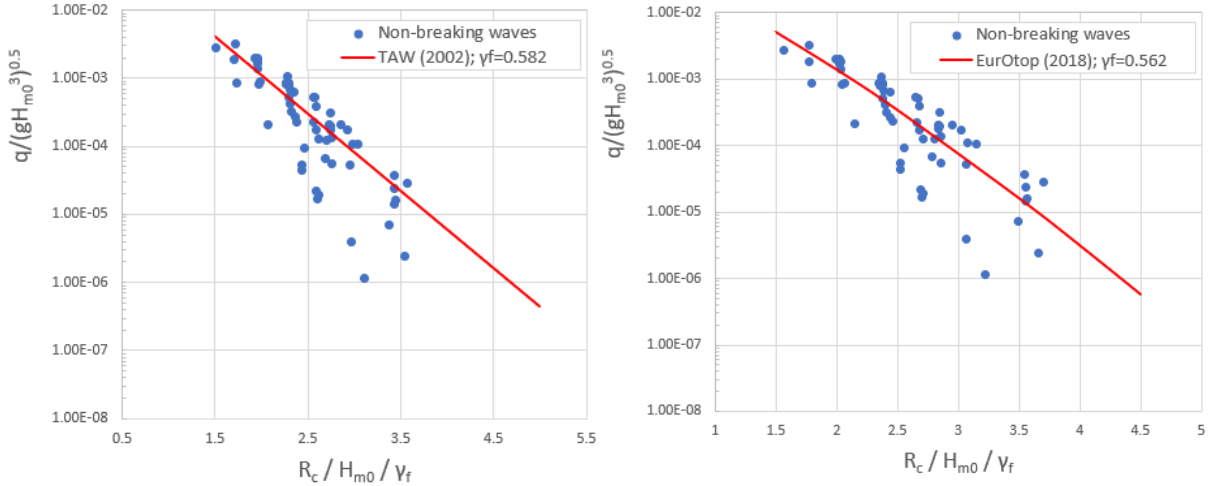

Figure 22 Measured wave overtopping discharges regarding non-breaking waves compared with TAW (2002) (left) and EurOtop (2018) (right) formulas with re-calibrated roughness factors.

To make quantitative comparisons between the measurements and the different guidelines and to compare the guidelines between themselves, the root-mean-squared-error-log (RMSLE) is used. The RMSLE is an error measure and can be defined as follows:

$$RMSLE = \sqrt{\frac{\sum_{i=1}^{n_{tests}} (\log(Q_{measured}) - \log(Q_{calculated}))^2}{n_{tests}}} \qquad \text{Equation 29}$$

Where: n_{tests} is the number of tests on which the RMSLE is based and $Q_{measured}$ and $Q_{calculated}$ are the non-dimensional values of the measured and calculated overtopping discharges, respectively ($Q = q/(gH_{m0}^3)^{0.5}$). It must be noted that in the following part of the data analysis the RMSLE is only based on the measured non-dimensional overtopping discharges larger than $Q_{measured} \geq 10^{-6}$. This is because smaller overtopping values are often less relevant as well as less reliable because of the presence of scale effects for small overtopping values.

The RMSLE is a variation of the root-mean-squared-error (RMSE). The advantage of the RMSLE compared to the RMSE is that the RMSLE handles relative errors better than the RMSE for datasets with a large range of values. The RMSE gives equal weight to all errors and is therefore more sensitive to outliers. RMSLE is considered to be more robust to the presence of outliers.

A lower value of the RMSLE implies a better fit between the described formula and measurements. In Table 2 the RMSLE values for non-breaking wave loading regarding the TAW (2002) and EurOtop (2018) formula are given, both with the standard tabulated values for the roughness factor as given in the guidelines and the optimized roughness factors which result in zero bias.

The TAW (2002) formula, for the standard tabulated roughness factor, is a better fit to the measurements than the EurOtop (2018) formula, which can also be seen in Figure 21. The TAW (2002) formula has a lower RMSLE and also the bias is closer to zero. Using the optimized roughness factors for both formulas for zero bias results in a slight increase of the RMSLE value for the TAW (2002) formula, while this decreases the RMSLE for the EurOtop (2018) formula by a large amount.

In this case it seems that the EurOtop (2018) expression with a roughness factor of γ_f = 0.562 is the best fit to the measurements, since it has a relatively low RMSLE compared to the other formulas and is unbiased. However, the RMSLE is still a significant value. This might be explained by the fact that both formulas are mainly designed for impermeable sea dikes, rather than permeable breakwaters, and therefore, the applicability of these formulas for rubble mound breakwaters is uncertain. Also, both formulas do not include a factor for the slope angle of the breakwater and a factor for the wave steepness, while they definitely have an influence on the wave overtopping discharge as was concluded in section 4.1. The measured overtopping discharges against the calculated overtopping discharges with both formulas and the various roughness factors can be seen in Figure 23.

Table 2 RMSLE (for Qmeasured >10-6) and bias for overtopping discharges of tests described by the TAW (2002) and EurOtop (2018) formulas for various roughness factors.

	TAW (2002); γ_f = 0.55	TAW (2002); γ_f = 0.582	EurOtop (2018); γ_f = 0.40	EurOtop (2018); γ_f = 0.562
RMSLE	0.4494	0.4843	1.4854	0.4525
Bias	1.44E-04	-	4.88E-04	-

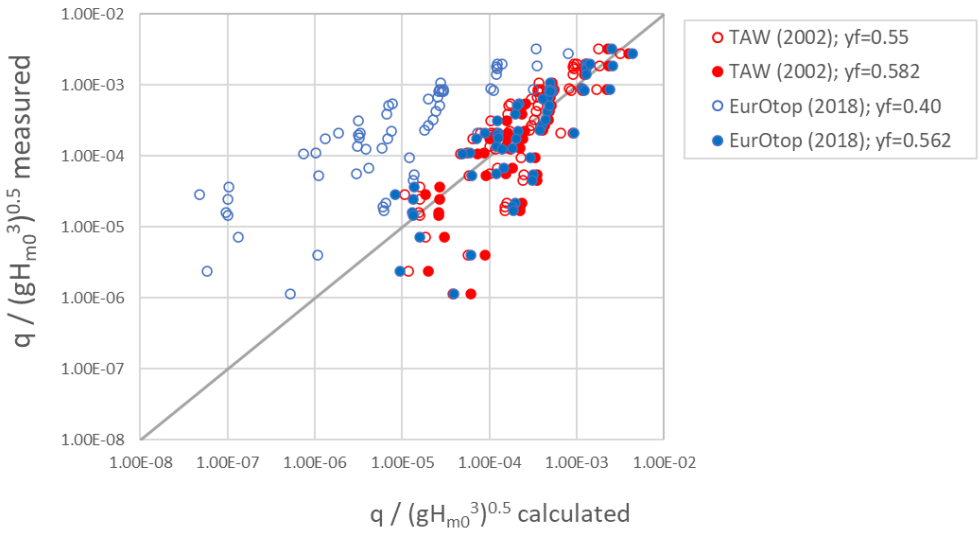

Figure 23 Measured wave overtopping discharges regarding breaking waves plotted against calculated overtopping discharges using TAW (2002) and EurOtop (2018) for various roughness factors.

In the formulas regarding non-breaking wave loading as proposed by Van Gent et al. (2022) and Irías Mata & Van Gent (2023), the steepness of the waves is taken into account which, as explained earlier qualitatively, has an influence on the wave overtopping discharge. In the formula proposed by Irías Mata & Van Gent (2023), also the slope angle of the rubble mound breakwater is taken into account. The formulas are repeated here as equation 30 and 31, respectively.

$$\frac{q}{\sqrt{g\,H_{mo}^3}} = 0.016\; s_{m-1,0}^{-1}\; exp\left[-\frac{2.4\;R_c}{\gamma_f\gamma_\beta\gamma_b\gamma_v\gamma_p H_{mo}}\right] \qquad \text{Equation 30}$$

$$\frac{q}{\sqrt{g\,H_{mo}^3}} = 0.03\; s_{m-1,0}^{-0.5}\; cot\alpha\; exp\left[-\frac{4\;R_c}{\gamma_f\gamma_\beta\gamma_b\gamma_v\gamma_p H_{mo}\xi_{m-1.0}^{0.5}}\right] \qquad \text{Equation 31}$$

With:

$$\gamma_f = 1 - 0.7\left(\frac{D_{n50}}{H_{mo}}\right)^{0.1}$$

The influence factors γ_β, γ_b, γ_v and γ_p are all set to 1. Figure 24 shows the measured wave overtopping discharges together with equation 30 and 31. Equation 31 appears to be a better fit to the measurements than equation 30, since the spread of the data around this equation is less, which indicates a more accurate prediction of the overtopping discharges by the formula. This is also supported by Table 3. The RMSLE for equation 31 is 0.4207, which is less than the RMSLE of 0.6003 for equation 30. The bias for equation 30 is 8.13E-05, indicating an underestimation of the wave overtopping discharges by the formula. The bias for equation 31 is -3.03E-05, indicating an overestimation.

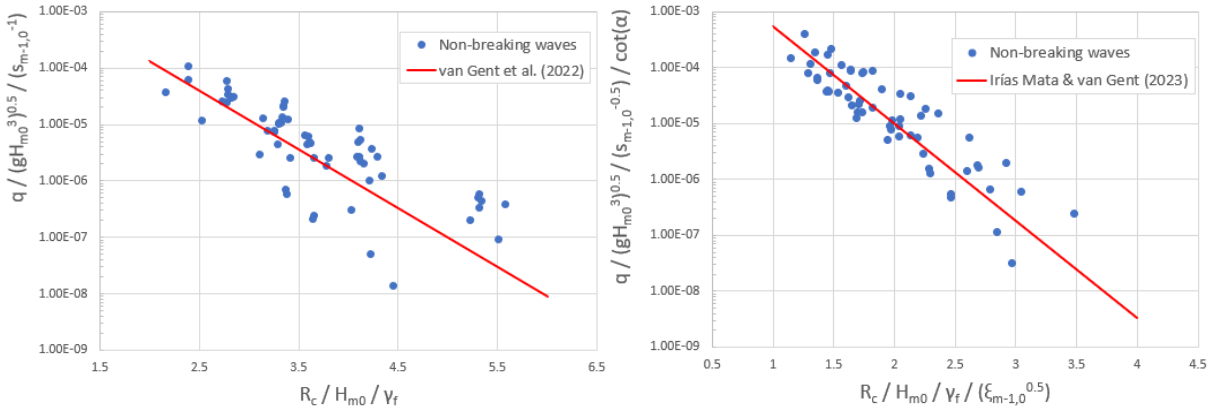

Figure 24 Measured wave overtopping discharges regarding non-breaking waves compared with Van Gent et al. (2022) (left) and Irías Mata & Van Gent (2023) (right).

It must be noted that the equation by Van Gent et al. (2022) is based only on physical model tests with a breakwater with a slope of 1:2. The RMSLE of this equation, when only the tests of the current test program with a slope of 1:2 are used for the computation, equals 0.4639, which is lower than the RMSLE when the whole test program (also tests with slope 1:1.5 and 1:4) is used. However, The RMSLE is still higher than the RMSLE of equation 31, which has a value of 0.4207.

One of the main differences between the two formulas is the inclusion of the slope angle of the breakwater in equation 31, directly in the formula as well as in the breaker parameter in the exponential part of the equation. This seems to improve the results of the formula, as was already expected qualitatively based on the measurements.

Next, the roughness factor is adjusted to get an optimal value which results in a bias as close to zero as possible. The roughness factor was depending on the ratio between the armour stone diameter D_{n50} and significant wave height H_{m0}. The factor 0.7 in this expression is adjusted to remove the bias from the formula. The optimal expression for the roughness factor for equation 30 becomes: $\gamma_f = 1 - 0.688 \left(\frac{D_{n50}}{H_{mo}}\right)^{0.1}$. Using this expression results in a RMSLE of 0.5645. The optimal expression for the roughness factor for equation 31 becomes: $\gamma_f = 1 - 0.705 \left(\frac{D_{n50}}{H_{mo}}\right)^{0.1}$. Using this expression results in a RMSLE of 0.4326.

However, it is found that for both equations the RMSLE is less when a constant optimized value of the roughness factor is used instead of the optimized expressions. The optimal constant value of the roughness factor is γ_f = 0.420 for equation 30 and γ_f = 0.406 for equation 31. Table 3 shows the RMSLE values for both formulas. The formulas with the optimized roughness factors can be seen together with the measurements in Figure 25.

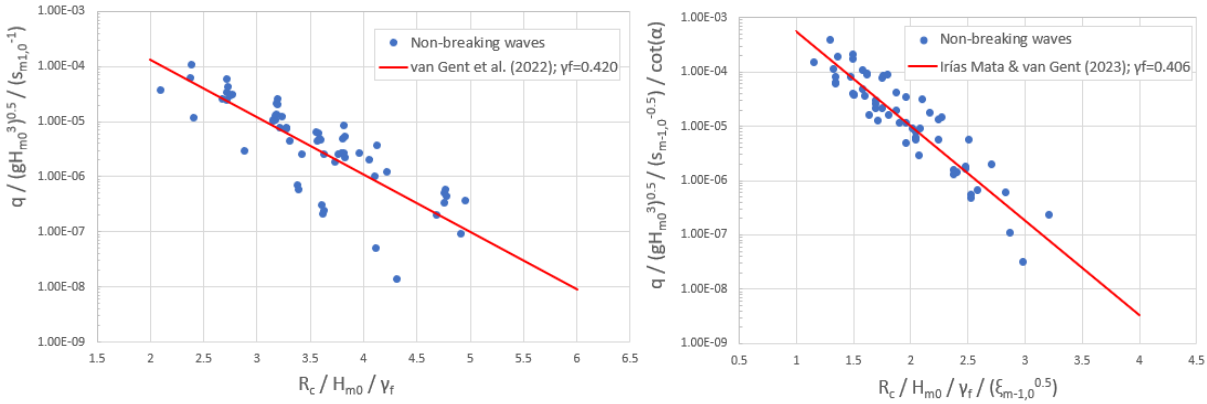

Figure 25 Measured wave overtopping discharges regarding non-breaking waves compared with Van Gent et al. (2022) (left) and Irías Mata & Van Gent (2023) (right).

According to Table 3, equation 31 is the best fit to the data when a constant value of the roughness factor of γ_f = 0.406 is applied. This expression has the lowest RMSLE. Therefore, it can be said that the re-calibrated formula by Irías Mata & Van Gent (2023) is more accurate in predicting the wave overtopping discharges of the current test program, based on the lowest RMSLE, compared to the re-calibrated formula by Van Gent et al. (2022). This is also illustrated in Figure 26, where it can be seen that the spread of the data around the line y=x is the lowest for the re-calibrated formula by Irías Mata & Van Gent (2023), thereby indicating a better fit to the measurements.

Table 3 RMSLE (for Qmeasured >10^{-6}) and bias for overtopping discharges of tests with non-breaking waves described by Van Gent et al. (2022) and Irías Mata & Van Gent (2023) for various roughness factors.

	Van Gent et al. (2022)	Van Gent et al. (2022); γ_f = 0.420	Irías Mata & Van Gent (2023)	Irías Mata & Van Gent (2023); γ_f = 0.406
RMSLE	0.6003	0.4934	0.4207	0.3466
Bias	8.13E-05	-	-3.03E-05	-

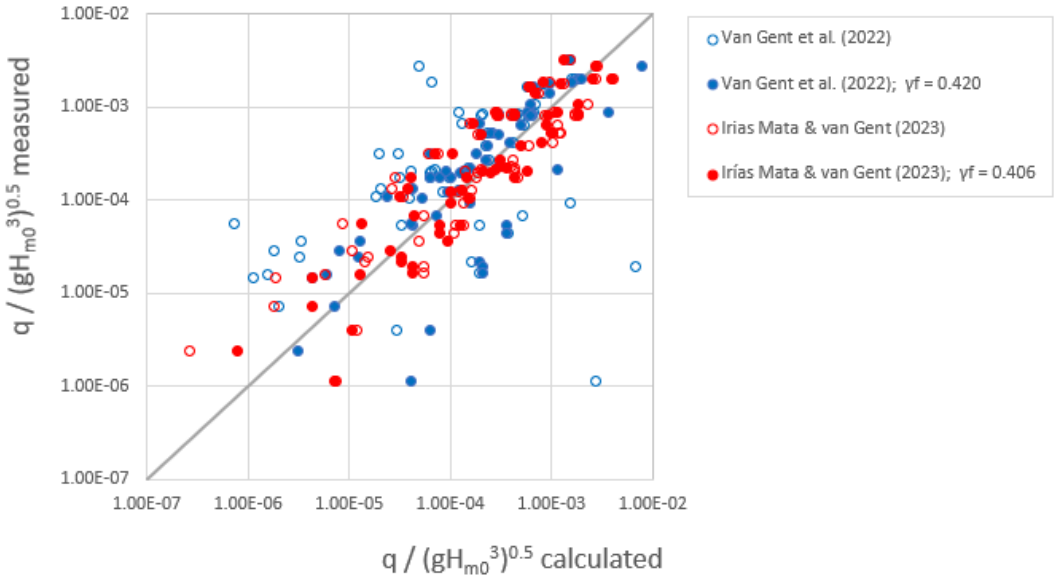

Figure 26 Measured wave overtopping discharges plotted against calculated overtopping discharges using Van Gent et al (2022) and Irías Mata & van Gent (2023) with various roughness factors.

The measured wave overtopping discharges against the calculated wave overtopping discharges for non-breaking waves with four different formulas, all four with the optimal re-calibrated roughness factors for zero bias, can be seen Figure 27. This figure shows that the largest deviations between measured and calculated wave overtopping discharges occur for the conditions with smaller wave overtopping discharges. It also illustrates that the best fit to the measured data is the formula as described in equation 31, by Irías Mata & Van Gent (2023), with a constant value of the roughness factor of γ_f = 0.406.

This equation has the lowest RMSLE and therefore it can be said that, regarding non-breaking waves, this equation is the most accurate in predicting wave overtopping discharges. In comparison with the EurOtop (2018) and TAW (2002) formulas, this expression includes the wave steepness and, in addition to Van Gent et al. (2022), also the slope angle of the breakwater is taken into account.

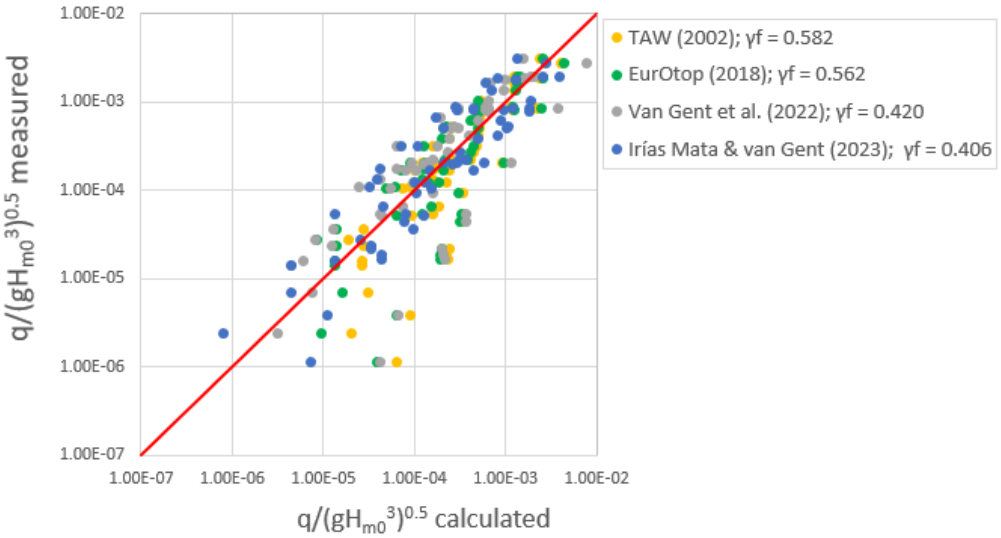

Figure 27 Measured wave overtopping discharges plotted against calculated overtopping discharges using different formulas with re-calibrated roughness factors.

4.2.2 Breaking waves

Regarding breaking waves, the measurements will be compared with two different guidelines. The formulas for the average wave overtopping discharge regarding breaking waves as presented in the EurOtop (2018) manual and TAW (2002) report are repeated here in equation 32 and 33, respectively. The main difference between these formulas and the formulas regarding non-breaking waves is the inclusion of the slope angle as tan(α) and the breaker parameter $\xi_{m-1,0}$, and with that also the wave steepness is included.

$$\frac{q}{\sqrt{g\,H_{mo}^3}} = \frac{0.023}{\sqrt{tan\alpha}}\gamma_b\,\xi_{m-1,0}\,exp\left[-\left(2.7\frac{R_c}{\xi_{m-1,0}H_{m0}\gamma_b\gamma_f\gamma_\beta\gamma_v}\right)^{1.3}\right] \qquad \text{Equation 32}$$

$$\frac{q}{\sqrt{g\,H_{mo}^3}} = \frac{0.067}{\sqrt{tan\alpha}}\gamma_b\,\xi_{m-1,0}\,exp\left[-4.75\frac{R_c}{\xi_{m-1,0}H_{m0}\gamma_b\gamma_f\gamma_\beta\gamma_v}\right] \qquad \text{Equation 33}$$

Figure 28 shows the measured wave overtopping discharges together with equation 32 and 33, with the standard tabulated values of the roughness factor of γ_f = 0.40 and γ_f = 0.55, as given in the guidelines, respectively. The influence factors γ_β, γ_b and γ_v are set to 1. From the figure it follows that the TAW (2002) formula overestimates the wave overtopping discharge by a relatively large amount. The EurOtop (2018) formula seems a better fit to the data. This is also supported by Table 4. The RMSLE for equation 32 is 0.4720, which is less than the RMSLE of 0.9655 for equation 33. The bias of equation 32 is 1.93E-04, indicating an underestimation of the wave overtopping discharges by the formula. The bias of equation 33 is -5.95E-04, indicating an overestimation.

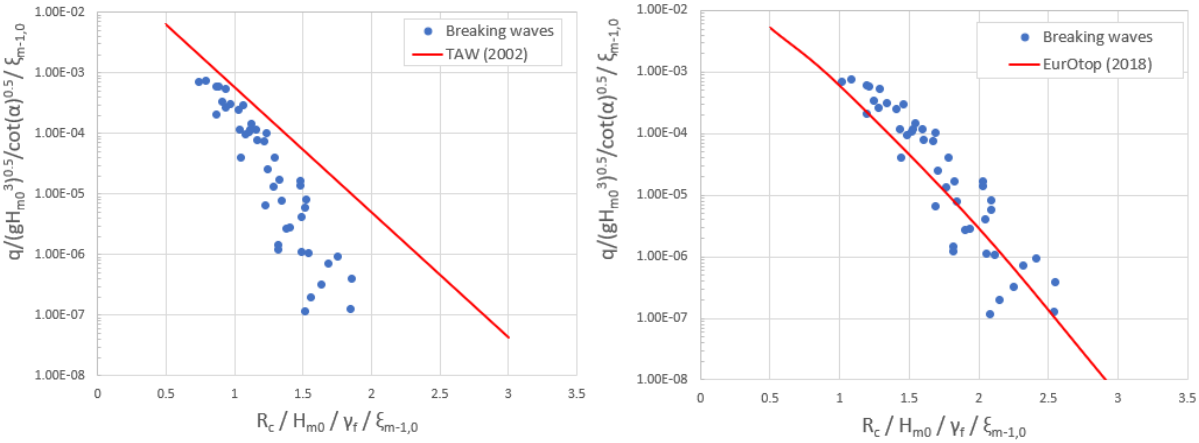

Figure 28 Measured wave overtopping discharges regarding breaking waves compared with the TAW (2002) (left) and EurOtop (2018) (right) formulas.

Next, the roughness factors are adjusted to an optimal value which results in a bias as close to zero as possible. For the TAW (2002) formula the bias becomes zero when a roughness factor of γ_f = 0.454 is applied. For the EurOtop (2018) formula the bias becomes zero when a roughness factor of γ_f = 0.453 is applied. Both expressions, with the optimal roughness factors for zero bias, can be seen together with the measurements in Figure 29.

From Figure 29 it follows that the EurOtop (2018) formula seems a better fit to the measurements due to the curvature of the line. This can also be concluded based on the values of the RMSLE. The RMSLE for the EurOtop formula, with a re-calibrated value of the roughness factor, is 0.4653, which is lower than the RMSLE of 0.5298 for the TAW (2002) formula, as can be seen in Table 4. However, the RMSLE is still relatively large. This might be explained by the fact that, just as was the case for non-breaking waves, both formulas are mainly designed for wave overtopping at impermeable sea dikes, rather than permeable breakwaters, and therefore the applicability of these formulas for rubble mound breakwaters is uncertain.

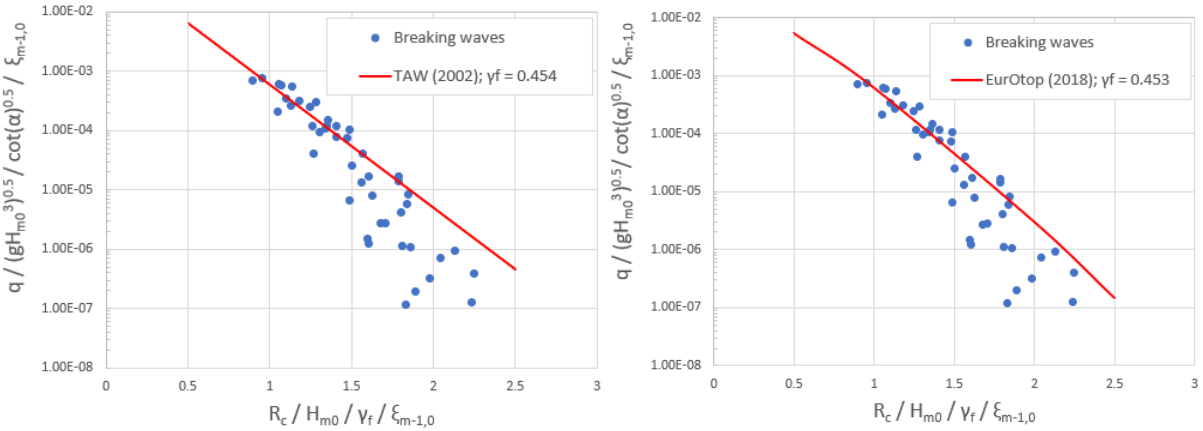

Figure 29 Measured wave overtopping discharges regarding breaking waves compared with the TAW (2002) (left) and EurOtop (2018) (right) formulas.

Table 4 RMSLE (for Qmeasured >10-6) and bias for overtopping discharges of tests described by TAW (2002) and EurOtop (2018) for various roughness factors.

	TAW (2002); γ_f = 0.55	TAW (2002); γ_f = 0.454	EurOtop (2018); γ_f = 0.40	EurOtop (2018); γ_f = 0.453
RMSLE	0.9655	0.5298	0.4720	0.4653
Bias	-5.95E-04	-	1.93E-04	-

The measured overtopping discharges regarding breaking waves plotted against the calculated discharges, computed by the TAW (2002) and EurOtop (2018) formulas, with various values of the roughness factor, can be seen in Figure 30. It is shown that for low overtopping discharges, the largest deviations between measured and calculated overtopping discharges occur. The TAW (2002) formula overestimates the overtopping discharges for these conditions. Meanwhile the EurOtop (2018) formula shows quite a consistent deviation for all overtopping discharges.

Figure 30 also illustrates that the best fit to the measured data is the formula as described in equation 32, with recalibrated value of the roughness factor of γ_f = 0.453. This equation has the lowest RMSLE and therefore it can be said that, regarding breaking waves, this equation is the most accurate in predicting wave overtopping discharges. Both the slope angle and the wave steepness are included in this equation.

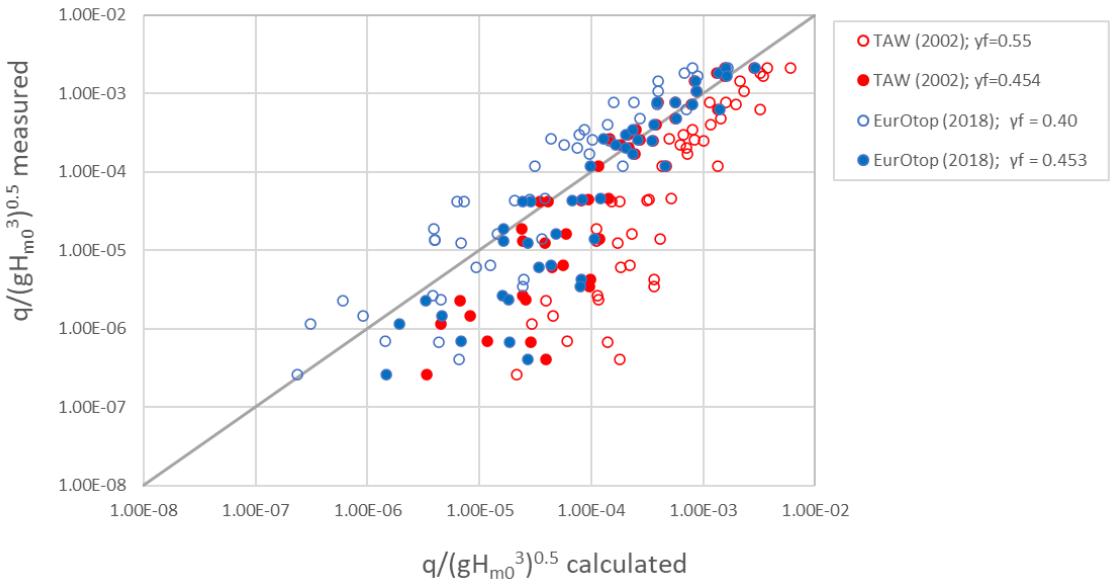

Figure 30 Measured wave overtopping discharges plotted against calculated overtopping discharges using different equations with re-calibrated roughness coefficients.

4.2.3 Conclusion

As a conclusion to whether the formulas in the guidelines fit the measurements a small resume is shown in Table 5 and Table 6. For non-breaking wave loading, equation 31 by Irías Mata & Van Gent (2023), with a re-calibrated value of the roughness factor of γ_f = 0.406, is the best fit to the measurements based on the lowest RMSLE. For breaking wave loading, equation 32 by the EurOtop (2018) manual, with a re-calibrated value of the roughness factor of γ_f = 0.453, is the best fit to the measurements based on the lowest RMSLE. These expressions are the most accurate in predicting the wave overtopping discharges from the current test program for non-breaking and breaking waves, respectively.

Table 5 RMSLE (for Qmeasured >10^{-6}) and bias for overtopping discharges of tests with non-breaking wave loading described by various formulas and roughness factors.

	RMSLE	Bias
TAW (2002); γ_f = 0.55	0.4494	1.44E-04
TAW (2002); γ_f = 0.582	0.4843	-
EurOtop (2018); γ_f = 0.40	1.4854	4.88E-04
EurOtop (2018); γ_f = 0.562	0.4525	-
Van Gent et al. (2022)	0.6003	8.13E-05
Van Gent et al. (2022); γ_f = 0.420	0.4934	-
Irías Mata & Van Gent (2023)	0.4207	-3.03E-05
Irías Mata & Van Gent (2023); γ_f = 0.406	0.3466	-

Table 6 RMSLE (for Qmeasured >10^{-6}) and bias for overtopping discharges of tests with breaking wave loading described by various formulas and roughness factors.

	RMSLE	Bias
TAW (2002); γ_f = 0.55	0.9655	-5.95E-04
TAW (2002); γ_f = 0.454	0.5298	-
EurOtop (2018); γ_f = 0.40	0.4720	1.93E-04
EurOtop (2018); γ_f = 0.453	0.4653	-

The wave overtopping discharges of all tests (breaking and non-breaking waves) are combined in Figure 32, and are compared to equation 31 for non-breaking waves and 32 for breaking waves, both with a re-calibrated value of the roughness factor. The comparison shows that the derived expressions describe the measured discharges reasonably. Most measurements differ no more than a factor 10 from the calculated overtopping discharges, except for a few outliers.

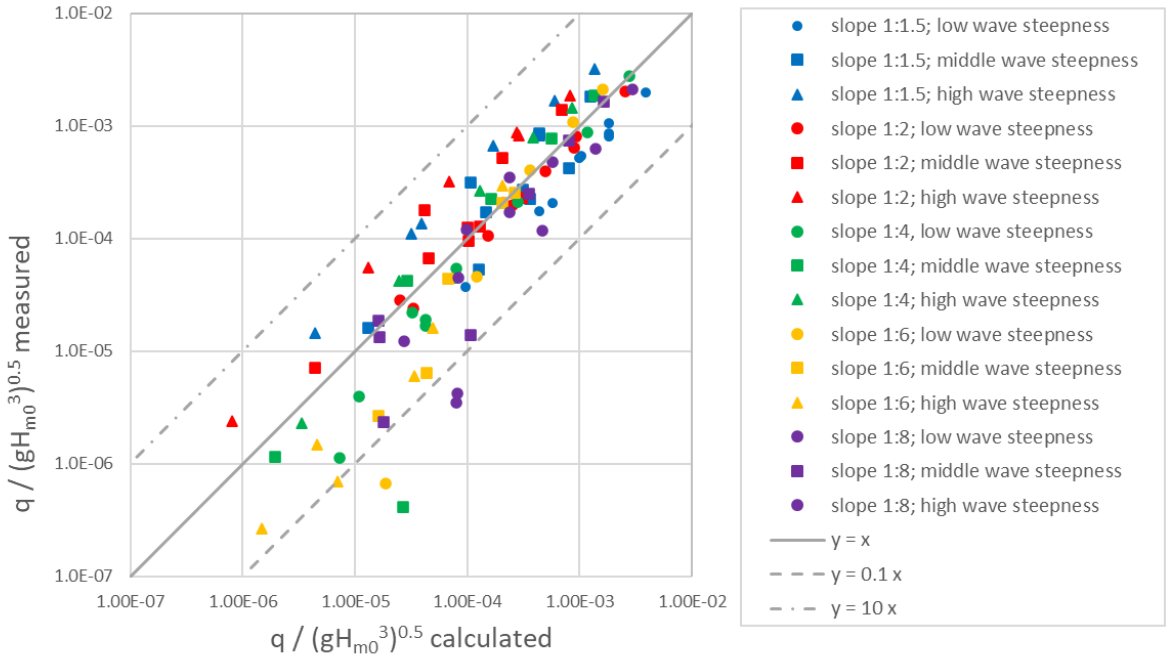

Figure 31 Measured wave overtopping discharges regarding breaking and non-breaking waves plotted against calculated overtopping discharges using equation 31 for non-breaking waves and 32 for breaking waves, with re-calibrated roughness coefficients.

4.3 Modified overtopping formula

4.3.1 Non-breaking waves

Regarding non-breaking wave loading, equation 31 by Irías Mata & Van Gent (2023) with a constant roughness factor of γ_f = 0.406 appears to give the best results in predicting wave overtopping discharges based on the lowest RMSLE. This equation already considers the wave steepness and slope angle and therefore, this formula is taken as a starting point. In Figure 32, this formula can be seen together with the measured overtopping discharges regarding non-breaking waves, with a distinction in slope angle and wave steepness.

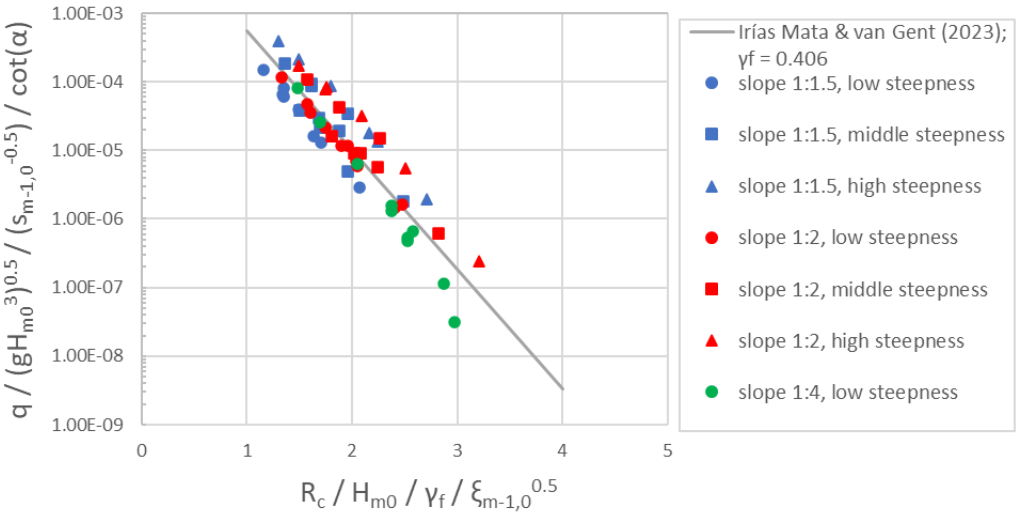

Figure 32 Measured wave overtopping discharges regarding non-breaking waves compared with the formula by Irías Mata & Van Gent (2023) with constant roughness factor of γ_f=0.406.

Optically, in general, it seems that for low wave steepnesses, the formula slightly overestimates the wave overtopping discharge, regardless of the slope angle. On the other hand, for middle and high steepnesses, the formula slightly underestimates the wave overtopping discharge. This can also be concluded based on Table 7. For a low wave steepness the bias is a relatively large negative value, which indicates an overestimation of wave overtopping discharges by the formula. For the middle and especially the high wave steepness conditions, the bias is a relatively large positive value, thereby indicating an underestimation of the overtopping discharges by the formula for these conditions. In Figure 33, the measured overtopping discharges can be seen together with the discharges as computed with equation 31. The scatter of the data around the line y=x in Figure 33 figure shows quite a consistent deviation.

Regarding the slope angle, it appears that the formula slightly overestimates the wave overtopping discharge for more gentle slopes, especially for the breakwater configuration with a slope of 1:4. However, since for this configuration only tests with a low wave steepness classify as non-breaking wave loading, it is yet unknown whether this is due to the influence of the slope angle or is a result of the low wave steepness. From Table 8 it follows that also for overtopping discharges of tests with a slope of 1:1.5 an overestimation of overtopping discharges is present, since for this slope the bias is a negative value of -6.90E-05.

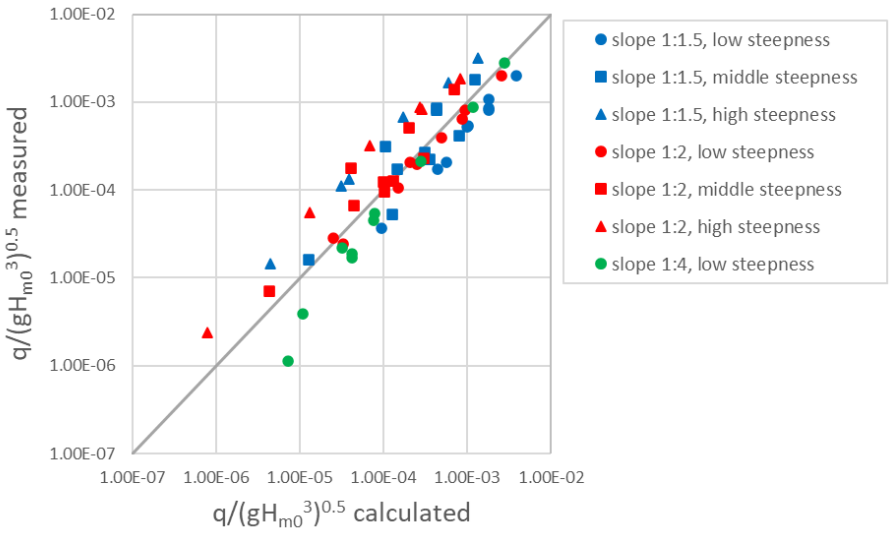

Figure 33 Measured wave overtopping discharges plotted against calculated overtopping discharges using the equation by Irías Mata & Van Gent (2023) with constant roughness factor of γ_f=0.406.

Table 7 RMSLE (for Qmeasured >10-6) and bias for overtopping discharges of tests described by equation 31 for varying wave steepness.

	Equation 31; γ_f = 0.406 all wave conditions	Equation 31; γ_f = 0.406 low wave steepness	Equation 31; γ_f = 0.406 middle wave steepness	Equation 31; γ_f = 0.406 high wave steepness
RMSLE	0.3466	0.2947	0.2762	0.5170
Bias	-	-2.84E-04	1.09E-04	5.08E-04

Table 8 RMSLE (for Qmeasured >10^{-6}) and bias for overtopping discharges of tests described by equation 31 for varying slope angle.

	Equation 31; γ_f = 0.406 all slopes	Equation 31; γ_f = 0.406 slope 1:1.5	Equation 31; γ_f = 0.406 slope 1:2	Equation 31; γ_f = 0.406 slope 1:4
RMSLE	0.3466	0.3640	0.3233	0.3560
Bias	-	-6.90E-05	1.01E-04	-5.05E-05

As was concluded earlier in section 4.1.1.2, for non-breaking waves the wave steepness plays a relevant role for wave overtopping at rubble mound breakwaters. It was concluded that, in general, for the same dimensionless crest freeboard, the lower the wave steepness, the higher the wave overtopping discharge, independent of the slope angle of the breakwater. In equation 31, this dependency is incorporated in the formula directly, by the factor $s_{m-1,0}^{-0.5}$, as well as in the breaker parameter $\xi_{m-1.0}^{0.5}$ in the exponential part of the equation. However, this dependency seems abundantly present, since the formula gives an overestimation of the wave overtopping discharge for low wave steepness conditions and an underestimation for high wave steepness conditions.

Therefore, to improve the accuracy of predictions of overtopping discharges by the formula, a factor is included that compensates for the abundantly present dependency of the wave steepness. This factor, $350s_{m-1,0}$, which is found empirically, also includes the wave steepness, but in this case with a positive exponent. By physical reasoning this does not make sense since a higher wave steepness should result in a lower wave overtopping discharge, which is not represented by this factor. However, this factor is a correction for the abundantly presence of the wave steepness dependency by the Iribarren number in the exponential part of the equation. The modified formula for non-breaking waves can be seen in equation 34.

$$\frac{q}{\sqrt{g\,H_{mo}^3}} = 10.5\,s_{m-1,0}\,cot\alpha\,exp\left[-\frac{4\,R_c}{\gamma_f\gamma_\beta\gamma_b\gamma_v\gamma_p H_{mo}\xi_{m-1.0}^{0.5}}\right] \qquad \text{Equation 34}$$

In Figure 34, this formula is shown together with the measurements for non-breaking waves. Comparing Figure 32 and Figure 34, it can be seen that the scatter of the data around the equation is less in Figure 34. This can also be concluded based on the RMSLE, which is shown in Table 9. The RMSLE for overtopping discharges of tests computed by equation 34 equals 0.1763, which is almost half of the RMSLE of equation 31, which has a value of 0.3466. Therefore, it can be said that equation 34 has a higher accuracy in predicting wave overtopping discharges for non-breaking waves from the present test program than equation 31.

Also, when a distinction is made in wave steepness, equation 34 gives better results than equation 31, as can be seen in Table 9. For every wave steepness, the absolute value of the bias for overtopping discharges of tests computed by equation 34 is closer to zero than computed by equation 31. There is no large overestimation of the overtopping discharge for low wave steepnesses anymore, and also the underestimation of the overtopping discharge for middle and low wave steepnesses becomes less.

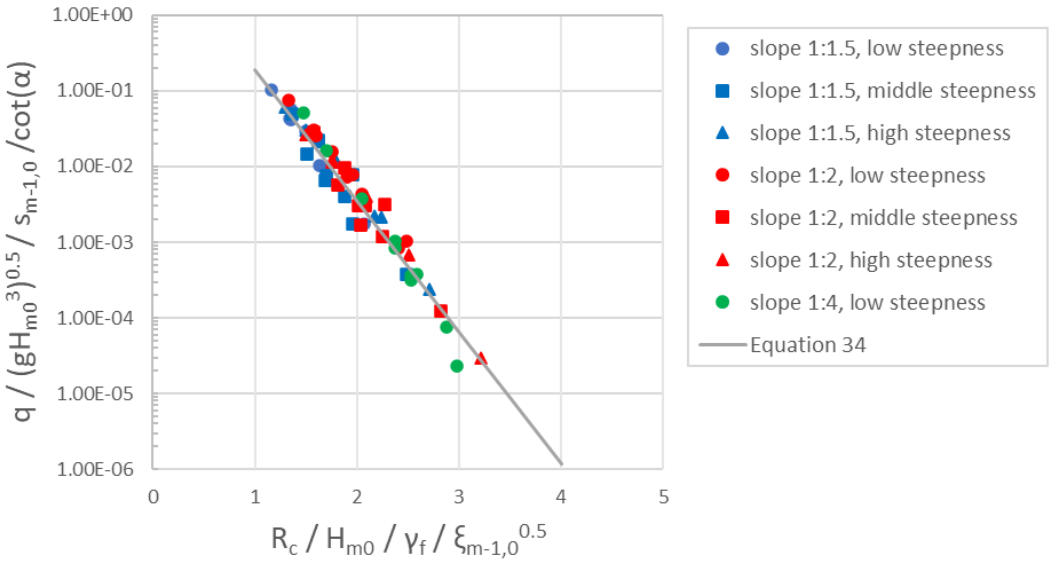

Figure 34 Measured wave overtopping discharges regarding non-breaking waves compared with equation 34.

Table 9 RMSLE (for Qmeasured >10-6) and bias for overtopping discharges of tests described by equation 34 for varying wave steepness.

	Equation 34; γ_f = 0.406 all wave steepnesses	Equation 34; γ_f = 0.406 low wave steepness	Equation 34; γ_f = 0.406 middle wave steepness	Equation 34; γ_f = 0.406 high wave steepness
RMSLE	0.1763	0.1725	0.2066	0.1260
Bias	7.69E-05	1.01E-04	2.56E-05	1.01E-04

As was shown earlier, in general, a more gentle slope (a higher cot(α)) leads to a lower wave overtopping discharge for the same dimensionless crest freeboard. This is contradictory to what might be expected from equation 31 and 34, where a higher cot(α) leads to a higher wave overtopping discharge at first sight, when the breaker parameter is ignored.

But of course, the slope angle is also present in the breaker parameter in the exponential part of the equation. A steeper slope leads to a higher breaker parameter, which results in a higher wave overtopping discharge for the same dimensionless crest freeboard. However, it seems that this dependency of the wave overtopping discharge on the slope angle is abundantly present in the exponential part of the equation. Therefore, it appears that the factor cot(α) in the expression is also some kind of compensation for an over- or underestimation of the wave overtopping discharge.

This can also be seen when the factor cot(α) is removed from the formula, which results in equation 35. In Table 10 it is shown that the bias for overtopping discharges of tests computed by equation 35 is a significant positive value for every slope angle. Therefore, it can be said that this formula underestimates the wave overtopping discharge, for every slope angle.

$$\frac{q}{\sqrt{g\,H_{mo}^3}} = 10.5\; s_{m-1,0}\;\; exp\left[-\frac{4\,R_c}{\gamma_f\gamma_\beta\gamma_b\gamma_v\gamma_p H_{mo}\xi_{m-1.0}^{0.5}}\right] \qquad \text{Equation 35}$$

Table 10 RMSLE (for Qmeasured >10^{-6}) and bias for overtopping discharges of tests described by equation 35 for varying slope angle.

	Equation 35; γ_f = 0.406 all slopes	Equation 35; γ_f = 0.406 slope 1:1.5	Equation 35; γ_f = 0.406 slope 1:2	Equation 35; γ_f = 0.406 slope 1:4
RMSLE	0.4047	0.2187	0.4398	0.6187
Bias	2.74E-04	2.38E-04	2.85E-04	3.38E-04

Table 11 shows the RMSLE and bias of equation 34 with a distinction between the different slope angles of the breakwater. Compared to equation 35, where the slope angle is not included directly in the formula by the factor cot(α), the absolute value of the bias for overtopping discharges of tests computed by equation 34 is closer to zero

for all slope angles. Therefore, it can be concluded that the factor cot(α) in equation 34 is a compensation for an underestimation of the wave overtopping discharge by the rest of the formula. Furthermore, the RMSLE of equation 34 is more than two times as low as the RMSLE of equation 35. Therefore, it can be said that equation 34 has a higher accuracy in predicting wave overtopping discharges for non-breaking waves than equation 35.

Table 11 RMSLE (for Qmeasured >10-6) and bias for overtopping discharges of tests described by equation 34 for varying slope angle.

	Equation 34; γ_f = 0.406 all slopes	Equation 34; γ_f = 0.406 slope 1:1.5	Equation 34; γ_f = 0.406 slope 1:2	Equation 34; γ_f = 0.406 slope 1:4
RMSLE	0.1763	0.1595	0.1836	0.1974
Bias	7.69E-05	1.80E-05	1.08E-04	1.49E-04

Furthermore, it was found that an increase of the power of the factor cot(α) in equation 34, from 1 to 1.1, further improves the accuracy of the predictions by the formula. This modification can be seen in equation 36. An increase of the power reduces the RMSLE to a value of 0.1734, as well as reduces the absolute value of the bias for every slope angle of the breakwater, which is shown in Table 12.

$$\frac{q}{\sqrt{g\,H_{mo}^3}} = 10.5\; s_{m-1,0}\; cot\alpha^{1.1}\; exp\left[-\frac{4\,R_c}{\gamma_f\gamma_\beta\gamma_b\gamma_v\gamma_p H_{mo}\xi_{m-1,0}^{0.5}}\right] \qquad \text{Equation 36}$$

Table 12 RMSLE (for Qmeasured >10-6) and bias for overtopping discharges of tests described by equation 36 for varying slope angle.

	Equation 36; γ_f = 0.406 all slopes	Equation 36; γ_f = 0.406 slope 1:1.5	Equation 36; γ_f = 0.406 slope 1:2	Equation 36; γ_f = 0.406 slope 1:4
RMSLE	0.1734	0.1631	0.1665	0.2108
Bias	4.87E-05	-9.30E-06	8.28E-05	1.12E-04

Next, the coefficients of equation 36 are re-calibrated to remove the bias of the formula. This results in the following formula for the dimensionless wave overtopping discharge at rubble mound breakwaters, with wave loading that can be characterized as non-breaking waves:

$$\frac{q}{\sqrt{g\,H_{mo}^3}} = 13.4\; s_{m-1,0}\; cot\alpha^{1.1}\; exp\left[-\frac{4.1\,R_c}{\gamma_f\gamma_\beta\gamma_b\gamma_v\gamma_p H_{mo}\xi_{m-1,0}^{0.5}}\right] \qquad \text{Equation 37}$$

The RMSLE for overtopping discharges of tests computed by this expression is 0.1722. In Figure 35, it can be seen that equation 37 is a rather good fit to the data, since the spread of the measurements around the equation is low. Figure 36 illustrates the measured against the calculated overtopping discharges computed by equation 31,

which was the starting point of this analysis, and the modified equation 37. The spread of data around the line y=x is much lower for equation 37 compared to equation 31. Furthermore, the RMSLE is more than two times as low, as is shown in Table 13. Therefore, it can be concluded that equation 37 is more accurate in predicting wave overtopping discharges than equation 31 for non-breaking waves.

Table 13 RMSLE (for Qmeasured >10-6) for overtopping discharges of tests described by equations 31 and 37.

	Equation 31	Equation 37
RMSLE	0.3466	0.1722

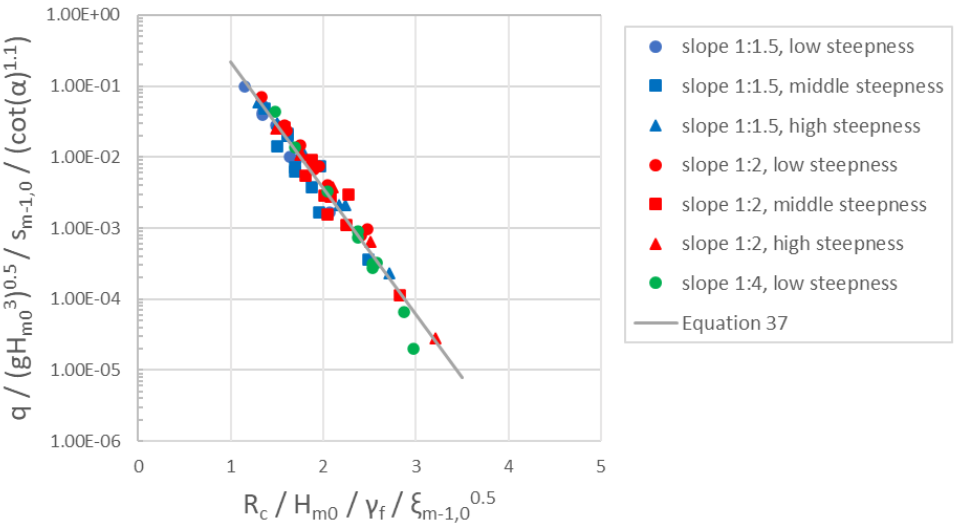

Figure 35 Measured wave overtopping discharges regarding non-breaking waves compared with equation 37.

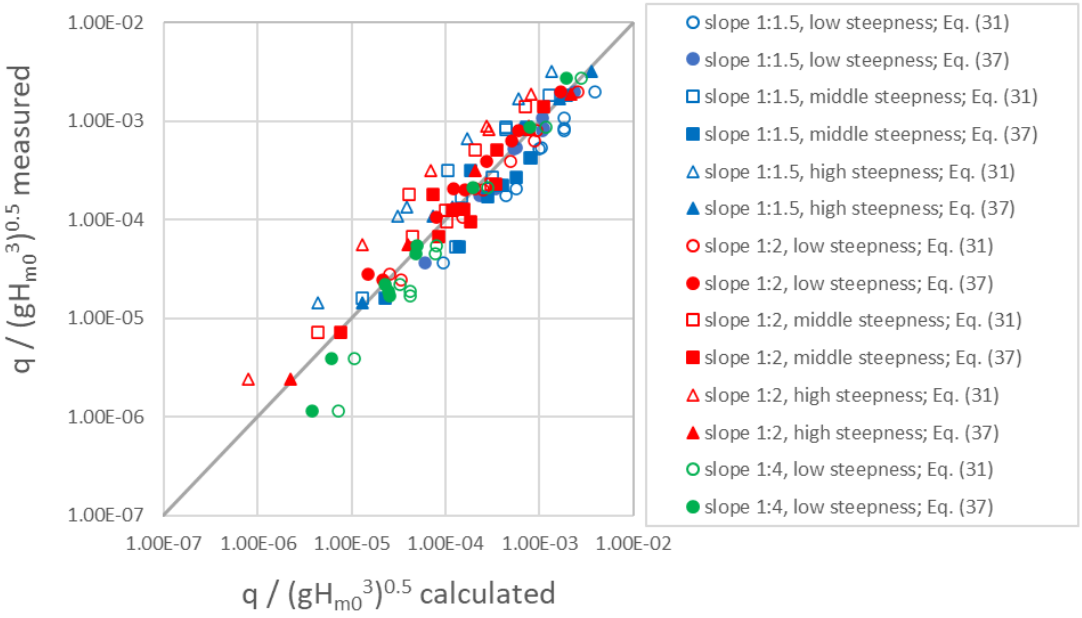

Figure 36 Measured wave overtopping discharges plotted against calculated overtopping discharges using equations 31 and 37.

4.3.2 Breaking waves

The wave overtopping discharge at rubble mound breakwaters with wave loading that can be characterized as breaking wave loading is best described by a recalibrated version of the breaking waves formula in the EurOtop (2018) manual. Using a roughness factor of γ_f = 0.453 appears to give the best results in predicting wave overtopping discharges based on the lowest RMSLE, as can be seen in Table 6. This formula, as shown in equation 32, was the best fit to the data and, therefore, will be taken as a starting point in this analysis. In Figure 37, this formula can be seen together with the measured overtopping discharges for breaking waves. Figure 38 illustrates the measured wave overtopping discharges plotted against calculated overtopping discharges using the EurOtop (2018) formula.

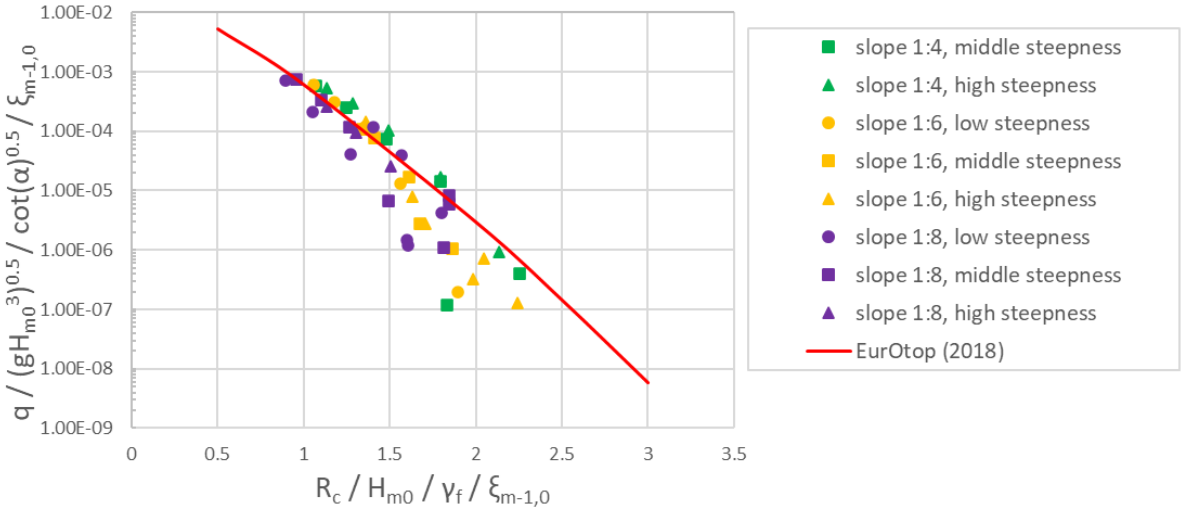

Figure 37 Measured wave overtopping discharges regarding breaking waves compared with the EurOtop (2018) formula with roughness factor of γ_f=0.453.

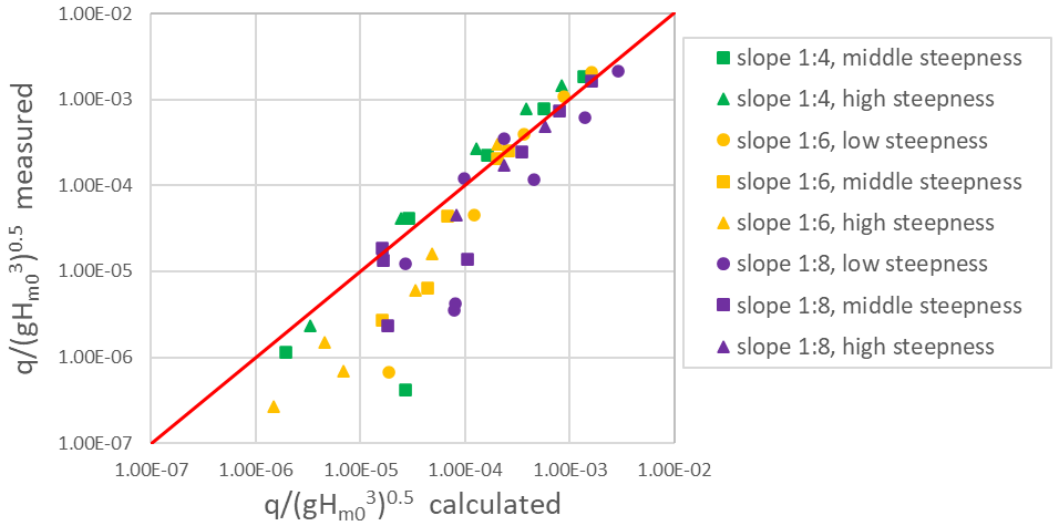

Figure 38 Measured wave overtopping discharges plotted against calculated overtopping discharges using the EurOtop (2018) formula with roughness factor of γ_f=0.453.

Following from Figure 37 and Figure 38, it seems that the formula fits the data well for higher wave overtopping discharges. For lower overtopping discharges, the formula overestimates the overtopping discharge significantly. It appears that the formula is a better fit for middle and high steepnesses than for low wave steepnesses since, in general, for low wave steepnesses, the formula overestimates the wave overtopping discharge. This can also be seen in Table 14. The expression is the best fit to the data for higher wave steepnesses, as it presents the lowest RMSLE. Again it is noted that the RMSLE is only based on the measured non-dimensional overtopping discharges larger than Qmeasured ≥ 10^{-6}.

For low wave steepnesses, the bias for overtopping discharges of tests described by equation 32 is a significant negative value, indicating an overestimation of the wave overtopping discharge by the expression. For middle and high wave steepnesses, the bias is a positive value, thereby indicating an underestimation of wave overtopping discharges.

Table 14 RMSLE (for Qmeasured >10-6) and bias for overtopping discharges of tests described by equation 32 for varying wave steepness.

	Equation 32; γ_f = 0.453 all wave steepnesses	Equation 32; γ_f = 0.453 low wave steepnesses	Equation 32; γ_f = 0.453 middle wave steepnesses	Equation 32; γ_f = 0.453 high wave steepnesses
RMSLE	0.4653	0.6002	0.4247	0.3521
Bias	-	-1.03E-04	2.21E-05	6.95E-05

Also, from Figure 37 and Figure 38, it appears that the formula is a better fit for steeper slopes of the breakwater, since the spread of the data around the equation is less for the measurements with a slope of 1:4 compared to those with a slope of 1:6 or 1:8. This can also be concluded based on Table 15. The RMSLE is considerably lower for calculations with a slope of 1:4 compared to a slope of 1:6 and 1:8. However, the bias is quite large for calculations with slope 1:4, indicating an underestimation of the wave overtopping discharge by the formula. The bias for overtopping discharges of tests described by equation 32 with a slope of 1:8 is a significant negative value, indicating an overestimation of the overtopping discharge.

Table 15 RMSLE (for Qmeasured >10-6) and bias for overtopping discharges of tests described by equation 32 for varying slope angle.

	Equation 32; γ_f = 0.453 all slopes	Equation 32; γ_f = 0.453 slope 1:4	Equation 32; γ_f = 0.453 slope 1:6	Equation 32; γ_f = 0.453 slope 1:8
RMSLE	0.4653	0.2129	0.4469	0.5690
Bias	-	1.71E-04	3.62E-05	-1.35E-04

To get more insight into the influence of the individual parameters of equation 32, the breaker parameter $\xi_{m-1,0}$ is deconstructed in the slope angle and wave steepness. The rewritten expression can be seen in equation 38.

$$\frac{q}{\sqrt{g\,H_{mo}^3}} = 0.023\ \ cot\alpha\ \ ^{-0.5}\ s_{m-1,0}^{-0.5}\ \ \gamma_b\ \ exp\left[-\left(2.7\frac{R_c}{\xi_{m-1,0}H_{m0}\gamma_b\gamma_f\gamma_\beta\gamma_v}\right)^{1.3}\right] \qquad \text{Equation 38}$$

The parameters in equation 38 outside the exponential part of the equation, $\cot\alpha\ ^{-0.5}$ and $s_{m-1,0}^{-0.5}$, make sense based on physical reasoning. As was shown earlier, for breaking waves, it followed that the more gentle the slope, the smaller the factor $\cot\alpha\ ^{-0.5}$ and the lower the wave overtopping discharge for the same dimensionless crest freeboard. Also, it was shown earlier that the higher the wave steepness, the lower the wave overtopping discharge. This is in accordance with the presence of $s_{m-1,0}^{-0.5}$ in the equation.

Equation 38 is adjusted empirically to obtain an expression which is the best fit to the measurements for breaking waves, based on the lowest RMSLE. This results in equation 39. The optimal powers of the slope angle cot(α) and the wave steepness $s_{m-1,0}$, are different compared to equation 38 (i.e. powers -0.5 and -0.5 in Eq. 38 and -1.8 and -1 in Eq. 39).

$$\frac{q}{\sqrt{g\,H_{mo}^3}} = 0.023\ \ cot\alpha\ \ ^{-1.8}\ s_{m-1,0}^{-1}\ \ \gamma_b\ \ exp\left[-\left(2.7\frac{R_c}{\xi_{m-1,0}H_{m0}\gamma_b\gamma_f\gamma_\beta\gamma_v}\right)^{1.3}\right] \qquad \text{Equation 39}$$

The corresponding RMSLE value of equation 39 is 0.3840, which is less than the RMSLE of equation 32, which has a value of 0.4653. The bias of equation 39 is 1.26E-04. From Table 16, it can be concluded that changing the power of cot(α) in equation 39 significantly improves the accuracy of the predictions of the wave overtopping discharges, especially for the more gentle slopes 1:6 and 1:8. Compared to equation 32, the RMSLE for overtopping discharges of tests described by equation 39 reduces from 0.4469 to 0.3335 for 1:6 slopes and from 0.5690 to 0.4723 for 1:8 slopes. For 1:4 slopes the RMSLE slightly increases from 0.2129 to 0.2418. It must be noted that, although equation 39 shows a lower RMSLE compared to equation 32, the absolute value of the bias has increased, mainly for tests with a slope of 1:6. Both spreading (RMSLE) and systematic differences (bias) are important factors to consider which formula is preferred for calculating wave overtopping discharges. It should be noted that the power of cot(α) is differed to achieve the lowest RMSLE for overtopping discharges of tests computed by equation 39.

Table 16 RMSLE (for Qmeasured >10-6) and bias for overtopping discharges of tests described by equation 39 for varying slope angle.

	Equation 39; γ_f = 0.453 all slopes	Equation 39; γ_f = 0.453 slope 1:4	Equation 39; γ_f = 0.453 slope 1:6	Equation 39; γ_f = 0.453 slope 1:8
RMSLE	0.3840	0.2418	0.3335	0.4723
Bias	1.26E-04	1.80E-04	9.35E-05	1.23E-04

Changing the power of $s_{m-1,0}$ also improves the accuracy of the predictions of wave overtopping discharges for every wave steepness as can be seen in Table 17. Compared to equation 32, the RMSLE for overtopping discharges of tests described by equation 39 reduces from 0.6002 to 0.4879 for low wave steepnesses, from 0.4247 to 0.3366 for middle wave steepnesses and from 0.3521 to 0.3246 for high wave steepnesses.

However, the absolute value of the bias of the overtopping discharges of tests described by equation 39, has slightly increased for every wave steepness. In general, it can be said that the formula underestimates the wave overtopping discharge, which can be concluded from the positive value of the bias, for every wave steepness. It should be noted that the power of $s_{m-1,0}$ is differed to achieve the lowest RMSLE for overtopping discharges of tests computed by equation 39. Equation 39 can be seen together with the measurements in Figure 39.

Table 17 RMSLE (for Qmeasured >10-6) and bias for overtopping discharges of tests described by equation 39 for varying wave steepness.

	Equation 39; γ_f = 0.453 all wave steepnesses	Equation 39; γ_f = 0.453 low wave steepnesses	Equation 39; γ_f = 0.453 middle wave steepnesses	Equation 39; γ_f = 0.453 high wave steepnesses
RMSLE	0.3840	0.4879	0.3366	0.3246
Bias	1.26E-04	1.15E-04	1.28E-04	1.35E-04

Next, the coefficients of equation 39 are re-calibrated to remove the bias of the formula, using the measurements regarding breaking waves. This results in the following formula for the dimensionless wave overtopping discharge at rubble mound breakwaters with wave loading that can be characterized as breaking waves:

$$\frac{q}{\sqrt{g\,H_{mo}^3}} = 0.058\ cot\alpha\ ^{-1.8}\ s_{m-1,0}^{-1}\ \gamma_b\ exp\left[-\left(2.7\frac{R_c}{\xi_{m-1,0}H_{m0}\gamma_b\gamma_f\gamma_\beta\gamma_v}\right)^{1.4}\right] \qquad \text{Equation 40}$$

In Figure 39, equation 40 can be seen together with the measurements for breaking waves. The RMSLE of equation 40 is 0.3619. Compared with the re-calibrated version of the breaking waves formula in the EurOtop (2018) manual, which was used as a starting point in this analysis, the RMSLE decreases significantly, as shown in Table 18. Therefore, it can be said that the accuracy in predicting wave overtopping discharges for breaking waves, is higher for equation 40 than for equation 32. This is also illustrated in Figure 40. In this figure, the measured wave overtopping discharges for breaking waves can be seen against the calculated overtopping discharges using equations 32 and 40. The spread around the line y=x is smaller for equation 40 than equation 32. This indicates a higher accuracy in predicting wave overtopping discharges.

Table 18 RMSLE (for Qmeasured >10-6) and bias for overtopping discharges of tests described by equation 32 and 40.

	Equation 32 (EurOtop (2018); γ_f = 0.453)	Equation 40
RMSLE	0.4653	0.3619

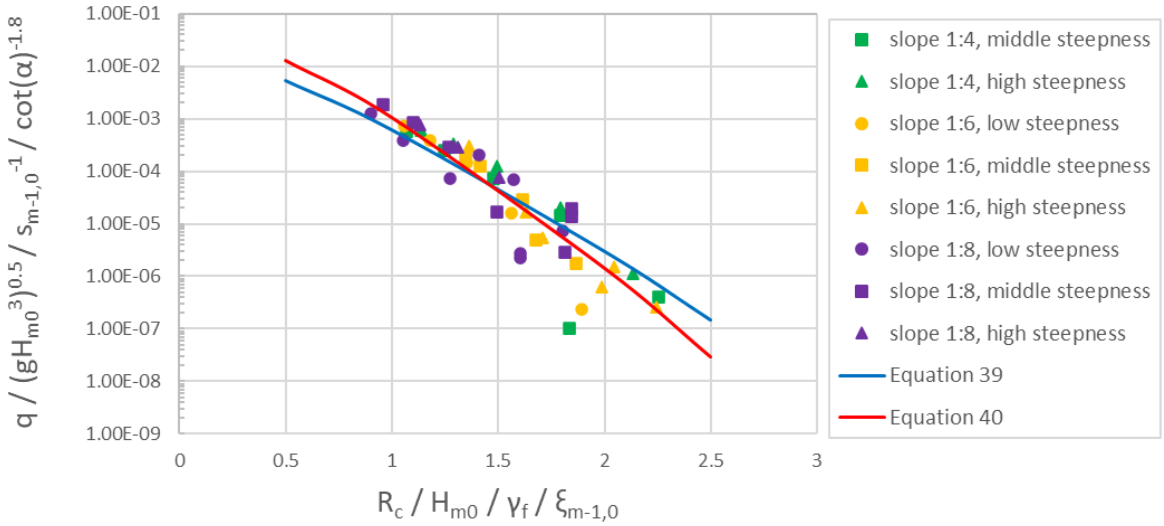

Figure 39 Measured wave overtopping discharges regarding breaking waves compared with equations 39 and 40.

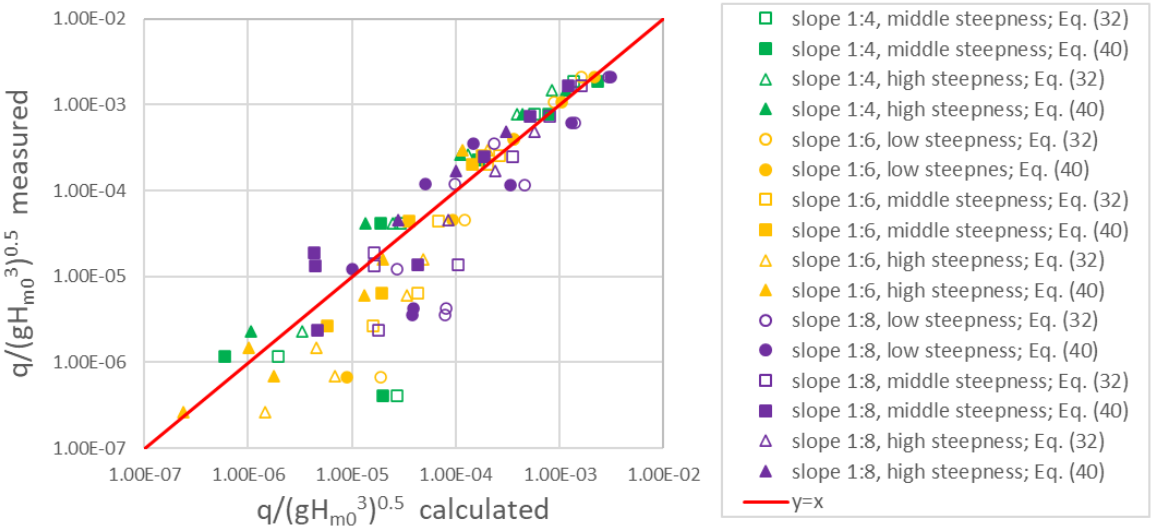

Figure 40 Measured wave overtopping discharges plotted against calculated overtopping discharges using the equations 32 and 40.

In addition to the modification of the EurOtop (2018) formula for breaking waves, also a straight line, on logarithmic scale, is fitted through the data. This resembles more a TAW like approach where no extra power is present in the exponential part of the expression as can be seen in equation 33. This modified TAW expression can be seen in equation 41 below.

$$\frac{q}{\sqrt{g\,H_{mo}^3}} = 0.65\ cot\alpha\ ^{-1.8}\ s_{m-1,0}^{-1}\ \gamma_b\ exp\left[-6.4\frac{R_c}{\xi_{m-1,0}H_{m0}\gamma_b\gamma_f\gamma_\beta\gamma_v}\right] \qquad \text{Equation 41}$$

Equation 40 and 41 are shown together with the data for breaking waves in Figure 41. It can be seen that in the range $1 \leq \frac{R_c}{H_{mo}\gamma_f\xi_{m-1,0}} \leq 2$, the two equations show a very similar behavior. The RMSLE (for Qmeasured > 10^{-6}) for overtopping discharges of tests described by equation 41 is slightly smaller than described by equation 40, as is presented in Table 19. This indicates a higher accuracy in predicting wave overtopping discharges for breaking waves by equation 41.

Table 19 RMSLE (for Qmeasured >10-6) and bias for overtopping discharges of tests described by equations 40 and 41.

	Equation 40	Equation 41
RMSLE	0.3619	0.3562

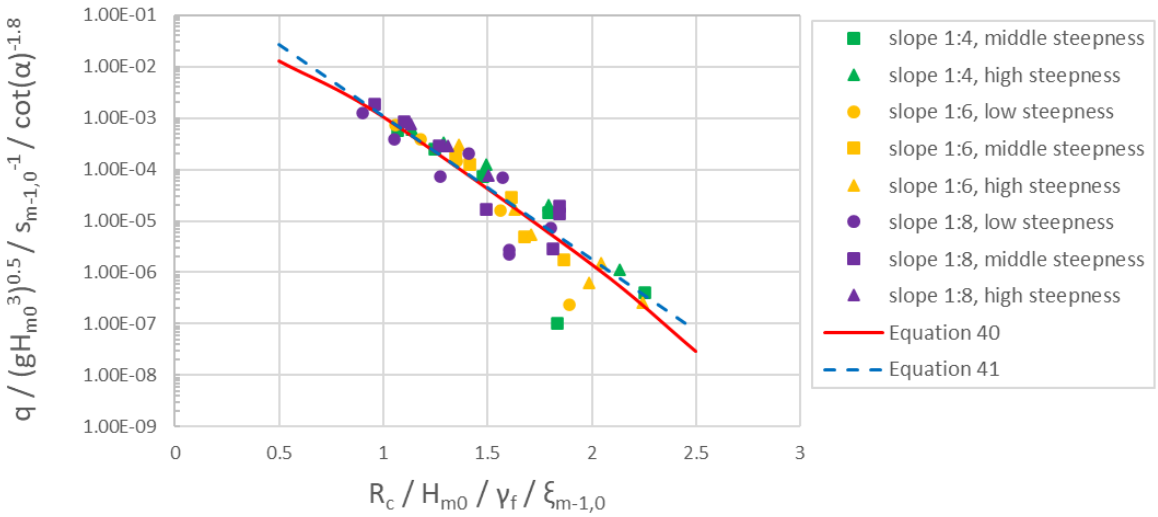

Figure 41 Measured wave overtopping discharges regarding non-breaking waves compared with equations 40 and 41.

4.3.3 Conclusion

As a conclusion to this part of the research, the proposed equation to calculate the wave overtopping discharge at permeable rubble mound breakwaters for wave loading that can be characterized as non-breaking wave loading is equation 37. The proposed equation to calculate the wave overtopping discharge at permeable rubble mound structures for wave loading that can be characterized as breaking wave loading is equation 41.

The wave overtopping discharges of all tests (breaking and non-breaking waves) are combined in Figure 42 and are compared to the proposed equations. The comparison shows that the derived expressions describe the measured discharges accurately, except for a few measurements with a very small discharge (Qmeasured < 10^{-6}), which are outside the range of practical relevance. Most measurements differ no more than

a factor 5 from the calculated overtopping discharges. For low as well as high wave overtopping discharges quite a consistent deviation between the measured and calculated discharges can be seen.

Also, no clear overestimation or underestimation of the calculated wave overtopping discharges can be spotted for varying slope angles or wave steepnesses. Therefore, it can be said that the two proposed formulas do not show any systematic differences in the calculation of the wave overtopping discharge for rubble mound breakwaters.

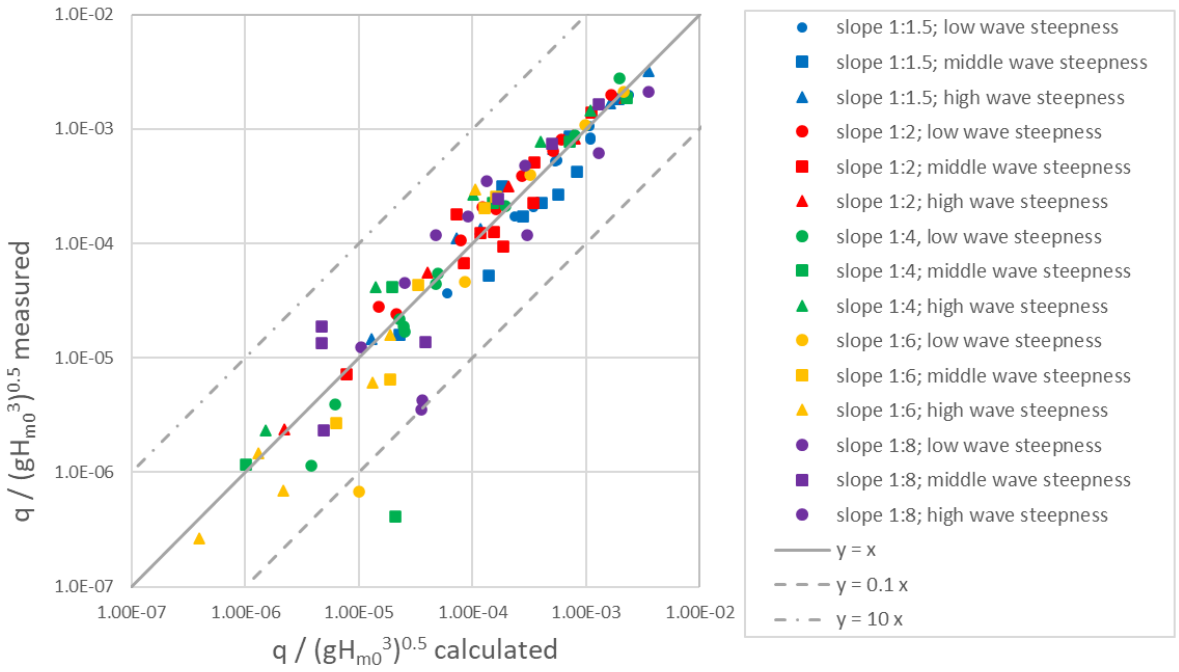

Figure 42 Measured wave overtopping discharges regarding breaking and non-breaking waves plotted against calculated overtopping discharges using the proposed equations in this thesis.

The RMSLE of the proposed equations is shown in Table 20.

Table 20 Proposed equation for breaking and non-breaking wave loading and RMSLE (for Qmeasured >10^{-6}) and bias for overtopping discharges of tests described by the proposed equation.

	Proposed equation	RMSLE
Non-breaking waves	Eq. (37)	0.1722
Breaking waves	Eq. (41)	0.3562

5. Discussion

The discussion consists of two different parts. In the first part, a reflection of the performed physical model tests is given. Possible inaccuracies in the set-up and execution of the physical model tests are discussed. In the second part, the applicability and limitations of this research are covered.

5.1 Reflection of physical model tests

Several inaccuracies might have occurred in the set-up of the physical model tests. These inaccuracies might have an influence on the measured wave overtopping at the breakwater. For example, the breakwater was placed between two glass walls inside the wave flume. These glass walls cause some friction on the incoming waves and, therefore, can cause a reduction in wave energy, which in its turn influences the wave overtopping at the breakwater. To account for these potential wall effects, the chute width was 0.9 m instead of 1.0 m, which was the width of the wave flume. However, it is unknown if the side walls still affected the wave overtopping at the breakwater, but the effects are expected to be negligible since wave propagation in a glass wall flume generally leads to hardly any energy dissipation. Furthermore, stones at the side of the breakwater, near the glass wall, can cause some frictional effects which reduce the wave energy and therefore influence the wave overtopping discharge. However, since a chute width of 0.9 m or smaller was used, this effect is also expected to be negligible.

During the tests with higher overtopping discharges, pumping of the overtopping box was needed to prevent the overtopping box from overflowing. The waves that overtopped the breakwater during this pumping were not taken into account in the total overtopping volume and thereby influencing the average wave overtopping discharge. Therefore, some inaccuracies might have occurred in the results of the tests. It was chosen to disregard the tests with a total pumping time, as percentage of the total duration of the specific test, higher than 11%, to keep these inaccuracies as low as possible. As a result of this, it is not expected that the pumping time has a relevant influence on the average wave overtopping discharge of the remaining tests that were used in the data analysis.

Furthermore, for each test a JONSWAP spectrum was schematized by generating 1,000 waves. Deviations in the overtopping discharges might have occurred for the same wave characteristics due to the uniqueness of the specific series of 1,000 waves.

Finally, also inaccuracies in the results due to the measuring equipment might have occurred. In total 17 wave gauges were used, which measured the wave characteristics in the wave flume, water depth inside the overtopping box and individual wave overtopping events on top of the breakwater. The wave gauges were calibrated with millimeter accuracy. Although the measuring error is expected to be negligible, differences in the results due to a measuring error cannot be completely ruled out.

A unique feature of the performed physical model tests was the reuse of the armour layer for every breakwater configuration. Reusing this armour layer implies that, for every test and every configuration, the positioning of the stones as well as the porosity of the armour layer at the part where waves run up the slope is equal. Because of this the roughness of the breakwater is also equal for every breakwater configuration and every test. Therefore, this method is particularly suitable to make comparisons between the configurations since it reduces inaccuracies in the measurements due to a difference in roughness, which can have an influence on the wave overtopping discharge.

5.2 Applicability and limitations of the research

The proposed formulas, to calculate wave overtopping discharges, in this thesis are based on the data gathered during physical model tests. The ranges of the most important parameters of these tests can be seen in Table 21. These ranges cover a wide variety of rubble mound structures. In total 114 tests have been taken into account in the data analysis at 5 various breakwater configurations, each with a different slope of 1:1.5, 1:2, 1:4, 1:6 and 1:8. Tests have been performed with a wide range of hydraulic parameters. The breakwaters were exposed to varying significant wave heights (0.095 m $\leq H_{m0} \leq$ 0.228 m) and wave steepnesses ($0.012 \leq s_{m-1,0} \leq 0.042$). Also, different water depths were used. This resulted in a wide range of the Iribarren number ($0.612 \leq \xi_{m-1,0} \leq 6.04$) and non-dimensional crest freeboard ($0.33 \leq R_c/H_{m0} \leq 2.08$). Furthermore, 55 Tests could be characterized as tests with breaking wave loading and 59 as tests with non-breaking wave loading.

Therefore, the proposed expressions are expected to be valid for a wide variety of rubble mound breakwaters. But there are limitations to the ranges of validity of the proposed expressions. The proposed expressions might be accurate outside the ranges of test conditions, however their validity is still unknown. Some important limitations of the research will now be discussed further.

During the physical model tests, no severe wave breaking occurred on the foreshore. The proposed expressions are based on these conditions. However rubble mound structures are often placed in relatively shallow water, where wave breaking on the foreshore is present. It is not unimaginable that wave breaking on the foreshore has an influence on wave overtopping at rubble mound breakwaters. However, as input for all computations on wave overtopping in the data analysis, the significant wave height at the toe of the structure is used.

In this research several influencing factors for wave overtopping at rubble mound structures were not studied. The influence of a crest wall, the influence of a berm and the influence of oblique waves were not taken into account. Therefore, it is yet unknown what the influence of a combination of a varying slope angle or wave steepness and for example, a berm, is on the wave overtopping discharge. In the data analysis, the influencing factors that were not studied were all set to 1.0, such that they do not have an influence on the wave overtopping discharge. However, the proposed equations

should still be validated whereby also the influencing factors for a crest wall, a berm and oblique waves are taken into account.

Also, it must be noted that the proposed expressions in this research are based on empirical relations between different parameters. Although empirical formulas are useful for the design of all kinds of coastal structures, these expressions do not necessarily represent all physical processes in reality. Therefore, they cannot always be accepted as the truth and extensive judgement of empirical formulas is always needed.

6. Conclusion and Recommendations

In the first part of this chapter the conclusions of the research will be given. In the second part, some recommendations for further research will be presented.

6.1 Conclusion

One of the parameters that plays a role in wave overtopping at breakwaters, that was less widely investigated compared to other parameters, was the slope angle of the outer slope of rubble mound breakwaters. In the current guidelines, no influence of the slope angle is accounted for in the formulas for wave overtopping of wave loading that can be characterized as non-breaking waves. However, numerical model results by Irías Mata & Van Gent (2023) showed that wave overtopping at rubble mound breakwaters strongly depend on the slope angle.

In the current guidelines, like the TAW (2002) and EurOtop (2018) manual, for wave overtopping for breaking waves, which is mainly the case for structures with a gentle slope, the slope angle of the structure is taken into account. However, these formulas are mostly based on physical model tests at breakwaters or dikes with an impermeable core and are therefore not applicable for rubble mound breakwaters with a permeable core.

This lead to the following research objective: gather more information about a possible relation between the slope angle of a rubble mound breakwater and the wave overtopping at this breakwater. The research question that was studied during this master thesis read as follows:

What is the influence of the slope angle of rubble mound breakwaters on wave overtopping?

To answer this research question, a literature study was done and physical model tests in the wave flume at Deltares in Delft, the Netherlands, were performed. The ranges of the most important parameters of the physical model tests can be seen in Table 21.

Table 21 Parameter ranges of test program

Parameter	Symbol	Values / Ranges
Seaward Slope [-]	$\cot \alpha$	1.5; 2; 4; 6; 8
Median nominal grain diameter [m]	D_{n50}	0.0317
Water depth [m]	d	0.6 – 0.825
Crest height [m]	h	0.9
Incident significant wave height at toe [m]	H_{m0}	0.095 – 0.228
Freeboard [m]	R_c	0.075 – 0.3
Wave Steepness [-]: $s_{m-1,0}=2\Pi H_{m0}/gT^2_{m-1,0}$	$s_{m-1,0}$	0.012 – 0.042
Iribarren number [-]: $\xi_{m-1,0}=\tan\alpha/s^{0.5}_{m-1,0}$	$\xi_{m-1,0}$	0.612 – 6.04
Number of waves [-]	N	1,000
Armour width in front of chute / crest element [m]	G_c	0.100
Chute width [m]	C_w	0.25; 0.5; 0.9
Non-dimensional Freeboard [-]	R_c/H_{m0}	0.33 – 2.08
Non-dimensional armour width in front of chute [-]	G_c/H_{m0}	0.44 – 1.05
Non-dimensional stone diameter [-]	D_{n50}/H_{m0}	0.14 – 0.33

The research question will now be answered based on multiple sub-questions:

1. ***Which parameters have an influence on wave overtopping at rubble mound breakwaters?***

This sub-question will be answered based on the performed literature study. All influencing parameters for wave overtopping can be divided into two different categories: wave characteristics and the structure's geometry. The main wave characteristics that play a role in wave overtopping at breakwaters are the significant wave height and wave period. An increase in significant wave height will result in an increase in wave overtopping discharge. Together, the wave height and wave period form the wave steepness. It was found that the wave steepness plays a role in wave overtopping for wave loading that can be characterized as breaking as well as non-breaking wave loading. A higher wave steepness results in a lower breaker parameter which causes waves to be plunging or spilling instead of surging. Plunging or spilling waves lose more energy while breaking and therefore a higher wave steepness results in less wave overtopping.

Rubble mound slopes have a rough surface which results in a higher frictional resistance on the approaching waves. Therefore a rubble mound structure dissipates more wave energy than a smooth slope. Furthermore a permeable core leads to more wave energy dissipation compared to an impermeable core. More wave energy dissipation leads to less wave overtopping.

Also, the angle of wave attack plays a role at wave overtopping. The larger the angle of wave attack, the less wave overtopping at the structure, both for breaking and for non-breaking wave loading.

Another influencing parameter is an influence factor for a berm. The presence of a berm has a reducing effect on the wave overtopping discharge, both for breaking and for non-breaking wave loading and permeable and impermeable breakwaters or seadikes. Regarding non-breaking waves at rubble mound breakwaters this reducing effect is also influenced by the wave steepness, as was found by Van Gent et al. (2022). They also found that the presence of a crest wall on top of a rubble mound breakwater is less effective than a corresponding structure with the same crest elevation but without crest wall.

2. ***What is the influence of the slope angle on wave overtopping when the wave characteristics stay the same and what is the difference between non-breaking and breaking waves?***

After the physical model tests and the associated data analysis it can be concluded that the slope angle has a large influence on wave overtopping at rubble mound breakwaters. It follows that the steeper the slope, the larger the wave overtopping

discharge for the same dimensionless crest freeboard. This relation can be seen both for breaking and for non-breaking wave loading. This trend is also captured regardless the wave steepness. For low, middle and high wave steepness conditions, it still followed that the gentler the slope of the breakwater, the lower the wave overtopping discharges for the same dimensionless crest freeboard.

When the wave characteristics stay the same it means that the breaker parameter is only depending on the slope angle of the breakwater. So a steeper slope means a higher breaker parameter. It was found that a higher breaker parameter corresponds to a higher wave overtopping discharge for the same dimensionless crest freeboard.

For wave loading that can be characterized as breaking as well as non-breaking waves, it applies that the steeper the slope, the larger the wave overtopping discharge for the same dimensionless crest freeboard. However, it appears that that the slope angle of the breakwater has a larger influence on the wave overtopping discharge for breaking wave conditions compared to non-breaking wave conditions. Therefore, it can be said that the dependency between the slope angle and the wave overtopping discharge is larger for breaking waves than for non-breaking waves.

According to literature, higher overtopping discharges for steeper slopes might be caused by a higher upward velocity in the run-up for steeper slopes. This increases the momentum and energy of the waves at the breakwater which causes in its turn more water to spill over the crest of the breakwater and therefore, more wave overtopping.

3. ***What is the influence of the wave steepness on wave overtopping at different slope angles?***

After the physical model tests and the associated data analysis, it can be concluded that the wave steepness has a large influence on wave overtopping at rubble mound breakwaters, both for non-breaking waves and for breaking waves. In general, it can be said that the lower the wave steepness, the larger the wave overtopping discharge for the same dimensionless crest freeboard. This relation was found regardless of the slope angle of the breakwater.

However, it follows that for more gentle slopes of the breakwater, the wave steepness has a larger influence on the wave overtopping discharge. Thus, the dependency between the wave overtopping discharge and the wave steepness becomes larger for more gentle slopes compared to steeper slopes. Gentle slopes, like 1:6 and 1:8, mostly lead to breaking wave loading. Therefore, it follows that the dependency between the wave steepness and the wave overtopping discharge is larger for breaking waves than for non-breaking waves.

4. ***What is the difference between the results of the physical model tests and the existing guidelines for wave overtopping and how can the guidelines be improved in order to obtain more accurate predictions of wave overtopping at rubble mound breakwaters?***

For wave loading that can be characterized as breaking waves, the influence of the wave steepness and slope angle of the breakwater on the wave overtopping discharge was already described in the TAW (2002) report and EurOtop (2018) manual. However, these formulas were mainly based on physical model tests with impermeable breakwaters or seadikes. In this research, it was found that also at permeable rubble mound breakwaters, the wave steepness and slope angle of the breakwater have an influence on the wave overtopping at this structure regarding breaking waves.

For wave loading that can be characterized as non-breaking waves, the influence of the wave steepness on the wave overtopping discharge at rubble mound breakwaters was reported by Van Gent et al. (2022) based on physical model tests. The influence of the slope angle of the breakwater on the wave overtopping discharge was found by Irías Mata & Van Gent (2023) based on numerical model results. In this research, the dependency between the wave overtopping discharge and the slope angle and wave steepness for non-breaking waves, was also found based on physical model tests.

Regarding non-breaking waves, four different formulas were compared with each other and the gathered data. The formula by Irías Mata & Van Gent (2023), as shown in equation 31, with a re-calibrated constant value of the roughness factor of $\gamma_f = 0.406$, is the best fit to the data. This equation has the lowest RMSLE and therefore it can be said that, regarding non-breaking waves, this equation is the most accurate in predicting wave overtopping discharges. The RMSLE for overtopping discharges of tests described by this formula is 0.3466.

Regarding breaking waves, two different formulas were compared to each other and the data. The formula as given in the EurOtop (2018) manual, with a re-calibrated value of the roughness factor, to get zero bias, of $\gamma_f = 0.453$, resulted in the most accurate predictions of wave overtopping discharges based on the lowest RMSLE. This formula can be found in equation 32. The RMSLE for overtopping discharges of tests described by this formula is 0.4653.

Both formulas that gave the best results in predicting wave overtopping discharges were modified to obtain even more accurate predictions for overtopping discharges. The proposed equation to calculate the wave overtopping discharge at permeable rubble mound breakwaters for wave loading that can be characterized as non-breaking waves reads as follows:

$$\frac{q}{\sqrt{g\,H_{mo}^3}} = 13.4\,s_{m-1,0}\;\;cot\alpha^{1.1}\;exp\left[-\frac{4.1\,R_c}{\gamma_f\gamma_\beta\gamma_b\gamma_v\gamma_p H_{mo}\xi_{m-1,0}^{0.5}}\right] \qquad \text{Equation 43}$$

With $\gamma_f = 0.406$; $\gamma_\beta = 1.0$; $\gamma_b = 1.0$; $\gamma_v = 1.0$; $\gamma_p = 1.0$

The RMSLE for overtopping discharges of tests described by equation 43 is 0.1722. This value is more than two times as low as the RMSLE of the expression by Irías Mata & Van Gent (2023).

The proposed equation to calculate the wave overtopping discharge at permeable rubble mound breakwaters for wave loading that can be characterized as breaking waves reads as follows:

$$\frac{q}{\sqrt{g\,H_{mo}^3}} = 0.65\ cot\alpha\ ^{-1.8}\ s_{m-1,0}^{-1}\ \gamma_b\ exp\left[-6.4\frac{R_c}{\xi_{m-1,0}H_{m0}\gamma_b\gamma_f\gamma_\beta\gamma_v}\right] \qquad \text{Equation 44}$$

With $\gamma_f = 0.453$; $\gamma_\beta = 1.0$; $\gamma_b = 1.0$; $\gamma_v = 1.0$

The RMSLE for overtopping discharges of tests described by equation 44 is 0.3562.

The wave overtopping discharges of all tests (breaking and non-breaking waves) are combined in Figure 43 and are compared to the proposed equations for either breaking or non-breaking wave loading. The comparison shows that the derived expressions describe the measured discharges accurately, except for a few measurements with a very small discharge, which are outside the range of practical relevance.

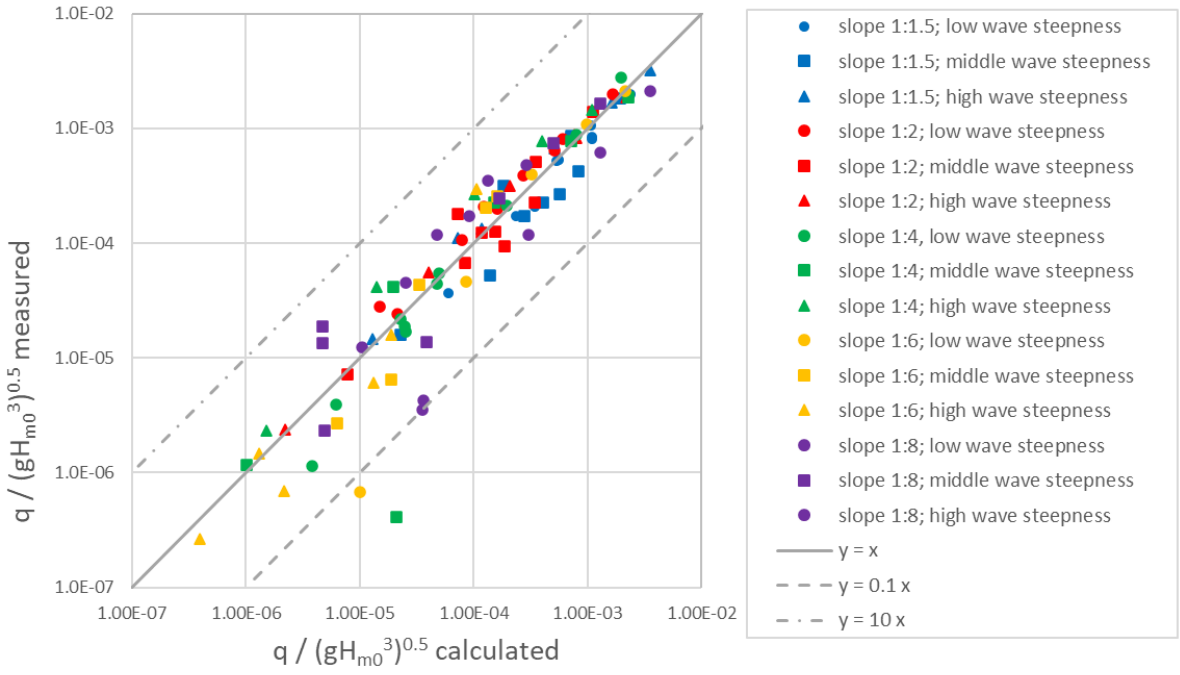

Figure 43 Measured wave overtopping discharges regarding breaking and non-breaking waves plotted against calculated overtopping discharges using the proposed equations in this thesis.

6.2 Recommendations

Some recommendations for future research are given below:

- Validate the proposed expressions for wave overtopping at rubble mound breakwaters for breaking and non-breaking waves, outside the parameter ranges that were used during the physical model tests in this research.

- Study the influence of wave breaking on the foreshore on wave overtopping at rubble mound breakwaters in combination with a varying slope angle of the seaward slope of the breakwater.

- Study the influence of crest walls, berms and obliquely incident waves on wave overtopping at rubble mound breakwaters in combination with a varying slope angle of the seaward slope of the breakwater.

- In this thesis, research was done to the influence of the slope angle and wave steepness on the average wave overtopping discharge. Conventionally the average wave overtopping discharge is used as a design criterion for coastal structures (Koosheh, et al., 2021). However nowadays, research indicates that large overtopping quantities can be the result of extreme overtopping events. This can cause high flow velocities and a thick water layer at the structure, which can cause damage at the dike or breakwater. Therefore, the average overtopping discharge may not be sufficient, and additional criteria may be required to describe extreme overtopping events. For instance, a criterion related to volumes within individual waves may be a suitable addition (Franco, et al., 1994).

  Therefore, it is further recommended to study the influence of the slope angle and wave steepness on volumes per overtopping wave, on percentages of overtopping waves and on flow velocities and flow depths during overtopping events. Data of volumes per overtopping wave and percentages of overtopping waves to do so, is gathered during the physical model tests.

- Currently, most studies that are performed regarding wave overtopping at coastal structures are based on physical model tests with dikes or breakwaters that either had a fully permeable or impermeable core. However also the degree of permeability might play a role in wave overtopping at dikes or breakwaters. Therefore it is advised to study the influence of the degree of permeability of the core of the breakwater. This can be done by performing physical model tests to different breakwater configurations, each with a different degree of permeability of the core.

Acknowledgements

This study was realized with the help of a TKI (Top Consortia for Knowledge and Innovation) subsidy (Delta Technology project Dynamics of Hydraulic Structures - DEL105) and the support of De Vries & van de Wiel (DEME) and Deltares.

References

Arkash, P. K. & Chaudhary, B., 2022. *Review of Literature on Design of Rubble Mound Breakwaters.*

Burcharth, H. F. & Liu, Z., 1995. *Rubble Mound breakwater Failure Modes.*

Chen, W., Gent, M. v., Warmink, J. & Hulscher, S., 2019. *The influence of a berm and roughness on the wave overtopping at dikes.*

CIRIA, CUR & CETMEF, 2007. *The Rock Manual. The use of rock in hydraulic engineering (2nd edition).*

De Ridder, M. P., Kramer, J., Biemand, J. P. d. & Wenneker, I., 2023. *Validation and practical application of nonlinear wave decomposition methods for irregular wave heights.*

Deltares, n.d. *Experimental Facility Scheldt Flume.* [Online] Available at: https://www.deltares.nl/en/research-facilities/wave-and-flow-facilities/scheldt-flume
[Accessed 24 August 2023].

EurOtop, 2018. *Manual on wave overtopping of sea defences and related structures.*

Franco, L., Gerloni, M. d. & Meer, J. v. d., 1994. *Wave overtopping on vertical composite breakwaters.*

Hughes, S., 1993. *Physical Models and Laboratory Techniques on Coastal Engineering,* Singapore.

Irías Mata, M. & Van Gent, M. R., 2023. *Numerical modelling of wave overtopping discharges at rubble mound breakwaters using OpenFOAM.*

Joosten, M., 2017. *Lecture Notes - Kansrekening en statistiek.*

Jumelet, D., Gent, M. R. v., Hofland, B. & Kuiper, C., 2024. *Satibility of rock-armoured mild slopes.*

Koosheh, A. et al., 2021. *Individual wave overtopping at coastal structures: A critical review and the existing challenges.*

Mansard & Funcke, 1980. *The measurement of incident and reflected spectra using a least squares method.*

Peña, E. & Anta, J., 2021. *Editorial—Physical Modelling in Hydraulics Engineering.*

Schiereck, G. J. & Verhagen, H. J., 2019. *Introduction to Bed bank and shore protection,* Delft Academic Press / VSSD.

TAW, 2002. *Technical Report Wave Run-up and Wave Overtopping at Dikes*.

Van Doorslaer, K., Rouck, J. d., Audenaert, S. & Duquet, V., 2015. *Crest modifications to reduce wave overtopping of non-breaking waves over a smooth dike slope*.

Van Gent, M. R., 1999. *Physical modelinvestigations on coastal structures with shallow foreshores; 2D Model tests with single and double-peaked wave energy spectra,* Delft.

Van Gent, M. R., 2020. *Influence of oblique wave attack on wave overtopping at smooth and rough dikes with a berm.*

Van Gent, M. R., Wolters, G. & Capel, A., 2022. *Wave overtopping discharges at rubble mound breakwaters including effects of a crest wall and a berm*.

Wolters, G. et al., 2009. *HYDRALAB III: Guidelines for physical model testing of rubble mound breakwaters.*

Appendix A: Breakwater Composition: Technical Drawing

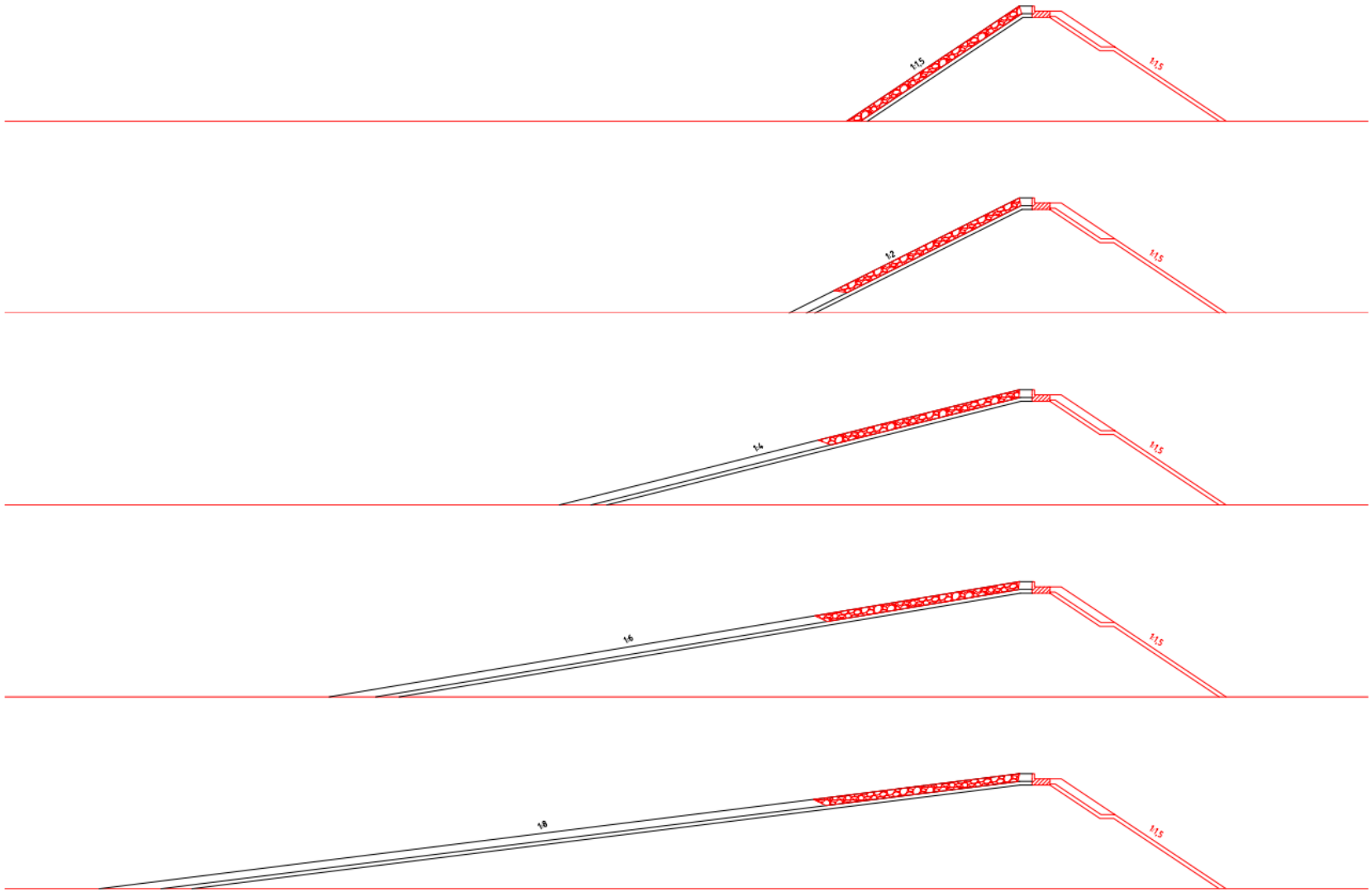

Figure 44 Technical drawing breakwater composition: different configurations (W. Stet, personal communication, June 2023).

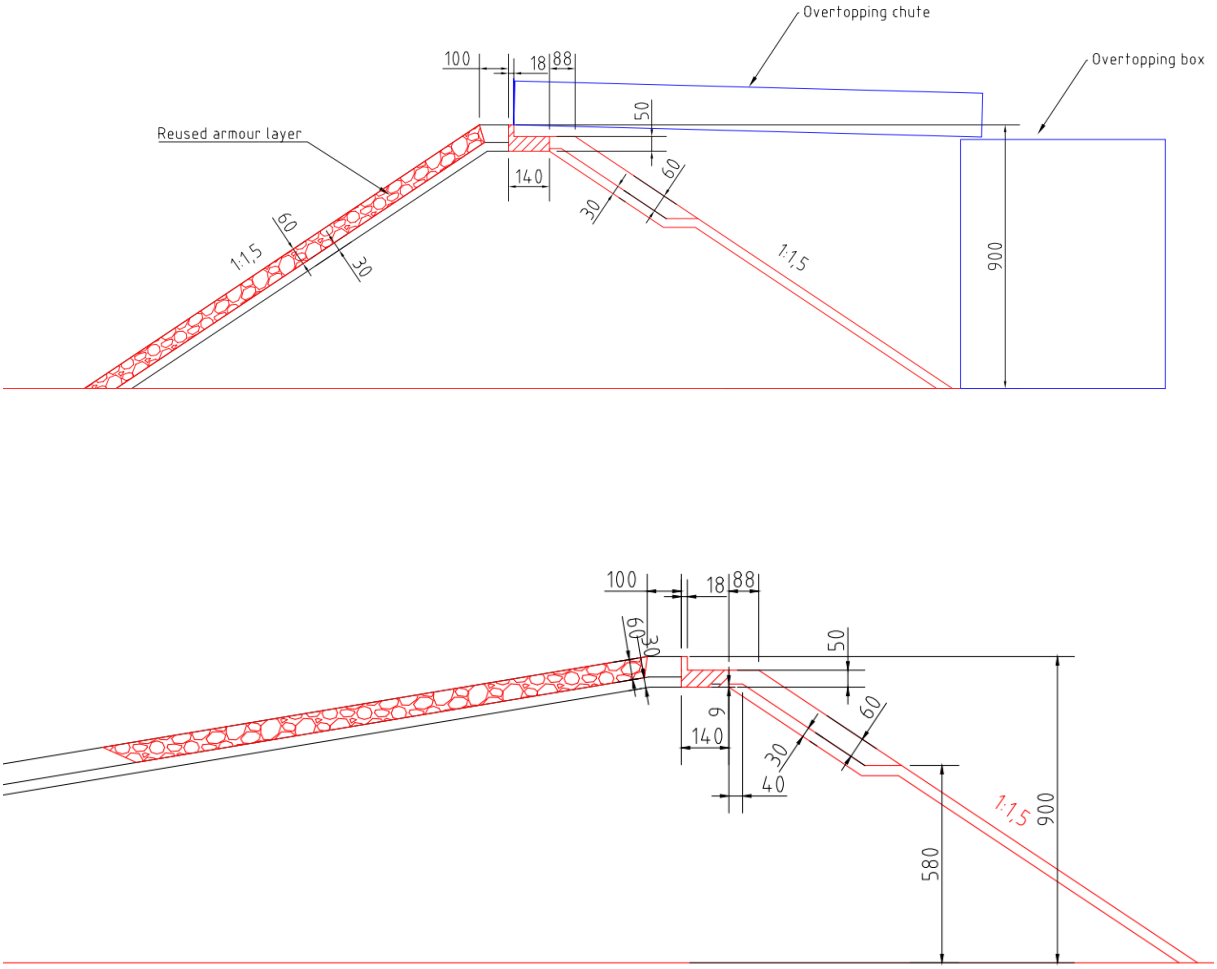

Figure 45 Technical Drawing breakwater composition (W. Stet, personal communication, June 2023).

Appendix B: Wave Gauge Positioning

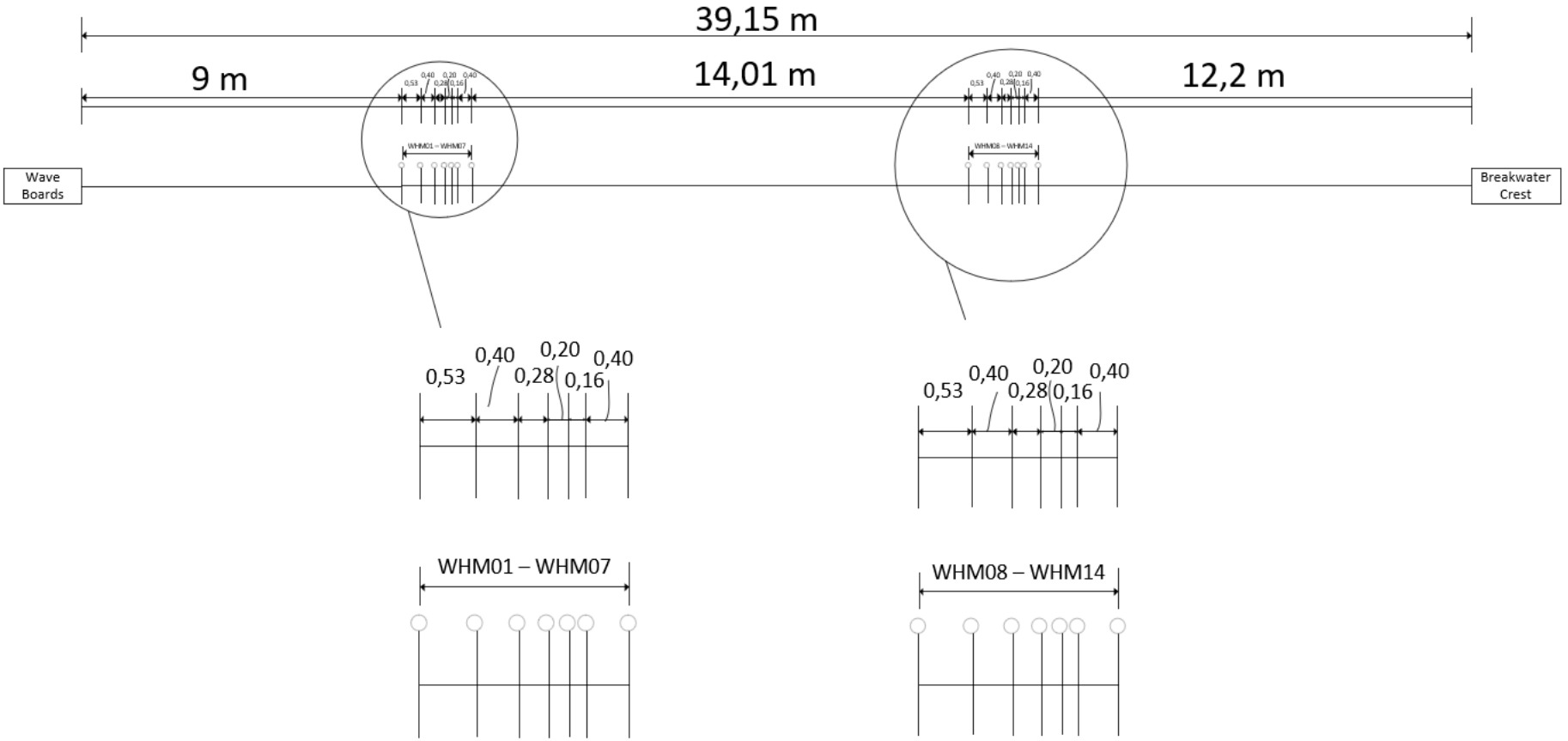

Figure 46 Wave gauge positioning in wave flume.

Appendix C: Wave running up a slope (T5753022)

Figure 47 Pictures of a wave running up the slope of the breakwater configuration with slope 1:8.

Appendix D: Full test program

In this appendix the full test program regarding the most important parameters can be found.

Table 22 Test program configuration 1 (slope 1:6).

Name	$H_{m0,toe}$ [m]	$T_{m-1,0,toe}$ [s]	T_p [s]	q [l/s/m]	q* [-]	R_c /H_{m0} [-]	$S_{m-1,0,toe}$ [-]	$\xi_{m-1,0}$ [-]
[redacted]								

Table 23 Test program configuration 2 (slope 1:4).

Name	$H_{m0,toe}$ [m]	$T_{m-1,0,toe}$ [s]	T_p [s]	q [l/s/m]	q* [-]	R_c /H_{m0} [-]	$S_{m-1,0,toe}$ [-]	$\xi_{m-1,0}$ [-]
[redacted]								

Table 24 Test program of configuration 3 (slope 1:2).

Name	$H_{m0,toe}$ [m]	$T_{m-1,0,toe}$ [s]	T_p [s]	q [l/s/m]	q* [-]	R_c / H_{m0} [-]	$S_{m-1,0,toe}$ [-]	$\xi_{m-1,0}$ [-]
[redacted]								

Table 25 Test program of configuration 4 (slope 1:1.5).

Name	$H_{m0,toe}$ [m]	$T_{m-1,0,toe}$ [s]	T_p [s]	q [l/s/m]	q* [-]	R_c / H_{m0} [-]	$S_{m-1,0,toe}$ [-]	$\xi_{m-1,0}$ [-]
[redacted]								

Table 26 Test program of configuration 5 (slope 1:8).

Name	$H_{m0,toe}$ [m]	$T_{m-1,0,toe}$ [s]	T_p [s]	q [l/s/m]	q* [-]	R_c /H_{m0} [-]	$S_{m-1,0,toe}$ [-]	$\xi_{m-1,0}$ [-.]